

# **STUDY ON POWER QUALITY ISSUES IN GRID CONNECTED WIND FARMS AND THEIR REMEDIAL MEASURES**

**March 2014**

**Project No. RD-RD-190-10**



A.D Thirumoorthy  
Principal Investigator  
Tamilnadu energy development Agency, Coimbatore

Dr. C. Chellamuthu  
Co-Principal Investigator  
RMK Engineering College, Kavaraipettai

## **ACKNOWLEDGEMENTS**

The Centre for Wind Energy Technology (C-WET) would like to acknowledge the experts from Tamilnadu Energy Development Agency , Coimbatore and RMK Engineering College, Kavaraipettai who have authored this report. C-WET also thanks the Ministry of New and Renewable Energy (MNRE) for their financial and technical support for the research and production of this report.

Major contributors in alphabetical order include :

Chellamuthu,C  
Thirumoorthy, A.D

RMK Engineering College  
Tamilnadu Energy Development Agency

## **NOTICE**

This report was prepared as an account of the work sponsored by Centre for Wind Energy Technology (C-WET). Neither C-WET nor any of their employees, makes any warranty, express or implied, or assumes any legal liability or responsibility for the accuracy, completeness, or usefulness of any information, apparatus, product, or process disclosed, or represent that its use would not infringe privately owned rights. Reference herein to any specific commercial product, process, or service by trade name, trademark, manufacturer, or otherwise does not necessarily constitute or imply its endorsement, recommendation, or favoring by C-WET. The views and opinions of authors expressed herein do not necessarily state or reflect those of C-WET.

No part of this report shall be either reproduced or otherwise be used in any form without the written permission of the C-WET and the proponent.

Available electronically at <http://www.cwet.res.in>

# CONTENT

CHAPTER NO.	TITLE	PAGE NO.
1	<b>Literature review</b>	
2	<b>Data collection and analysis of wind farm located at peedampalli substation</b>	1
	2.1 Introduction	5
	2.2 Fixed speed Induction generator	5
	2.3 Power quality analyzer- Dranetz PX5.8	6
	2.4 Power quality analyzer- Fluke Serial No 435	12
	2.5 Comparison of data collected from the power quality analyzers	13
	2.6 Conclusion	15
3	<b>Simulation of the peedampalli substation</b>	
	3.1 Introduction	16
	3.2 Simulation model	17
	3.3 Layout of Peedampalli substation	19
	3.4 Simulation model of the peedampalli substation	21
	3.5 Steady state analysis of peedampalli wind farm	23
	3.5.1 Simulation result of wind farm for various bus bar voltages	23
	3.5.2 Frequency Variations	25
	3.5.3 Simulation of wind electric system for various wind speeds	27
	3.6 Dynamic analysis of grid connected wind farm	28
	3.6.1 Short Circuit Analysis	30
	3.6.2 Load Variation	33
	3.6.3 Flickering	34

3.6.4	Harmonic load flow	36
3.7	Comparison between results of measurement and simulation	36
3.7.1	Simulation of voltage sag	37
3.7.2	Transient voltage due to capacitor switching	38
3.7.3	Tripping of the wind generator	40
3.7.4	Swell	42
3.8	Conclusion	44
<b>4</b>	<b>Data collection and analysis of wind farm located at Pethappampatty wind farm</b>	
4.1	Introduction	46
4.2	Power Quality Analyzer – Dranetz BMI	51
4.3	Time Plot (Pethappampatty)	56
4.4	Power Quality Analyzer-Fluke 434	58
4.5	Power Quality Analyzer-Hioki 3390	60
4.6	Conclusion	62
<b>5</b>	<b>Data collection and analysis of wind farm at chinnaputhur substation</b>	
5.1	Introduction	64
5.2	Substation layout	64
5.3	Analysis of recorded events	67
5.3.1	Transients	67
5.3.2	Impulsive transients	69
5.3.3	Sag	70
5.4	Analysis of overall recorded events	71
5.4.1	Voltage time plot	71
5.4.2	Time plot of current	73
5.4.3	Flickering	74

5.4.4	Frequency	76
5.5	Conclusion	77
<b>6</b>	<b>Modelling and controlling concept of the variable speed wind turbine with PMSG in DIgSILENT</b>	
6.1	General	78
6.2	Simulation tools	79
6.3	Simulation model of individual blk using dsl	80
6.3.1	Modelling of mechanical side block	81
6.3.1.1	Speed measurement	81
6.3.1.2	Synchronous generator model	83
6.3.1.3	Frame	84
6.3.1.4	Composite Model	85
6.3.2	Modelling of frequency converter	85
6.3.2.1	Frequency converter	87
6.3.2.2	Generator side controller	90
6.3.2.3	Grid side controller	93
6.3.2.4	Frame	96
6.3.2.6	Composite Model	97
6.4	Grid connection	98
6.5	Conclusion	100
<b>7</b>	<b>Analysis and simulation of E2 wind farm feeder in chinnaputhur substation</b>	
7.1	Introduction	101
7.2	Load flow studies	103
7.3	Steady state simulation of the e2 feeder connected to grid	105
7.3.1	Simulation of E2 feeder system for various bus bar voltages	105

7.3.2	Frequency variations	108
7.3.3	Simulation of E2 feeder system for various wind speeds	110
7.4	Dynamic simulation of the grid connected wind electric system	113
7.4.1	System performance under deterministic wind speeds	113
7.4.2	Dynamic behavior of the wind turbine driven PMSG under grid faults	117
7.4.3	Flickering	120
7.5	Comparison of simulation result with measurement	121
7.5.1	Introduction	121
7.5.2	Simulation of voltage sag	121
7.5.3	Tripping of the wind generator	123
7.5.4	Swell	124
7.6	Conclusion	125
<b>8</b>	<b>Remedial measures and suggestions for improving power quality</b>	
8.1	Improvement Techniques	127
8.2	Capacitor application	127
8.3	Re-Conductoring	128
8.4	Bifurcation	128
8.5	Load balancing	129
8.6	Feeder reconfiguration	129
8.7	Fact devices	130
8.8	Implication of poor power quality	130
8.9	Custom power solutions	131
8.10	Advantages of power conditioning	131

8.11 Fault ride through	132
8.12 Suggestions	133
<b>References</b>	<b>138</b>

## ABBREVIATION

C	Capacitance of DC-Link Capacitor
E	Electromotive Force (Induced Voltage)
$i_{ds}$	Direct Axis Stator Current
$I_f$	Excitation Current
IGBT	Insulated Gate Bipolar Transistor
$i_{qs}$	Quadrature Axis Stator Current
$I_s$	Stator Current
m	Number of Phases
MPPT	Maximum Power Point Tracking
N	Total no Transformer
p	Number of Pole Pairs
$P_{eq}$	Equivalent Real Power in p.u
$P_{gen}$	Generator Active Power
PMSG	Permanent Magnet Synchronous Generators
$P_{ref}$	Real Power Reference
$Q_{eq}$	Equivalent Reactive Power in p.u
$Q_{gen}$	Generator Reactive Power
$Q_{ref}$	Reactive Power Reference
RMS	Root Mean Square
RRF	Rotor Reference Frame
$R_s$	Stator Reactance
S	Apparent Converter Power
$S_{eq}$	Equivalent Apparent Power in p.u
SFRF	Stator Flux Reference Frame
$T_e$	Electromagnetic Torque
$U_{DC}$	Link Voltage
$U_h$	Voltage Representing the Main Field
$U_s$	Stator Voltage
$V_{dc_{ref}}$	DC Voltage Reference
$X_f$	Field Winding Reactance
$X_h$	Main Reactance
$X_{s\sigma}$	Stator Leakage Reactance
$Z_{eq}$	Equivalent Impedance
$\omega_{gen}$	Generator Rotational Speed

$\delta$	Load Angle
$\Psi_E$	DC Excited Flux
$\phi$	Power Factor
$\Omega_{gen}$	Mechanical Generator Speed
$\Delta U_{DC}$	Allowed Voltage Ripple
$\omega$	Electrical Frequency of the Grid
$C_p$	Power Coefficient
$H_m$	Inertia Constant
$i_{ds}$	Direct Axis Stator Current
$i_{qs}$	Quadrature Axis Stator Current
$K_s$	Spring Constant
$L_i$	Inductance
$p$	Pole
PCC	Point of Common Coupling
$P_s$	Stator Real Power
$P_{st}$	Flicker Emission from the Wind Turbine
$Q_s$	Stator Reactive Power
RMS	Root Mean Square
$R_s$	Stator Resistance
$V_{wg}(t)$	Gust Component
$V_{wr}(t)$	Ramp Component
$V_{wt}(t)$	Turbulence Component
$\beta$	Blade Angle
$\lambda$	Tip Speed Ratio
$\Psi_k$	Network Impedance Angle
$\omega_s$	Synchronous Speed
$\omega_m$	Mechanical Speed
$\Psi_i$	Flux Linkage

# **CHAPTER 1**

## **LITERATURE REVIEW**

The wind energy sector has grown significantly in India despite ups and downs. Today, after having surmounted many problems, wind energy development in India is known to be a very mature industry. In India, wind farms are concentrated in rural areas, where transmission and distribution grids tend to be very weak and often lack the capacity to tie-in large amounts of wind power. The insufficient capacity of the power system can cause large variations in steady state voltage and power outages. Substations are not always equipped with automatic voltage regulators, further adding to the complications and instability. Inadequate grid capacity and equipment affect both the efficiency and operation of the wind turbines. Thus with the increasing penetration of wind power, there is a need to study the impact of their interconnection to grid.

In India FSIG (Fixed Speed Induction Generator) is the most commonly used machine. A few turbines are equipped with DDSG (Direct Drive Synchronous Generator). So, this project will focus on the modeling of FSIG and DDSG systems. Analysis will be carried out with detailed and reduced order models. Complexities of the various parts of a wind electric system model, such as aerodynamic conversion, drive-train and generator representation will be analyzed. Machines may be represented with active stall and pitch mechanisms. The inverter modeling will be taken up for DDSG systems. Finally, a comparison of both the models for WECS will be done. A conclusion on the option of generator and its parameters to allow a higher penetration of wind power into the grid may be provided.

In this work, the steady state behavior of WECS will be studied using load flow analysis. It is important to study the dynamic performance because the performance of wind turbines is affected by disturbances in the grid frequency variations, voltage quality and fluctuations in steady state voltage. Wind power output is reduced during disturbances simply because turbines go off-line in an

outage. Frequency variations lead to changes in rotor speed, subsequently impacting performance and output. Voltage imbalances can cause the turbine to trip off-line and lead to efficiency losses in induction generators. The weak Indian grid networks can exacerbate these problems, making development difficult for rural areas with insufficient grid capacity. In this project, the impact of connecting FSIG and DDSG on the transient stability will be compared.

The impact of wind generation on power systems is no longer negligible if high penetration levels are going to be achieved. It is very important to boost the transfer capability of the transmission system while improving the utilization of transmission assets to accommodate high penetration of wind power on the network. Hence, this project may lead to certain recommendations to improve the wind power participation.

Overall, this project will present a preliminary analysis of the impact of high wind power penetration in the planning and operation of the Indian power system. A consolidated study of the impact of wind power with the Indian data is not available so far. The outcome of this project may be in terms of recommendations for the appropriate integration of the new wind generation foreseen for the Indian power system.

Over the past few years, several efforts have been made in the research and development for the study of grid connected Wind Energy Conversion Systems (WECS). As larger wind electric system are brought into service, it becomes increasingly important to predict their effect on the utility grid. This requires development of appropriate models for WECS. Work is being carried out on mainly two types of generators that are commonly used with commercial wind turbines. They are fixed-speed with directly grid coupled squirrel-cage induction generator (FSIG), and variable-speed based on a direct-drive synchronous generator (DDSG).

One of the problems with wind energy generation is the dependence of the injected power on the wind speed. The wind speed cannot be predicted, but the

probability of a particular wind speed occurring can be estimated. This can be done by assuming a Weibull or a Rayleigh probability distribution. Once the wind speed is known, the power injected into the grid can be calculated by means of the wind turbine power curve. Therefore, assessment of steady state performance of electrical networks with WECS is not as simple as with conventional generation and can be planned from a probabilistic point of view only. Several researchers in India and abroad have developed steady state models for various types of WECS and demonstrated the application of these models for both deterministic and probabilistic load flow analysis.

The fast growth of wind power in India has led to the concern about the impact of WECS on the dynamics of electric power systems. With the increase in wind power penetration into the utility grid, the power quality and the dynamic security of the power system might be affected because of the following reasons:

- i. The behavior of WECS may be different from conventional generation.
- ii. The wind turbines are connected in clusters in the form of wind farm mainly into the weak electrical grids and
- iii. The present connection requirements of wind farms do not have the capacity to handle such high penetration levels. Thus the dynamic analysis and the power quality issues of grid connected WECS becomes very important.
- iv. Various wind farms are identified, to measure the power quality events at the substation. Three power quality analyzer of Fluke 435, Dranetz PX5.8 and Hioki are connected at the individual wind turbine and group circuit breaker.

## **CHAPTER 2**

### **DATA COLLECTION AND ANALYSIS OF WIND FARM LOCATED AT PEEDAMPALLI SUBSTATION**

#### **2.1 Introduction**

The wind farm of fixed speed induction generator is identified at the Coimbatore district in Tamilnadu for measuring the power quality issues. Two power quality analyzer Fluke and Dranetz are connected at the individual wind turbines and at the Group control circuit breaker. The various power quality events such as sag, swell, impulsive transient, oscillatory transient and interruption are measured.

#### **2.2 Fixed Speed Induction Generator (FSIG)**

TEDA has selected peedampalli substation Coimbatore district for recording the power quality events with the help of power analyzers according to EN50160 standard. The substation consists of six fixed speed wind turbine units connected through 11kv line. The schematic diagram of peedampalli wind farms, its location and distances from the substation are shown in Figure 2.1.

The each wind turbine generates 600KW at 690V. The total capacity of this wind farm is 3.6MW. The fixed speed squirrel cage Induction generator directly connected to LV side of transformer rated at 800KVA, 690V/11KV. The HV side of the transformer is connected to 11KV common feeder. The 11KV peedampalli substation is connected to 110KV substation through transformer rated at 16MVA, 11KV/110KV

Two data loggers were installed at different location in wind farm substation to record the Voltage quality or disturbance according to EN50160 European standard. The Power quality Analyzer manufactured by Dranetz was installed at group control circuit breaker at 11KV substation. Another power quality analyzer manufactured by Fluke435 was installed at wind station, No: SE859 on the LV side of 690V/11KV transformer. The period of recording of the events in the system is from 24.07.2011 to 21.08.2011, (29 days).

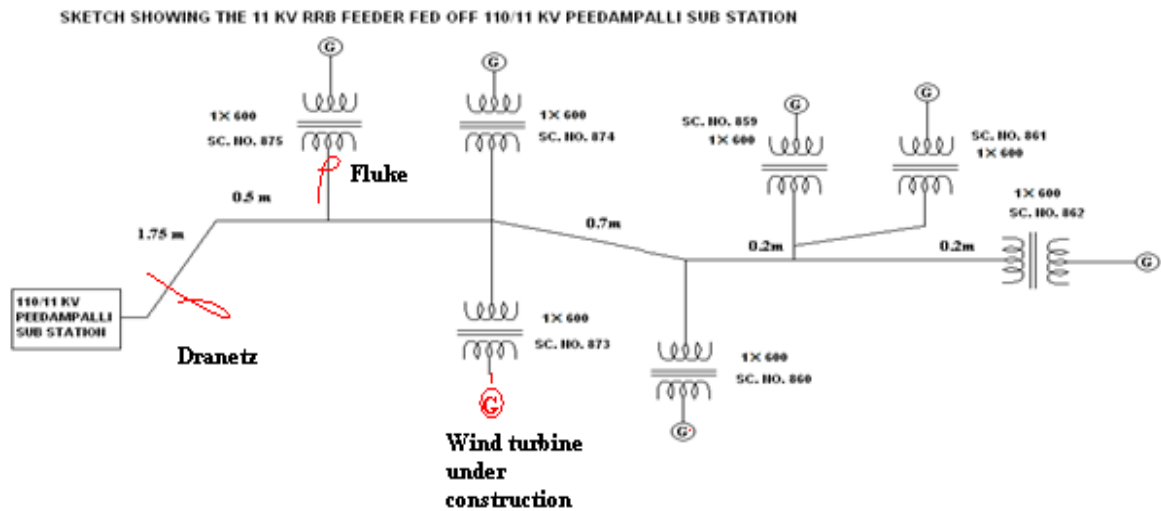


Figure 2.1: Layout of peedampalli substation

### 2.3 Power quality analyzer- Dranetz PX5.8

Dranetz power quality analyzer has been connected at wind farm feeder from 24.7.2011 to 21.8.2011, as the wind flow is at maximum during this period. About 140 events were recorded during this period and 75 events were found without any repetition and they are taken for further analysis. From the recorded data, 34 impulse transient events, only 1 oscillatory transient event, 26 sag events, 3 swell events and 2 interruption events were identified. The Figures 2.2 to 2.10 show a few recorded voltage quality events.

The recorded voltage quality event were

#### 1. Transient

- Impulse transient
- Oscillatory transient

#### 2. Sag

- Short duration instantaneous sag
- Short duration momentary sag
- Short duration temporary sag
- Long duration under voltage

#### 3. Swell

- Short duration instantaneous swell
- Short duration momentary swell

### 4. Interruption

- Short duration temporary interruption
- Long duration interruption

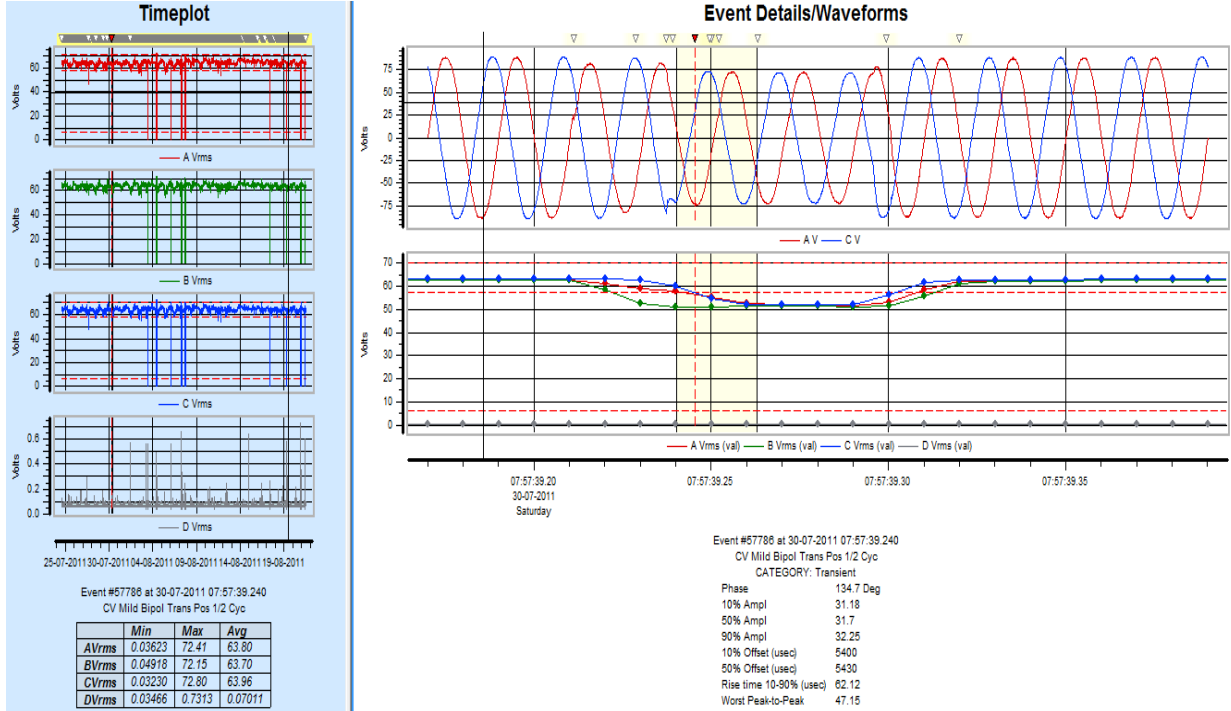


Figure 2.2: Transient event 57786 on 30-7-11

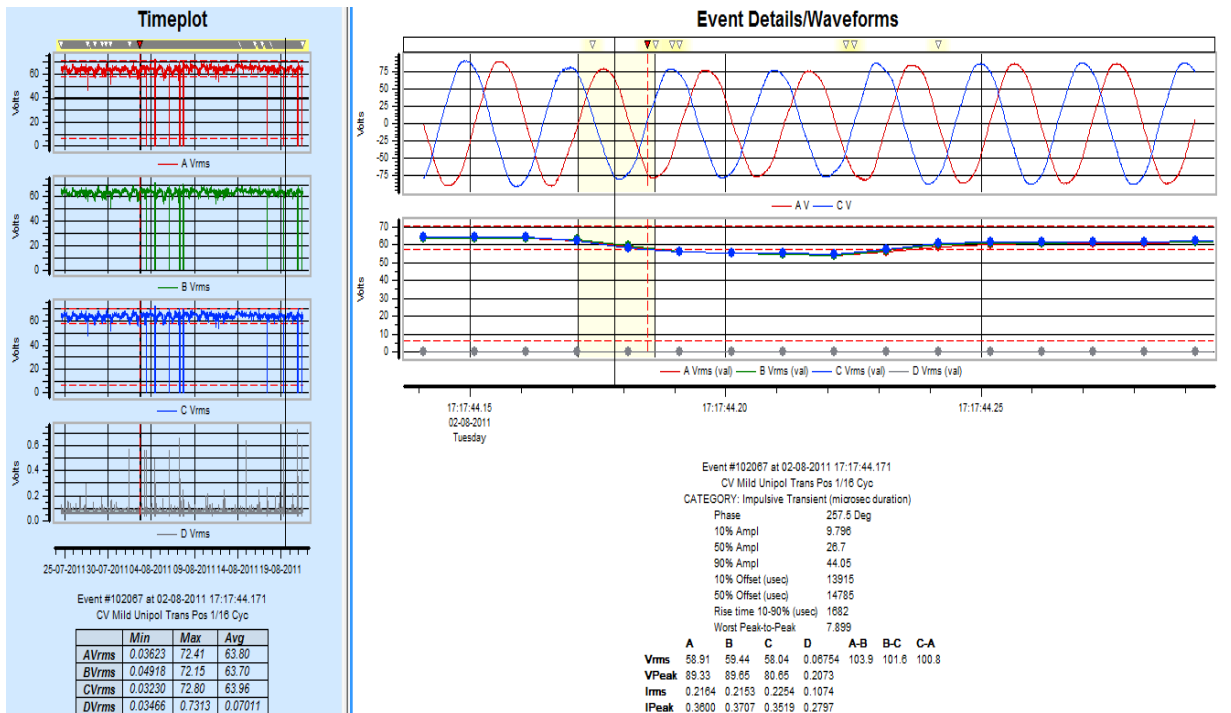
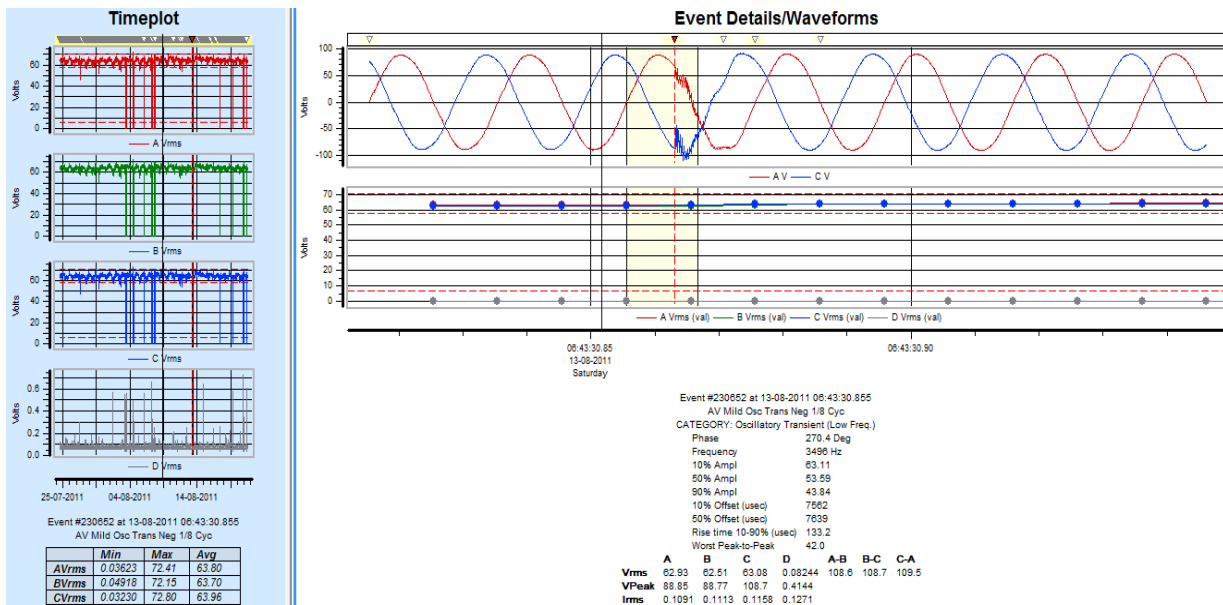
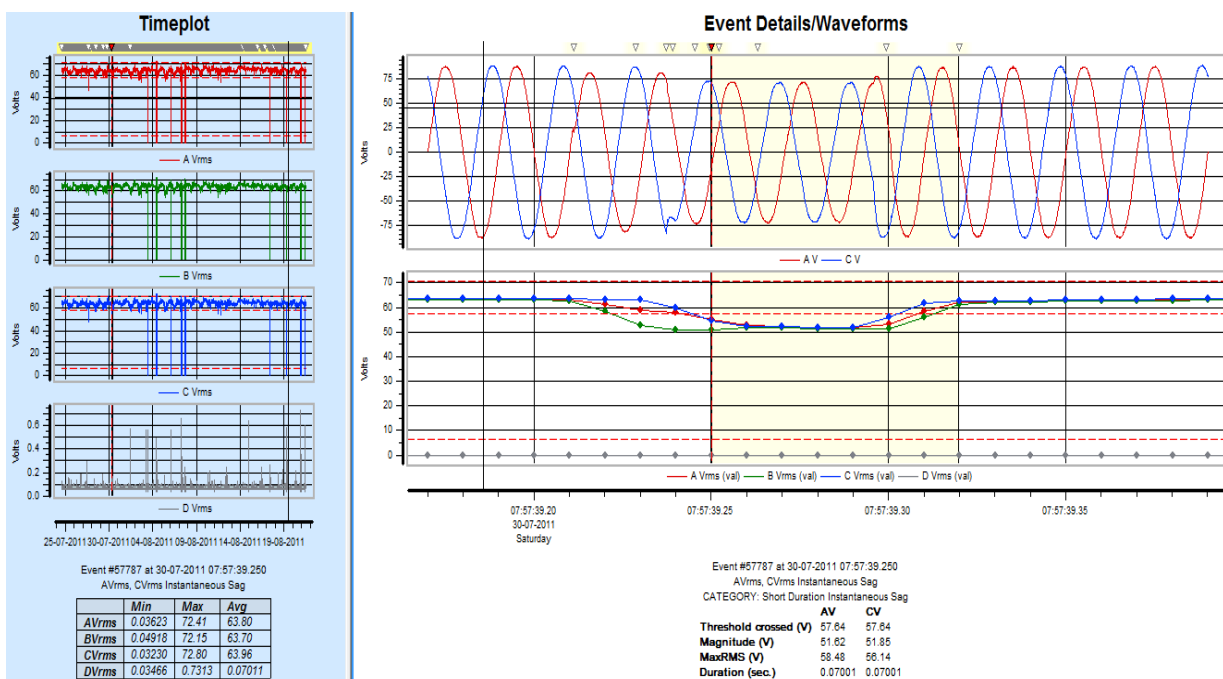


Figure 2.3: Impulsive transient event 102067 on 2-8-11



**Figure 2.4: Oscillatory transient 230652 on 13-8-11**



**Figure 2.5: Short duration instantaneous sag 57787 on 30-7-11**

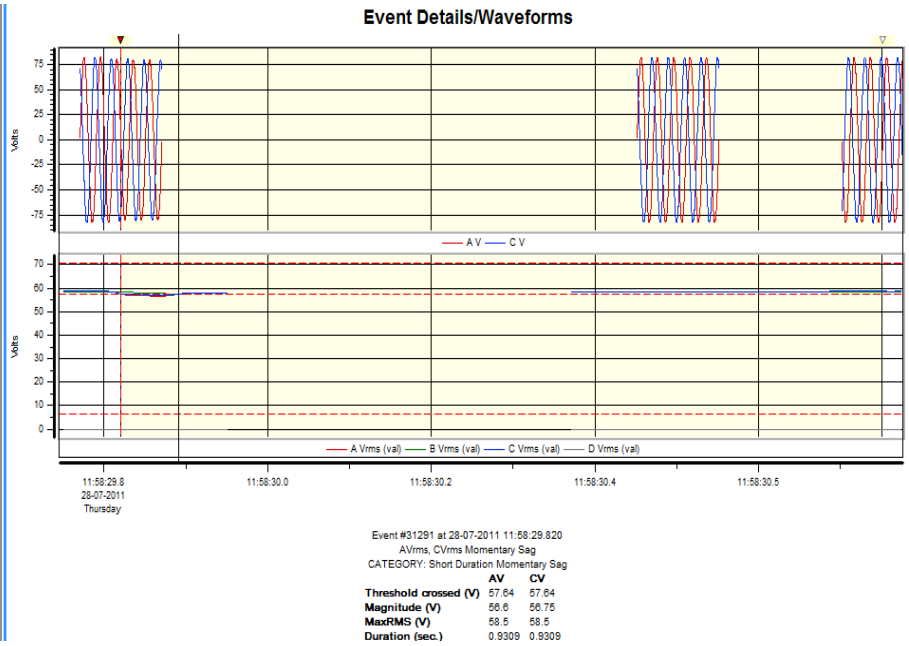
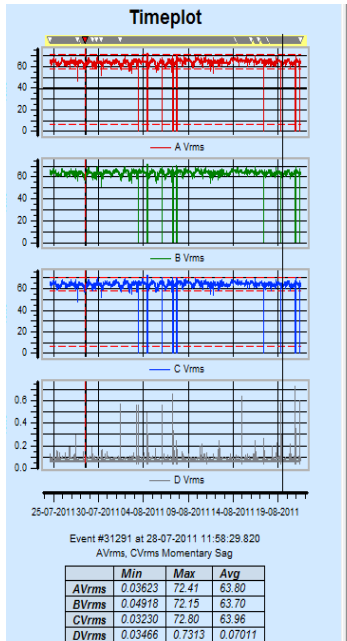


Figure 2.6: Short duration momentary sag 31291 on 28-7-11

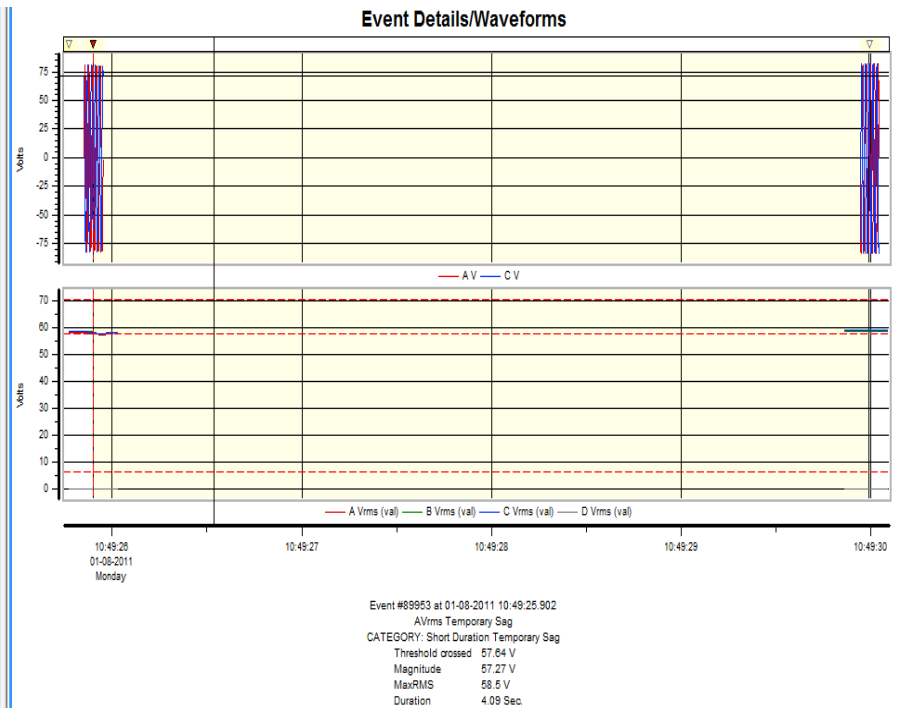
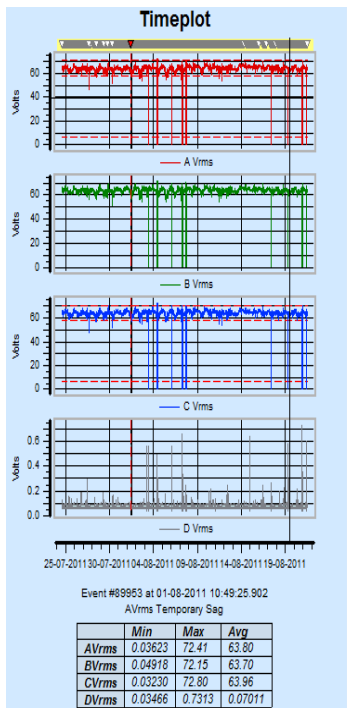
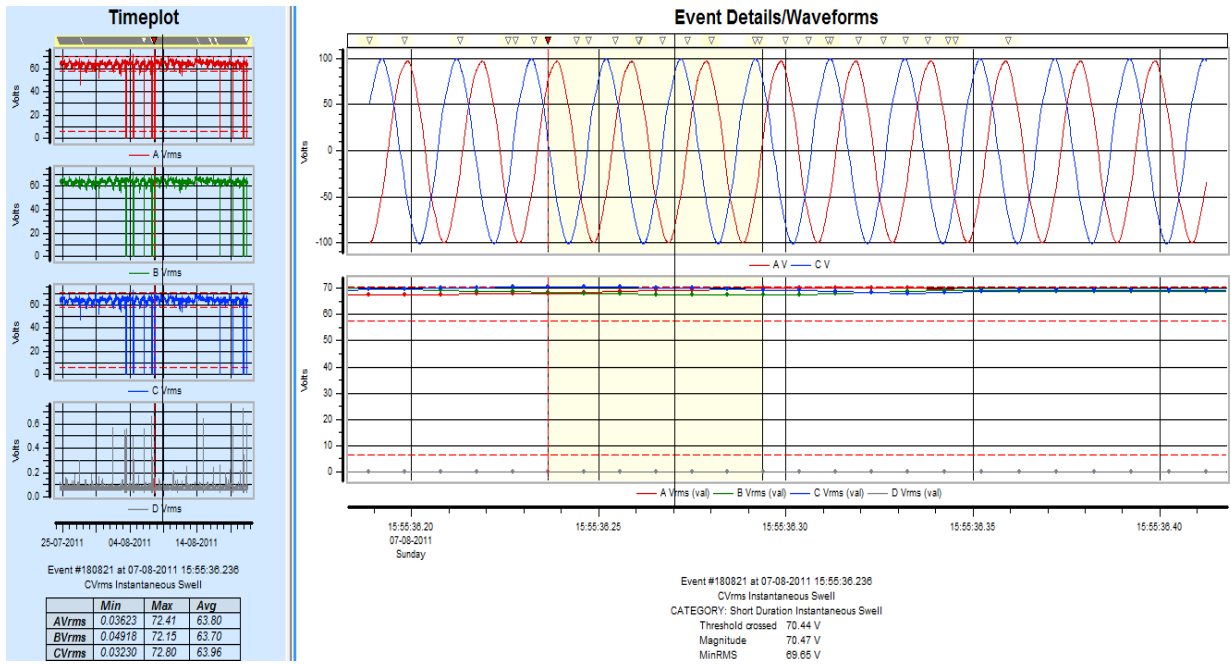
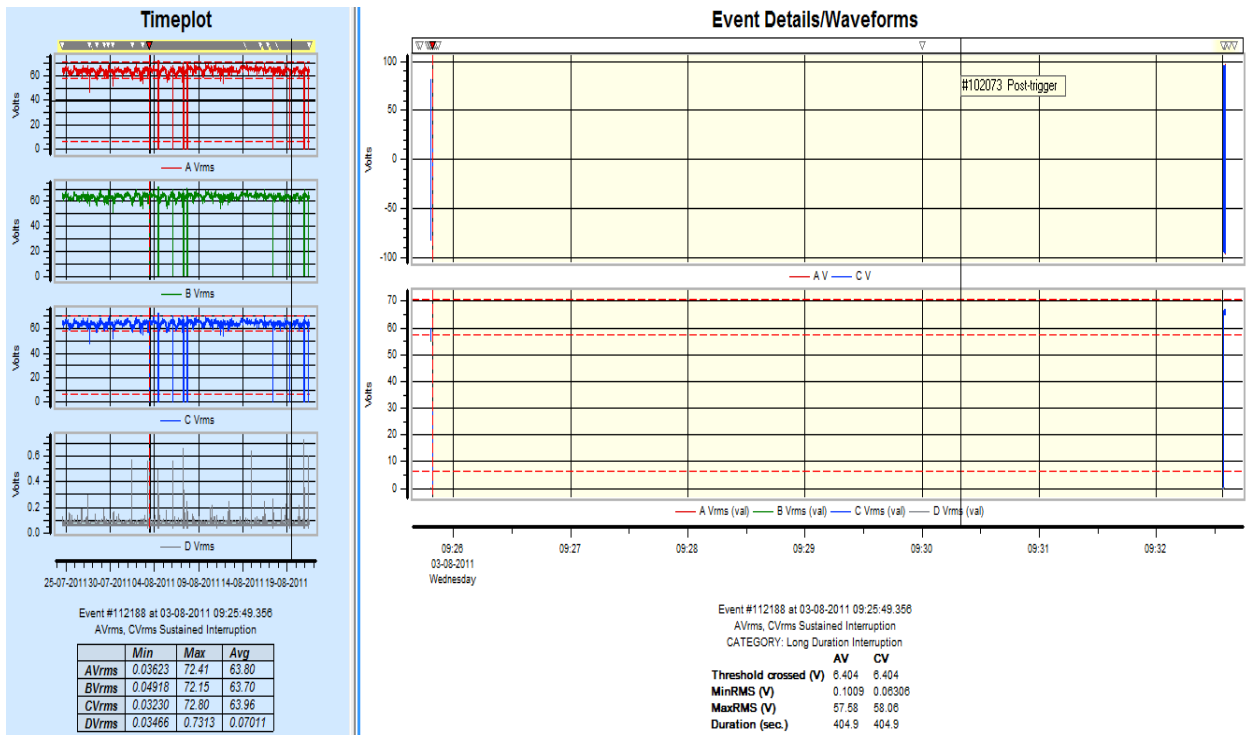


Figure 2.7: Short duration temporary sag event 89953 on 1-8-11



**Figure 2.8: Short duration instantaneous swell event 180821 on 7-8-11**



**Figure 2.9: Long duration interruption event 112188 on 3-8-11**

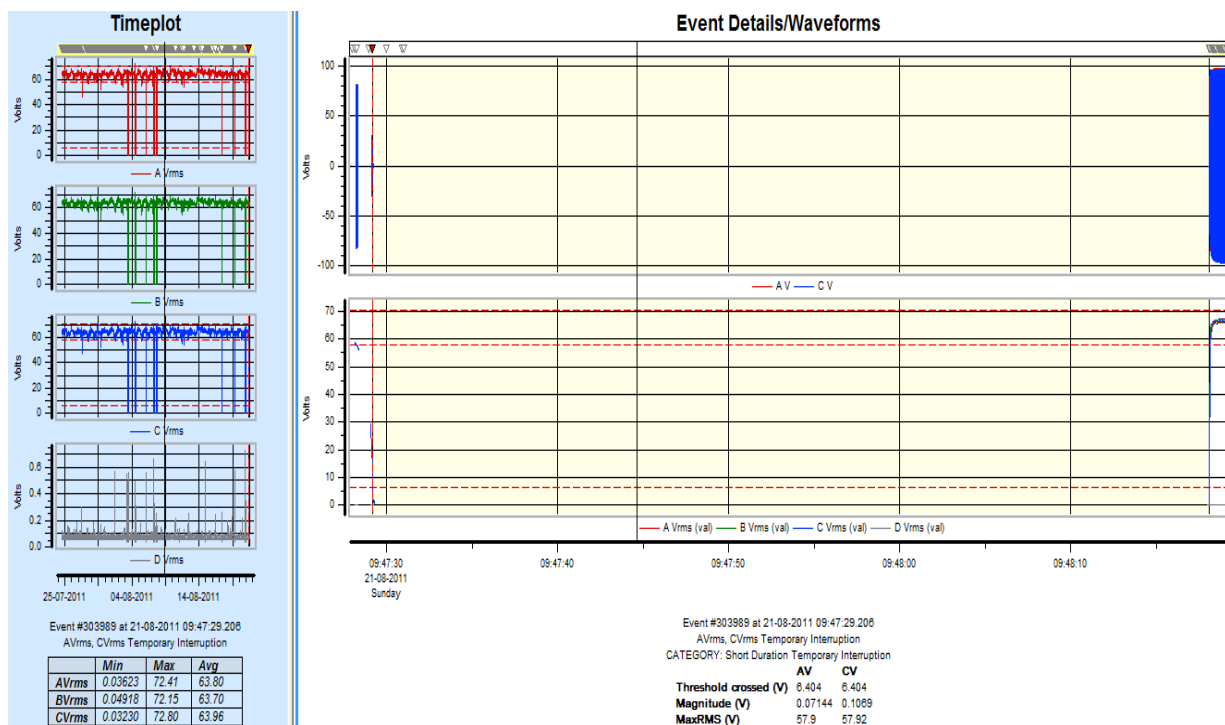


**Figure 2.10: Short duration temporary interruption event 303989 on 21-8-11**

### 2.3 Power quality analyzer- Fluke Serial No 435

The second power quality analyzer used was Fluke 435. This was connected to wind station, No: SE859 on the LV side of the transformer rated 80MVA, 690V/11KV. The Fluke 435 instrument recorded events only on 13 days out of 29 days, the remaining 16 days there were no issues to record in the system and the system was operating normally on these days. The recorded graphs are shown in Figure 2.11.

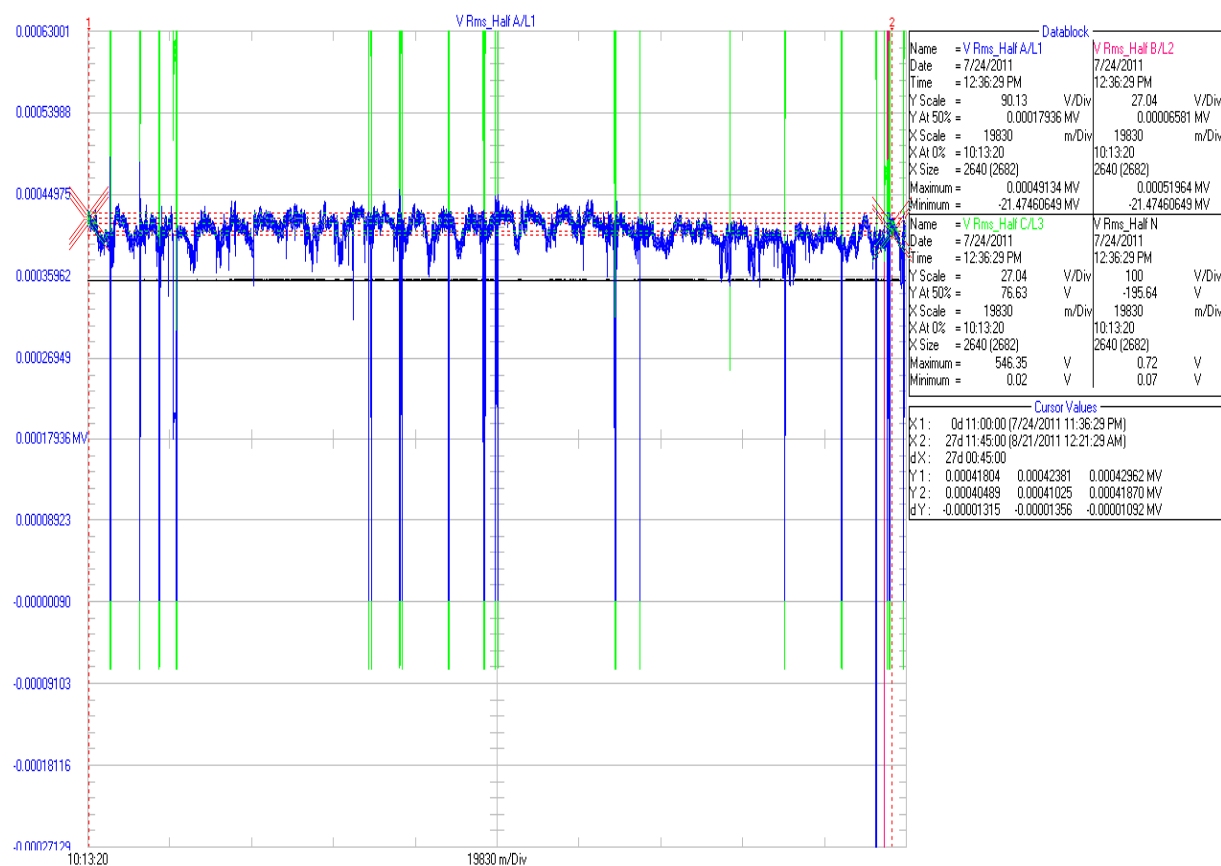


**Figure 2.11: Recorded graph for duration of 7/24/11 to 8/21/11**

## 2.4 Comparison of data collected from the power quality analyzers

The power quality analyzer installed at wind farm feeder records the same data recorded by the power quality analyzer installed at the wind farm feeder. There is a time lag of data 2 microseconds between the two readings. 26 events of fluke 435 match with the same 26 events of Dranetz analyzer. The Figures 2.12 and 2.13 shows the transient and short duration momentary sag events.

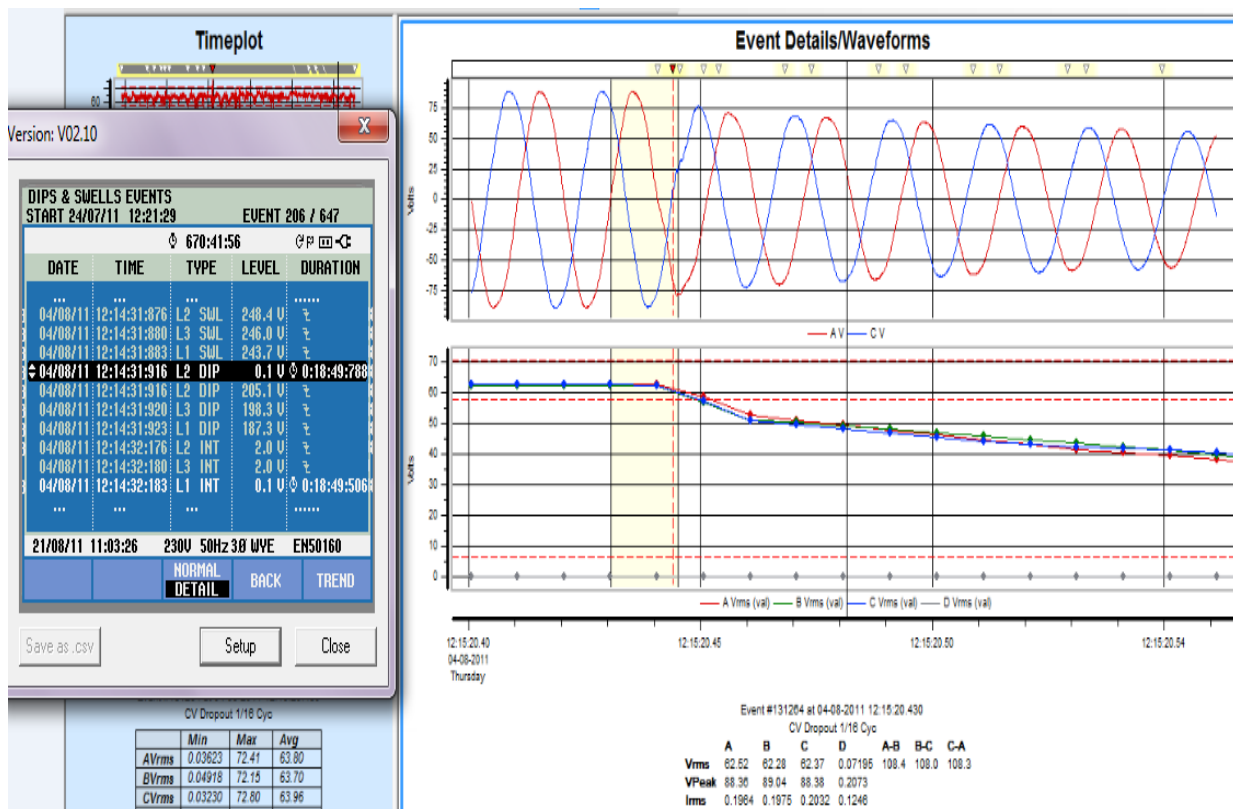


Figure 2.12: Impulsive transient event 131264 on 4-8-11

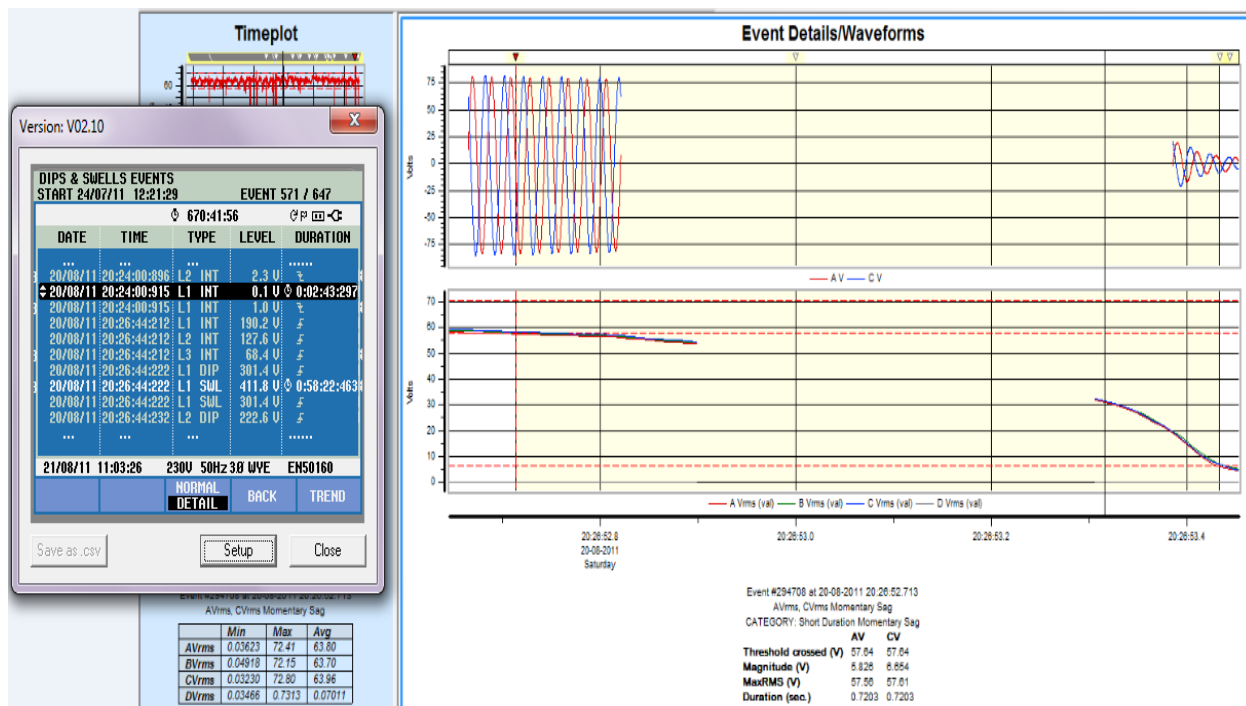


Figure 2.13: Short duration momentary sag event 294708 on 20-8-11

## 2.5 Conclusion

The power quality issues related to grid connected wind farm have been recorded and the possible causes are identified. Two power quality analyzers of different manufacturers are used at Peedampalli substation, Coimbatore district from 24.7.11 to 21.8.11(29 days). The Fluke 435 series analyzer installed at wind turbine on LV side of transformer and the Dranetz analyzer was installed at substation. Totally 78 mutually exclusive events such as Transient, Sag, Swell and Interruptions were recorded. 26 data recorded by the fluke 435 matches with 26 same data of Dranetz in spite of a microsecond delay. 34 Impulse transients of time duration of nanosecond to microsecond were recorded. 10% to 20% voltage spikes were due to Switching of capacitance, Switching of isolator and utility fault clearing. It is observed that system stability was maintained even with these disturbances. An oscillatory transient is a sudden change in the steady state condition of the voltage, current or both, at both the positive and negative signal limits, oscillating at the natural system frequency. Only 1 oscillatory transient has been identified. Totally 27 events of Sag were recorded. The main reason for sag was due to sudden increase in the load. It was seen from the recorded graph, voltage drop varied from 40% to 60% of the nominal value. Totally 3 events of Swell due to sudden removal of load and sudden change in wind speed were recorded. Voltage rise was about 10% of nominal value. There were 2 events of Interruption due to switching of wind turbine and sudden drop in wind speed for the period ranging from second to minute.

It is observed from the various events, 35 events were transient in nature and about 27 sag events, totaling to 78. Therefore, dynamic simulation of Peedampalli substation in DIgSILENT was necessary to study the sag and transient events

## CHAPTER 3

### SIMULATION OF THE PEEDAMPALLI SUBSTATION

#### 3.1 Introduction

The steady and dynamic state stabilities are analyzed for the grid connected Peedampalli wind farm located at Coimbatore district. The power quality analyzers Dranetz and Fluke were connected at this substation to record the various power quality issues. The general structure of fixed speed wind electric system is shown in Figure 3.1

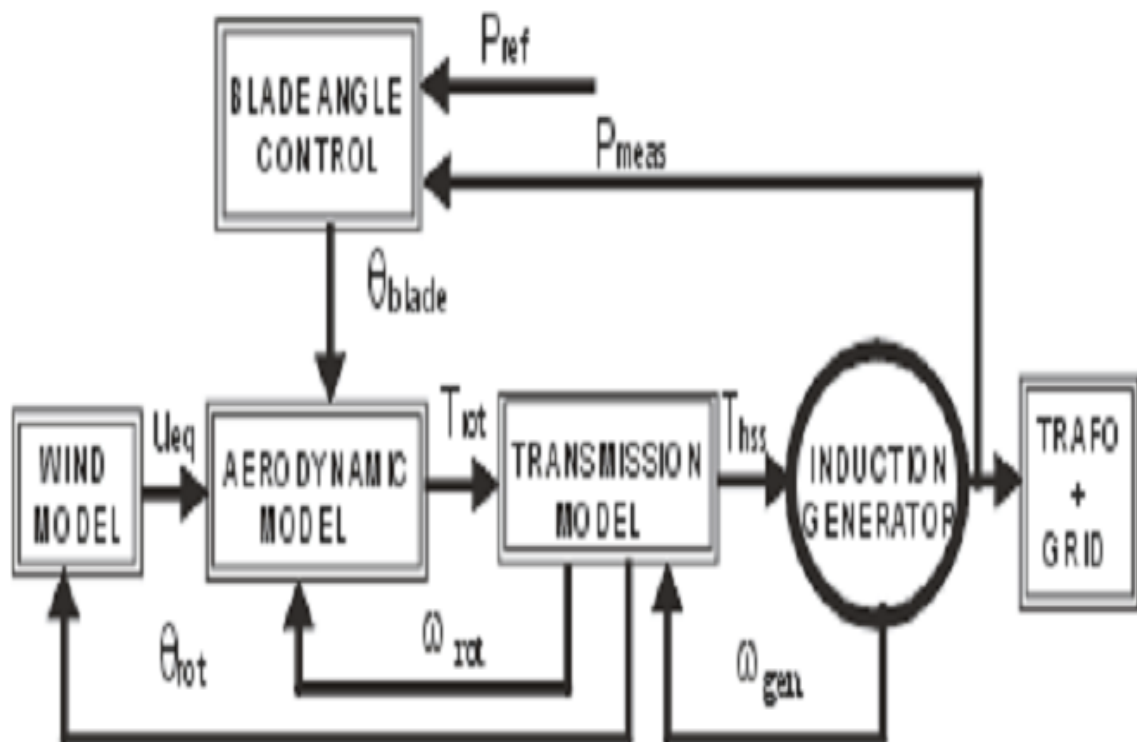


**Figure 3.1: General structure of fixed speed wind electric system**

#### 3.2 Simulation model

The important task is to model the wind farm accurately to predict the performance of wind electric system. DIGSILENT 14.6 power factory is more suitable for analyzing the grid connected wind farm. The models available in the

software provide the ability to simulate load flow, RMS fluctuations and transient events in the same environment. DIgSILENT provides a comprehensive library models for electrical components in the power system e.g. generators, motors, power plant controllers, dynamic loads and various passive network elements, such as lines, transformers, static loads and shunts. In the present study , we used the grid model with the electrical components of wind turbine and built in standard component models available in the DIgSILENT library. The models of the wind speed, aerodynamic model, shaft model, and pitch angle control model of the wind turbines are implemented in the Dynamic Simulation Language (DSL). Each individual model are built with individual block definition (blk). The mathematical equations of the individual model are written in the block definition in DSL form. The values of parameter variable are entered with help of common model. A Frame is a type of block definition which includes a number of slots for integrating the various blocks defined. All the individual blocks such as turbine blk, shaft model blk, pitch angle controller blk and built in model of Induction machine (ASM blk) are connected together through the slot with help of Frame definition. The Figure 3.2 shows the frame definition block. In order to connect the wind electric system to the grid, the composite model is used. In the composite model, a frame is selected for linking the individual slots to the variables of the common model. The Figure 3.3 shows the composite model of wind electric system. In this software, the simulation of EMT (Electromagnetic Transient), RMS (Electromechanical Transient), Fault, Optimal load, Reliability and Harmonic load flow including Flickering can be carried out.

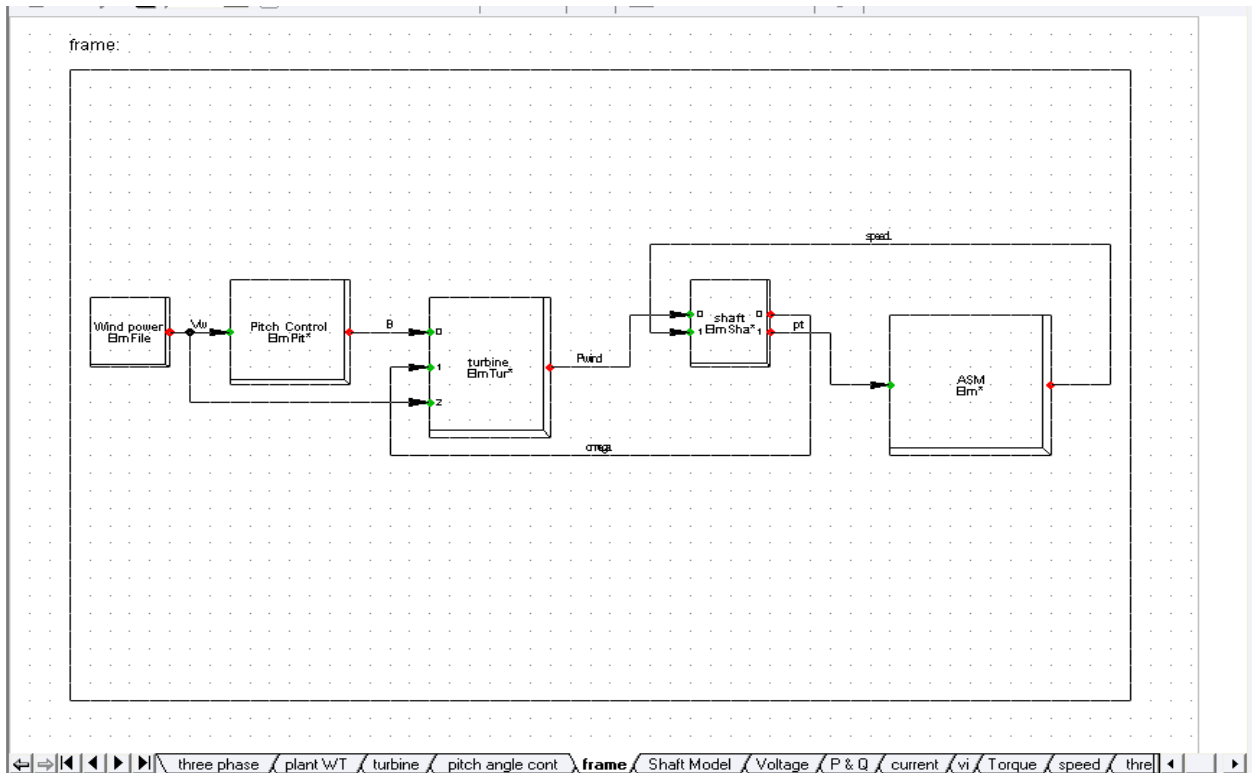


**Figure 3.2: Frame definitions to form slots to integrate all the blocks**

Composite Model - WindGen\Plant WT.ElmComp \*

Basic Data | Description

Name:

Frame:

Out of Service

Slot Definition:

	Slots BlkSlot	Net Elements Elm*,Sta*,IntRef
▶ 1	ASM	✓ GWT
2	Turbine	✓ Turbine
3	Pitch Control	✓ Pitch Control
4	Shaft	✓ Shaft

Slot Update      Step Response Test

**WindGen**

- + WindGen
- Plant WT
  - dsl Pitch Control
  - dsl Shaft
  - dsl Turbine

**Figure 3.3: Composite model of fixed speed wind electric system**

### 3.3 Layout of Peedampalli substation

The layout of the active stall controlled peedampalli wind farm is shown in Figure 3.4. It consists of six wind generator each with capacity 600kW at 690V is taken for the analysis. The total capacity of this wind farm is 3.6MW. The shaded part in the layout indicates the wind generator under erection work. Each wind turbine is connected to an 11 kV bus bar. The induction generators, soft-starters and the capacitor banks for reactive power compensation and step up transformer are placed at the foot of wind turbine. The control of active and reactive power is based on the measured reactive power at the point of common coupling. The wind turbine controller must be able to adjust the production of wind turbine, according to the demands imposed by the system operator. In case of normal operating conditions, the wind turbine has to produce maximum power. In power limited operation mode, the wind turbine has to limit its production to the rated power for wind speed greater than rated values.

The voltage generated by the squirrel cage generator is directly connected to LV side of a transformer rated at 800kVA, 690V/11kV. The HV side of the transformer is connected to 11kV common feeder using underground cable at voltage level of 11kV. The 11kV Peedampalli substation is connected to 110kV substation through a transformer rated at 16MVA. At this location, different wind farm are also connected to the substation as shown in Figure 3.5.

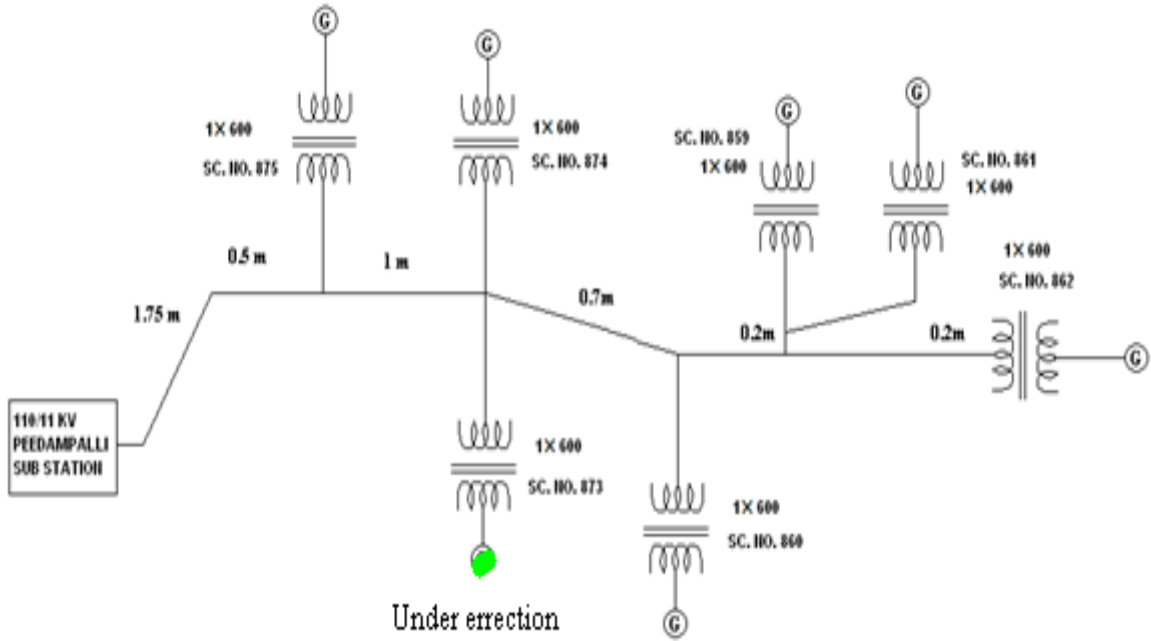


Figure 3.4 Layout of peedampalli substation

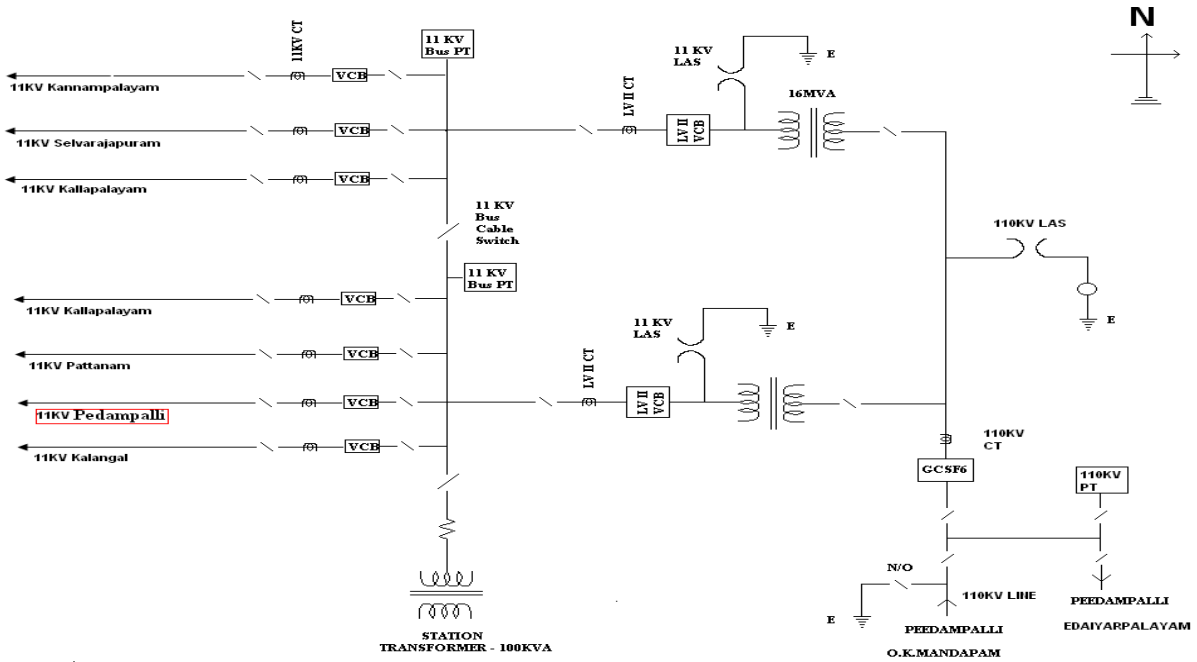
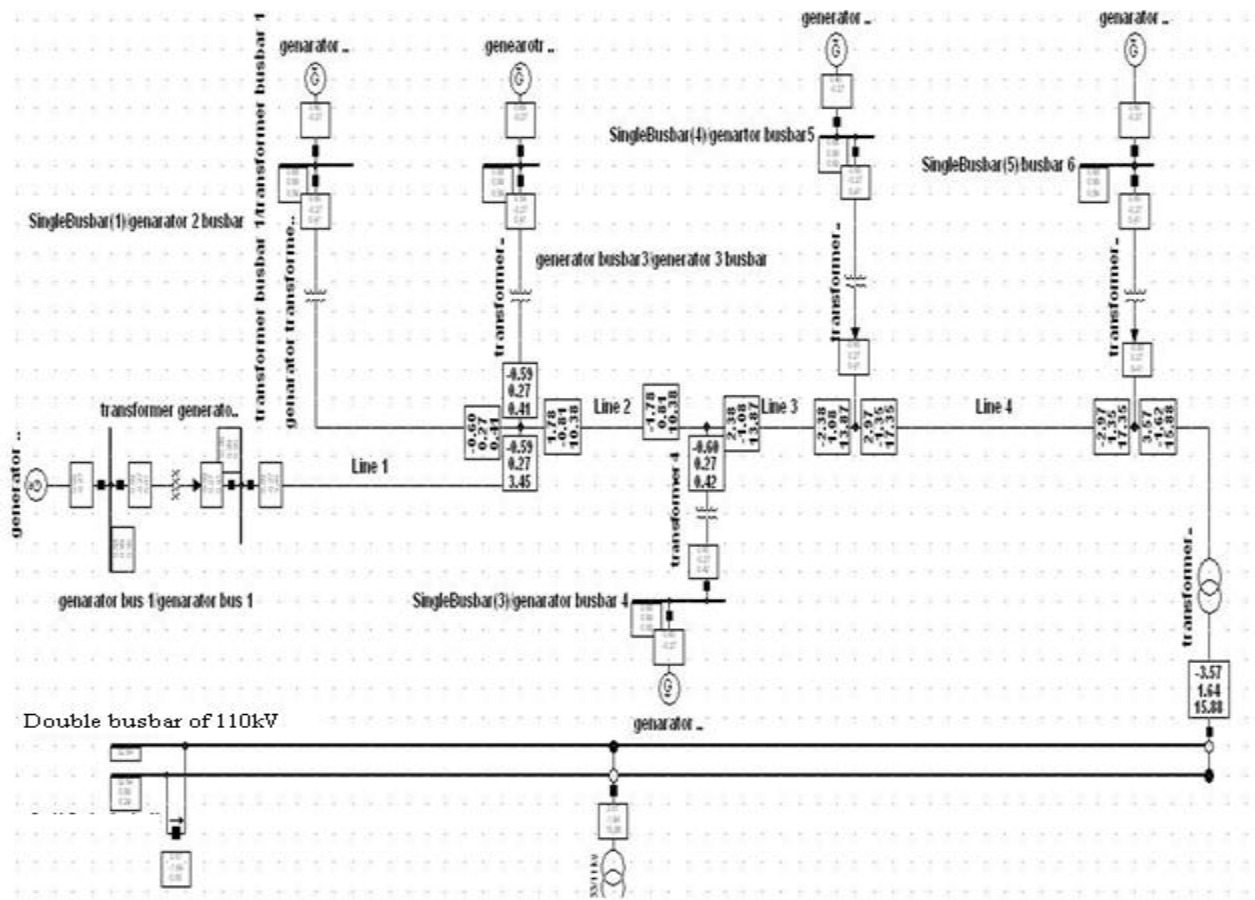


Figure 3.5 Sketch of 11kV /110kV Substation

### 3.4 Simulation model of the peedampalli substation

With help of power system component in DIgSILENT, the wind farm is built similar to the substation layout diagram. The Figure 3.6 shows the simulated load flow data of the peedampalli substation. Each generator generates 0.6MW real power; total power flow at the 110kV feeder is 3.6MW. The Figure 3.7 shows the load flow analysis of the entire grid connected wind farm and shows the Real and Reactive power flow in generators 4, 5 and 6. The Figure 3.8 shows the Real and Reactive power flow produced by the generators 1, 2 and 3.



**Figure 3.6 Simulation model of the Peedampalli substation in DIgSILENT**

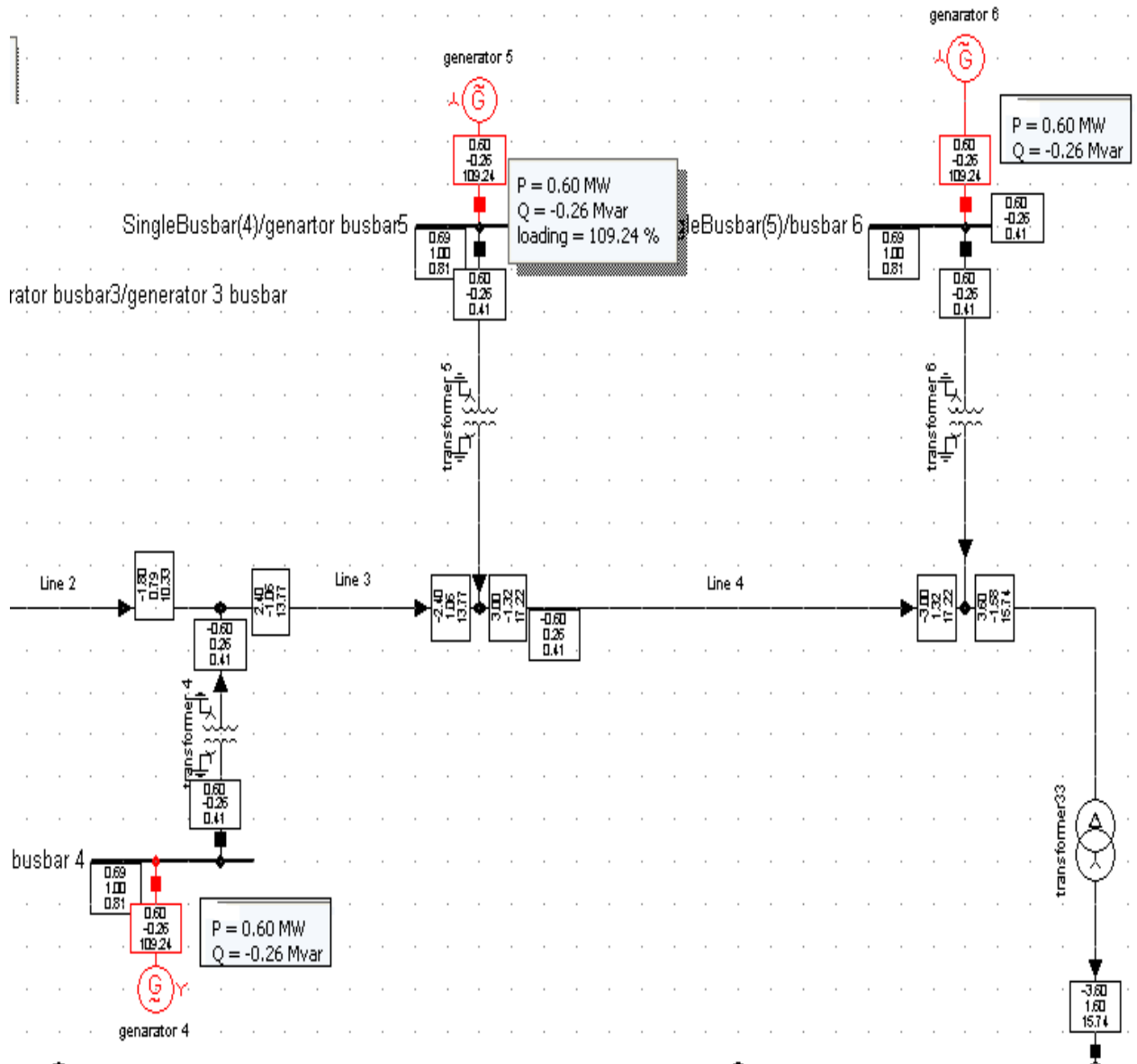


**Figure 3.7 Load flow diagram of peedampalli substation for generators 4, 5, and 6**

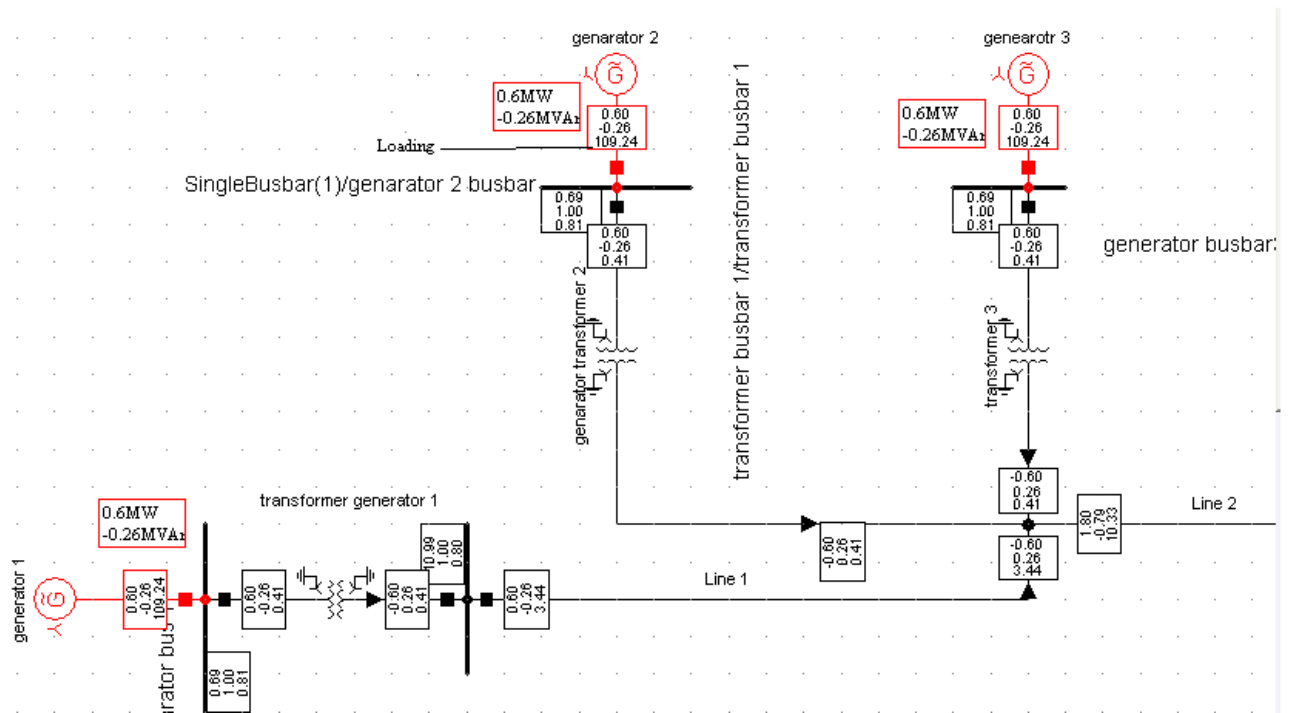


**Figure 3.8 Load flow data for generators 1, 2 and 3**

### 3.5 Steady state analysis of peedampalli wind farm

The steady state stability is analyzed for variation in Voltage and Wind speed as discussed in sec 3.3.

#### 3.5.1 Simulation result of wind farm for various bus bar voltages

Due to load variation and fault in the power system, the grid bus bar voltages may increase or decrease. The 110kV grid bus bar voltage is varied in steps. As the grid voltage is increased, the generated power remains constant and the current decreases. The generator absorbs more reactive power from the grid. The voltage of the various bus bars increase above the nominal value as shown in Table 3.1. If the grid voltage is decreased in steps the generated current increases and reactive power absorption from the grid decreases as shown in Table 3.2 at rated wind speed. The performance of generator G1 which is far away from the grid bus bar and G6 which is near to the grid bus bar are considered for comparison.

**Table 3.1 Grid Bus bar Voltage Increased from 110kV to 121 kV**

Si. No	Power system component	Rating	RMS simulation of steady state analysis
1.	Generator 1	0.6MW,0.69kV -0.33MVAR,0.546kA	0.60MW,0.71kV,-0.33MVAR, 0.5 kA
2.	Generator 6	0.6MW,0.69kV, -0.33MVAR, ,0.546kA	0.60MW,0.71kV, -0.33MVAR,0.50kA
3.	Feeder 11kV	11kV	12.1kV
4.	Feeder 110kV	110kV	121kV
5.	Grid Frequency	50Hz	50Hz

**Table 3.2 Grid Bus bar Voltage decreased from 110kV to 100 kV**

Si. No	Power system component	RMS simulation of steady state analysis
1.	Generator 1	0.60MW,0.63kV,-0.29MVAR,0.6kA
2.	Generator 6	0.60MW,0.63kV,-0.29MVAR,0.6kA
3.	Feeder 11kV	10kV
4.	Feeder 110kV	100kV
5.	Grid Frequency	50Hz

### 3.5.2 Frequency variations

Frequency variation in the power system depends upon the power demand. When the generated power and the load demand are equal, the value of frequency is 50Hz. Under the light load condition, the excess generated power is absorbed by the external grid. The frequency of the each bus bar remains constant as shown in Table 3.3. When the load is increased above the generated power, the

external grid supplies the power to compensate extra load. Therefore the bus bar frequency is remaining constant as shown in Table 3.4. In this software, there is a facility to increase or decrease the grid frequency. The grid frequency is increased to 51Hz from 50Hz. It is observed that the generator real power and current is increased but the generator bus bar voltage remain constant as shown in Table 3.5. As the grid frequency decreased, it is observed that generator real power and current is decreased but voltage remain constant as shown in Table 3.5a.

**Table 3.3 Frequency variation at each bus bar with light load**

Si.No	Element Name	Frequency Value
1	Generator Bus 1	50
2	Generator Bus 2	50
3	Generator Bus 3	50
4	Generator Bus 4	50
5	Generator Bus 5	50
6	Generator Bus 6	50
7	Feeder 11 kV	50
8	Feeder 110 kV	50

**Table 3.4 Frequency variation at each bus bar when the load is more than generation**

Si.no	Element Name	Frequency Value
1	Generator Bus 1	50
2	Generator Bus 2	50
3	Generator Bus 3	50
4	Generator Bus 4	50
5	Generator Bus 5	50

6	Generator Bus 6	50
7	Feeder 11kV	50
8	Feeder 110kV	50

**Table 3.5 Increase in grid frequency from 50Hz to 51Hz**

Si. No	Power system component	RMS simulation of steady state analysis
1.	Generator 1	0.66MW,0.69kV,-0.33MVAR,0.6kA,51Hz
2.	Generator 6	0.66MW,0.69kV,-0.33MVAR,0.6kA,51Hz
3.	Feeder 11kV	11kV
4.	Feeder 110kV	110kV
5.	Grid Frequency	51Hz

**Table 3.5a Decrease in grid frequency from 50Hz to 49Hz**

Si. No	Power system component	RMS simulation of steady state analysis
1.	Generator 1	0.58MW,0.69kV,-0.30MVAR,0.52kA,49Hz
2.	Generator 6	0.58MW,0.69kV,-0.30MVAR,0.52kA,49Hz
3.	Feeder 11kV	11kV
4.	Feeder 110kV	110kV
5.	Grid Frequency	49Hz

### 3.5.3 Simulation of wind electric system for various wind speeds

If the wind velocity decreases below its rated value (12m/s), the generated power also decreases. The fixed speed wind generator is also known as constant voltage source, generates constant voltage from rated wind velocity 12m/s to cut in speed 3.5m/s as shown in Tables from 3.6 to 3.7. As the wind velocity is reduced gradually, the generated power and current reduce accordingly. The speed and real power variations depend upon the speed of the wind. When the wind velocity

comes nearer to the cut in speed of 3.5m/s, the induction generator behaves like an induction motor and starts absorbing the reactive and real power from the grid as shown in the Table 3.8 (negative sign in real and reactive powers indicate its absorbs the power ).

**Table 3.6 Wind velocity (V=12m/s)**

Si. No	Power system Component	RMS simulation of steady state analysis
1	Generator 1	0.6MW,-0.3MVAR, 0.526kA
2.	Generator 6	0.6MW,-0.3MVAR, 0.526kA
3.	Feeder 11kV	11kV
4.	Feeder 110kV	110kV

**Table 3.7 Wind velocity (V=8m/s)**

Si. No	Power System Component	RMS simulation of steady state analysis
1	Generator 1	0.35MW,-0.15MVAR, 0.21kA
2.	Generator 6	0.35MW,-0.15MVAR, 0.21kA
3.	Feeder 11kV	11kV
4.	Feeder 110kV	110kV

**Table 3.8 Wind velocity (V=3m/s) Motor action**

Si. No	Power System Component	RMS simulation of steady state analysis
1	Generator 1	-0.15MW,-0.1MVAR, 0.12kA
2.	Generator 6	-0.15MW,-0.1MVAR, 0.12kA
3.	Feeder 11kV	11kV
4.	Feeder 110kV	110kV

### 3.6 Dynamic analysis of grid connected wind farm

In the dynamic analysis, the wind speed is assumed to vary from cut in speed to cut out speed (3.5m/s to 20m/s) as shown Figure 3.9. As the wind turbines are a few Km apart, the wind speed at individual wind turbines are assumed to have different values in the simulation. The wind generator 1 which is a few km away from grid bus bar and the generator 6 which is nearer to the grid bus bar are taken for the analysis. Various scenarios such as Transient stability analysis, three phase fault, and sudden increase of load, load flow harmonics and flickering are simulated. The electromechanical transient (RMS) simulation is executed for 600 seconds and the various data such as real power, reactive power, current, electrical and mechanical torques are recorded.

The pitch controlled wind turbine used in this model. When the speed of the wind is varying, the power generated is equal to or less than that of the rated value as shown in Figure 3.10. When the speed is below the rated value, the pitch control mechanism is deactivated. The induction generator absorbs the reactive power from the grid or from the capacitor banks.

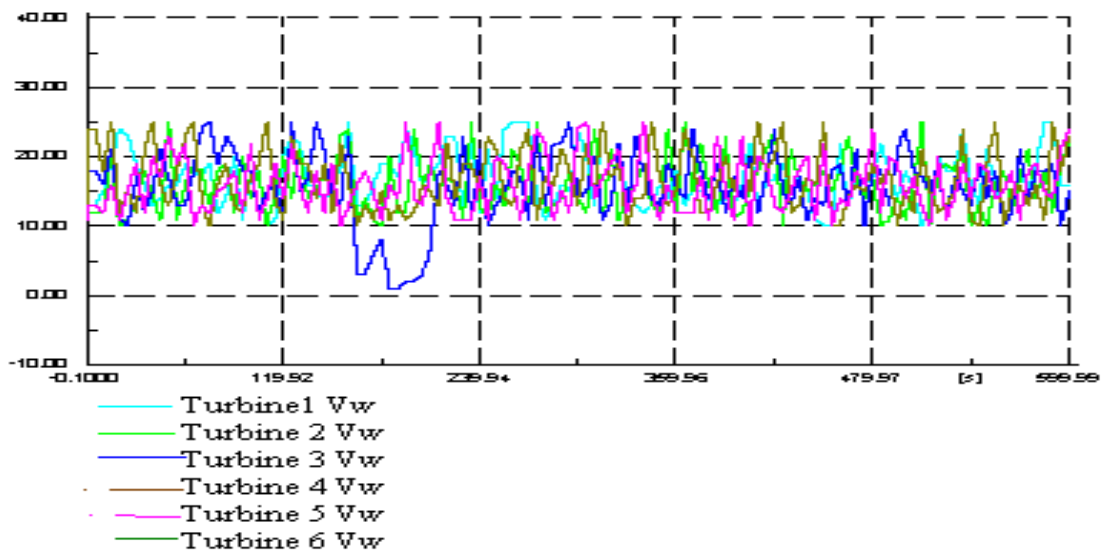


**Figure 3.9 Variations of wind speed for different wind turbines**

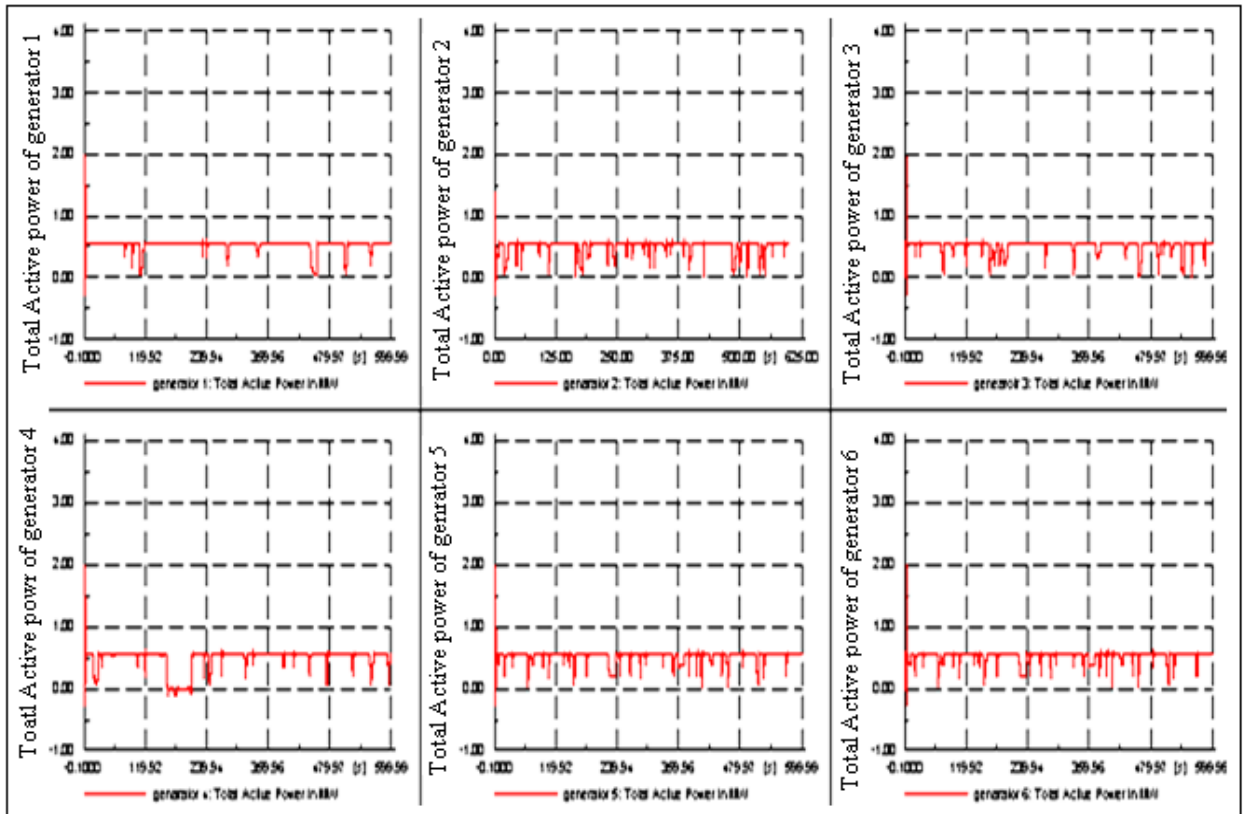


**Figure 3.10 Active power generation of different generator**

### 3.6.1 Short circuit analysis

The three-phase symmetrical fault is applied at 11kV bus bar  $t=5$  secs for the duration of 500ms in the simulation time of 20 seconds. The voltage at 11kV bus bar drops to zero and other bus bar voltages are decreased drastically. The Figures 3.11 and 3.12 show the active power and the voltage dip in the generators 1 and 6. The Figure 3.13 shows that the generator current increases by 2 to 5 times of the rated current. Depending on the severity of the fault and location of the fault, the generator current may increase to a high value. The difference between the mechanical input and electrical output power causes acceleration in the rotor and therefore, the rotor speed increases as shown in Figure 3.14

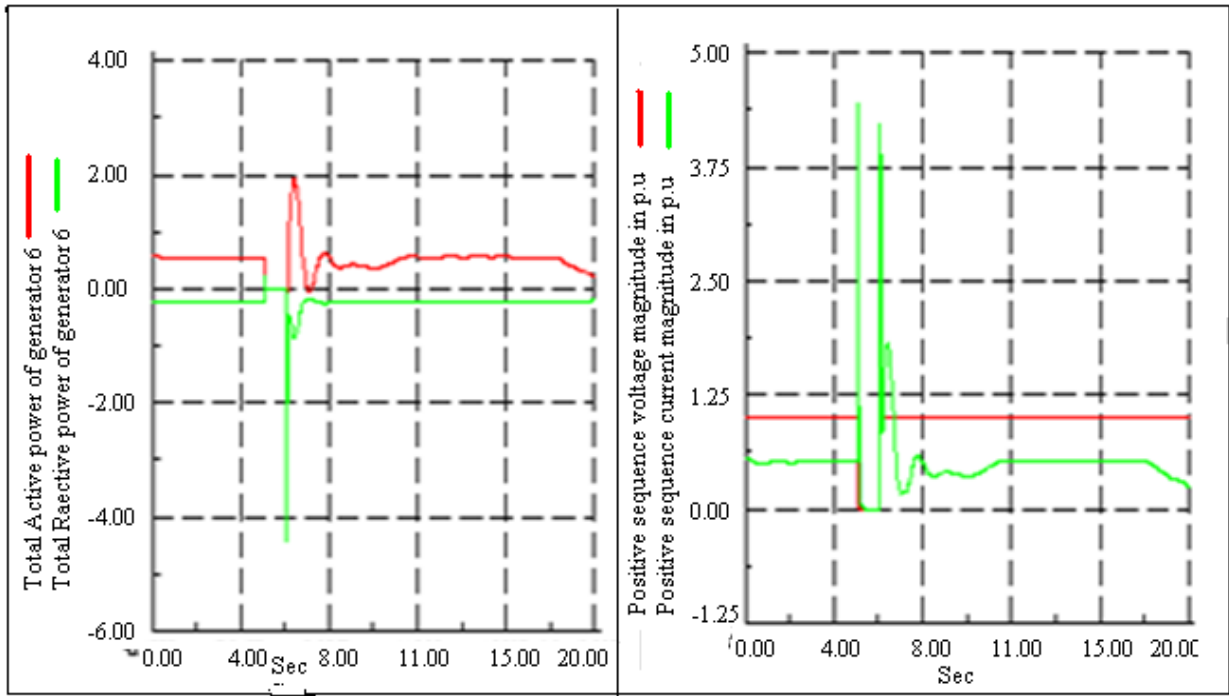


**Figure 3.11: Variation of active power, reactive power, voltage and current at generator 6 during the short circuit**

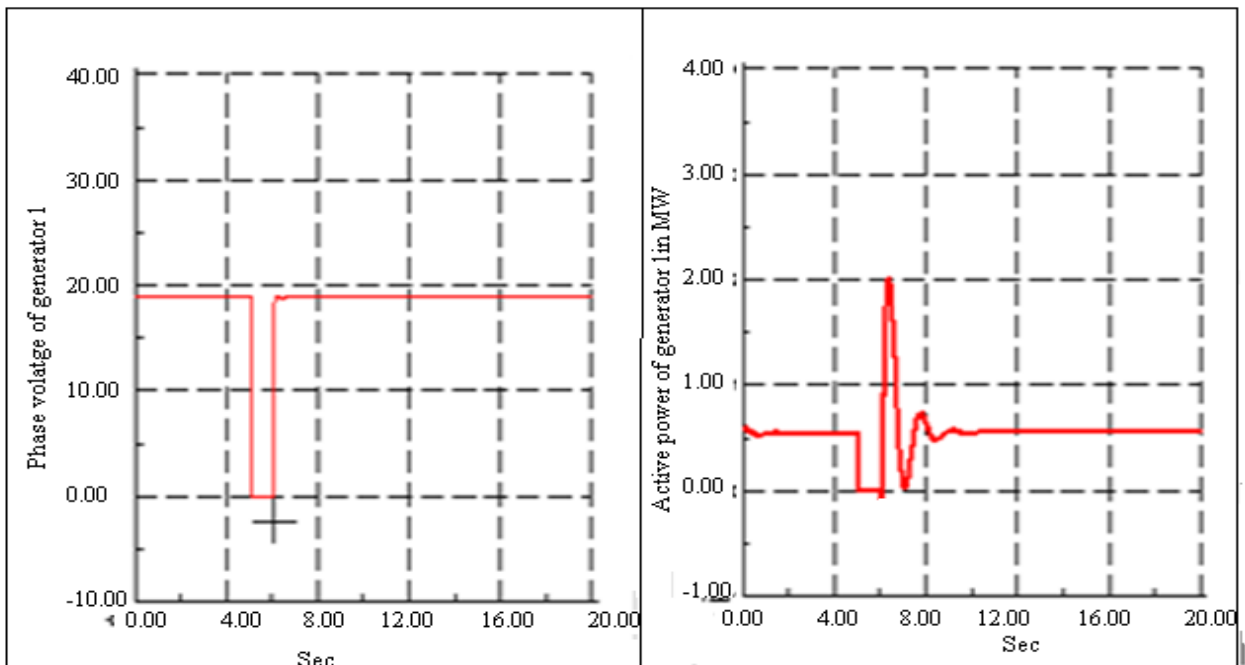


**Figure 3.12: Voltage dip at generator bus bar and the active power of generator 1 during the short circuit**

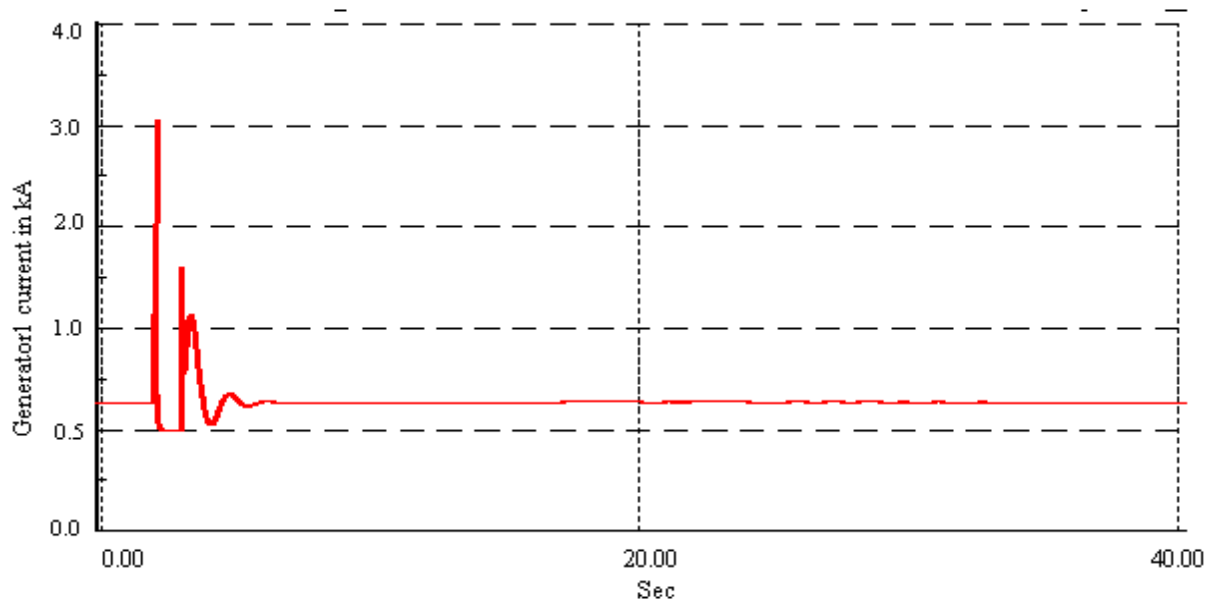


**Figure 3.13: Variation in generator 1 current during the short circuit**

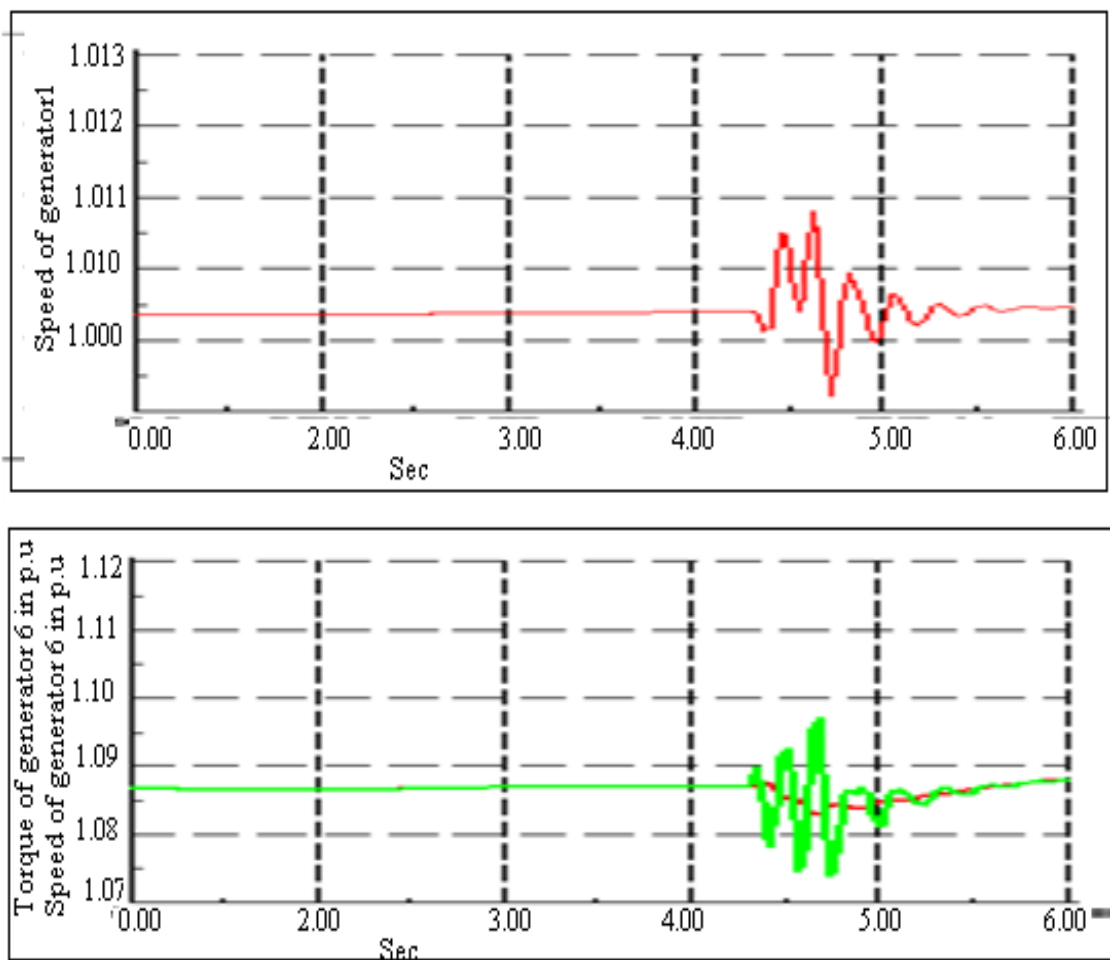


**Figure 3.14: Speed and torque oscillation during the short circuit interval**

### 3.6.2 Load variation

At the 11kV bus bar, an industrial load of 3.6MW is suddenly switch on at  $t=300$ secs for a short span of time. During this interval, there is a sudden dip in the voltage level at 11kV feeder and generator buses as shown in Figures 3.15 and 3.16.

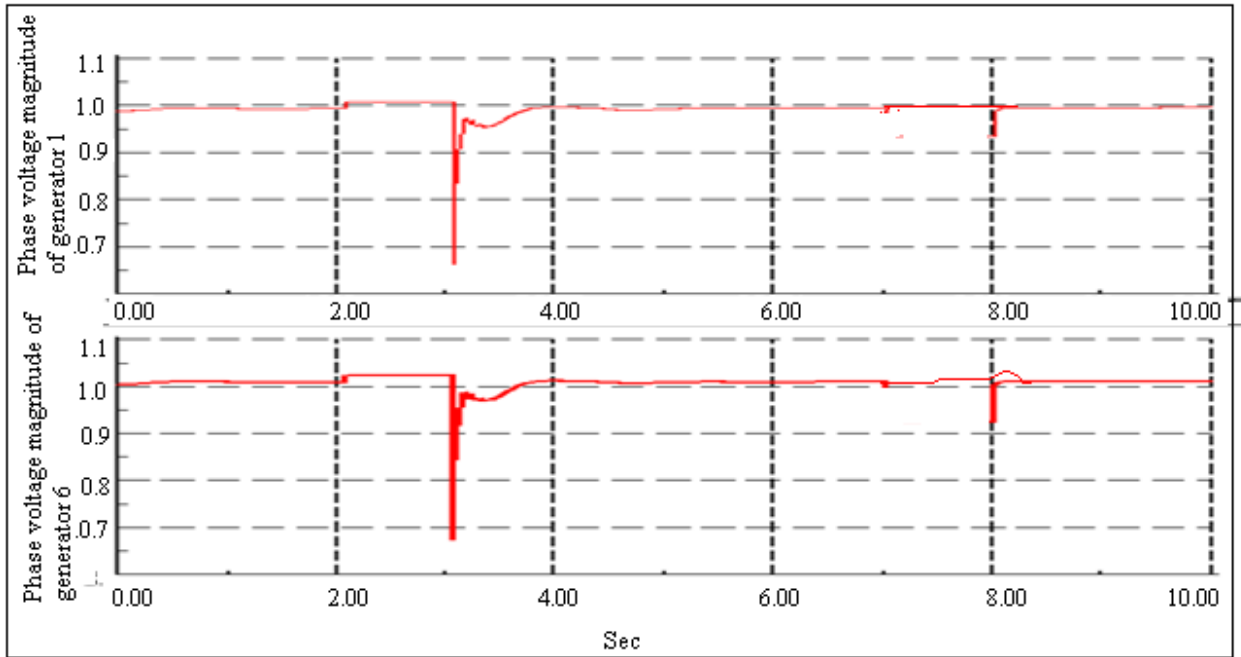


**Figure 3.15: Voltage sag at the bus bars during sudden increase in the load**

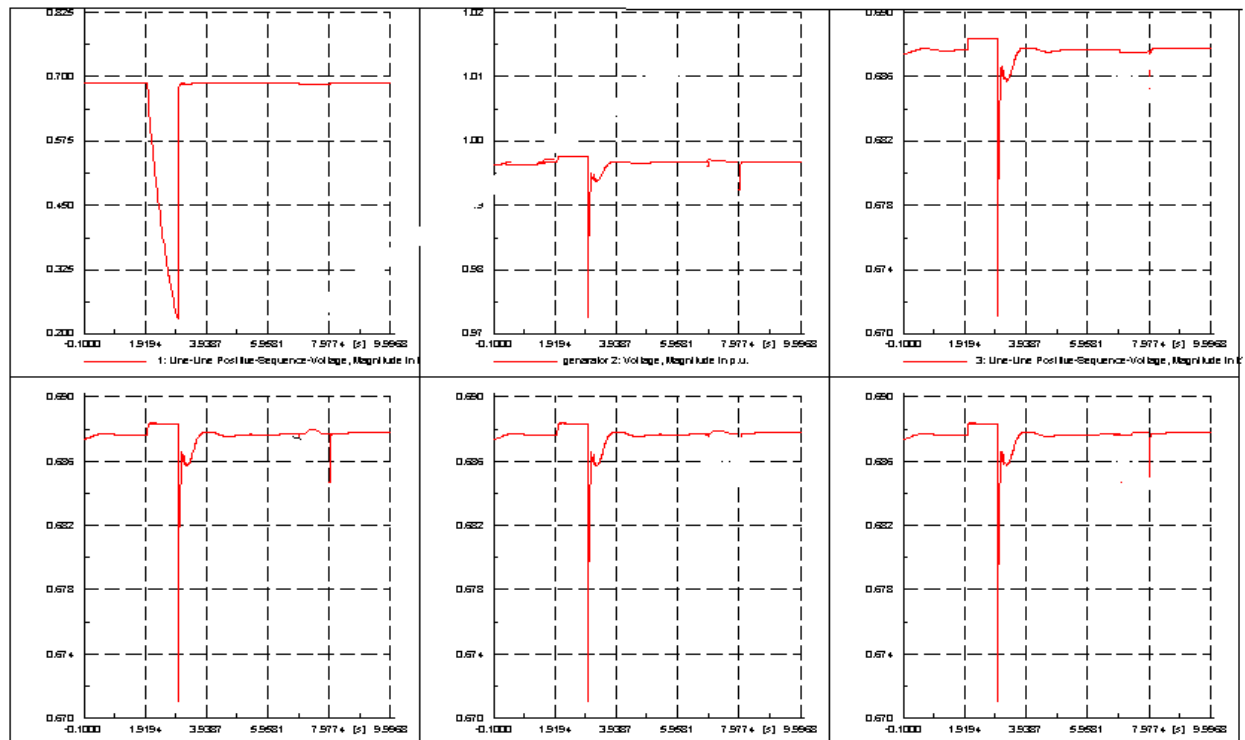


**Figure 3.16: Line voltages of Generator bus bars during sudden increase in load**

### 3.6.3 Flickering

The IEC 61000-4-15 standard specifies the function and design of apparatus for the measurement of flicker, termed the "Flicker meter". The Power Factory provides a Flicker meter command for the calculation of the short-term and long-term flicker according to IEC 61000-4-15.

The continuous and switching operations give different types of flickering. With the help of harmonic load flow in the DIgSILENT software the long term and the short term flickering due to continuous and switching operations can be calculated with the constant wind speed of 12m/s and with SCC equal to 15MVA for various grid impedance angles (30°, 50°, 70°, 85). The Table 3.9 shows the flickering data at the various generator bus bar for 30° impedance value at wind speed  $V_w=12\text{m/s}$  and  $\text{SSC}=15\text{MVA}$ . The value of  $P_{st}$ , and  $P_{lt}$  for continuous and switching operations for 30° are plotted and shown in Figures 3.17.

**Table 3.9 Flickering data at the bus bar for 30° impedance value for  
Vw=12m/s and SSC=15MVA**

Si. No	Element	Short-Term Flicker Disturbance Factor Continuous Operation	Long-Term Flicker Disturbance Factor Continuous Operation	Short-Term Flicker Disturbance Factor Switching Operation	Short-Term Flicker Disturbance Factor Switching Operation
1.	Generator 1 bus bar	0.085264	0.085264	0.223803	0.214897
2.	Generator 2 bus bar	0.085264	0.085264	0.223803	0.214896
3.	Generator 3 bus bar	0.085264	0.085264	0.223803	0.214896
4.	Generator 4 bus bar	0.085264	0.085264	0.223803	0.214896
5.	Generator 5 bus bar	0.085263	0.085264	0.223802	0.214896
6.	Generator 6 busbar	0.08526	0.085263	0.223799	0.214893
7.	Transformer busbar 1	0.084779	0.08526	0.223793	0.214887
8.	Feeder 11kV	0.066404	0.084779	0.222508	0.213653
9.	Feeder 110 kV	0.047914	0.066404	0.174282	0.167346

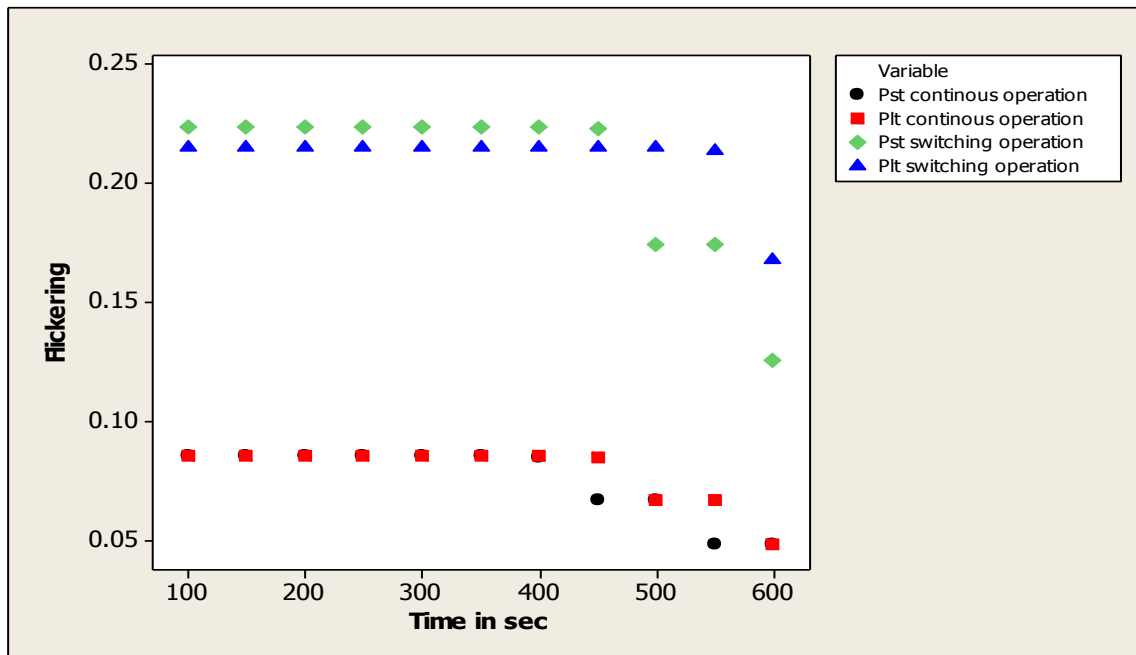


**Figure 3.17: Plot of  $P_{st}$ , and  $P_{It}$  for continuous and switching operations for  $30^\circ$**

The RMS simulation is executed for minimum of 600sec. The values of  $P_{st}$  and  $P_{It}$  measured with help flicker meter are 0.084563 and 0.225468 respectively.

### 3.6.4 Harmonic load flow

With help of harmonic load flow, the harmonic level can be calculated in a grid connected wind farm. The fixed speed wind farm did not inject any harmonic into the grid. In this software, harmonic any order can be manually entered into the load or with help of rectifier circuit. The diode rectifier circuit is connected at the generator bus bar. The injected harmonic by the rectifier circuit is estimated at the grid. The measured harmonics at the grid are depicted as shown on Figure 3.18.

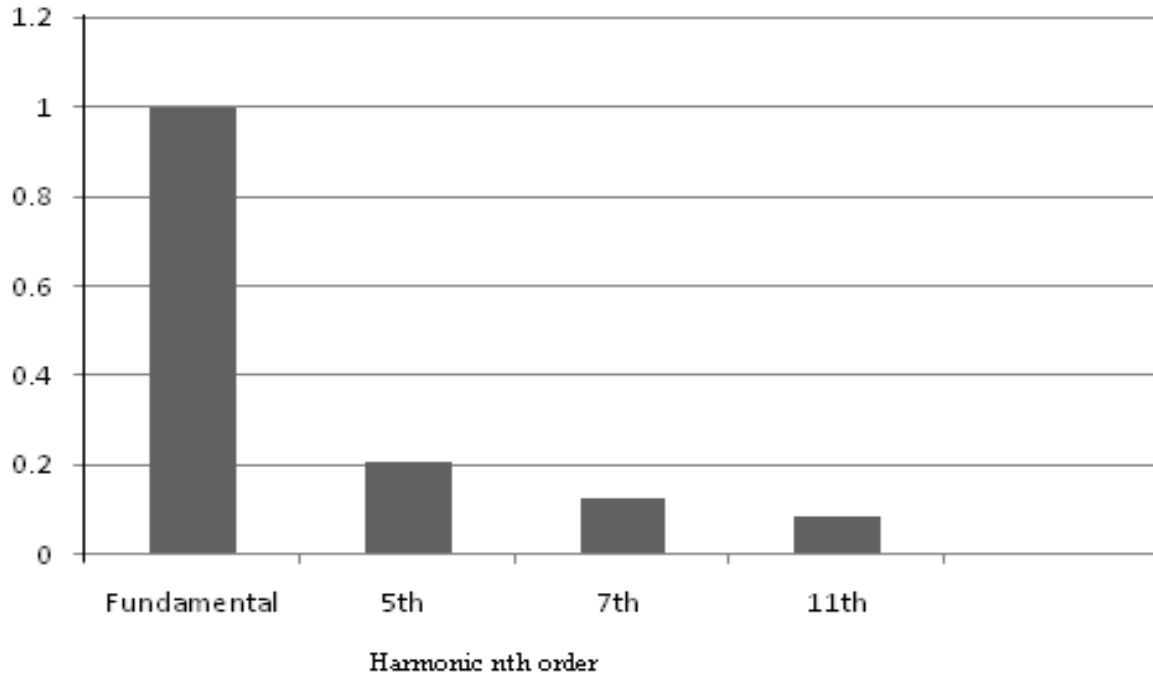


**Figure 3.18 Harmonics measured at the grid**

### **3.7 Comparison between results of measurement and simulation**

The comparison between the results of the simulations and measurements was done to validate the model developed. The power quality instrument manufactured by Dranetz was connected at the common breaker of the wind farm. During this study, power quality issues such as voltage sag, Interruption, Oscillatory transient and Interruption were recorded.

#### **3.7.1 Simulation of voltage sag**

Voltage sag is defined as the decrease (between 10% and 90%) in RMS voltage at the power frequency for the duration of 0.5 cycles to 1 minute. In the network design considered, the motor at the 11kV bus bar is not started until eighth second. The switching on of this motor results in a sag in the voltage on the 11kV line. The motor on the 11kV bus bar is started on the eighth second and it has caused a sag in voltage in the 11kV bus bar. The sags are momentary in nature as shown in the Figure 3.19. The Voltage sag measured at the wind feeder is depicted in Figure 3.20. The dip in voltage is due to the sudden load variation and the starting of motor. .

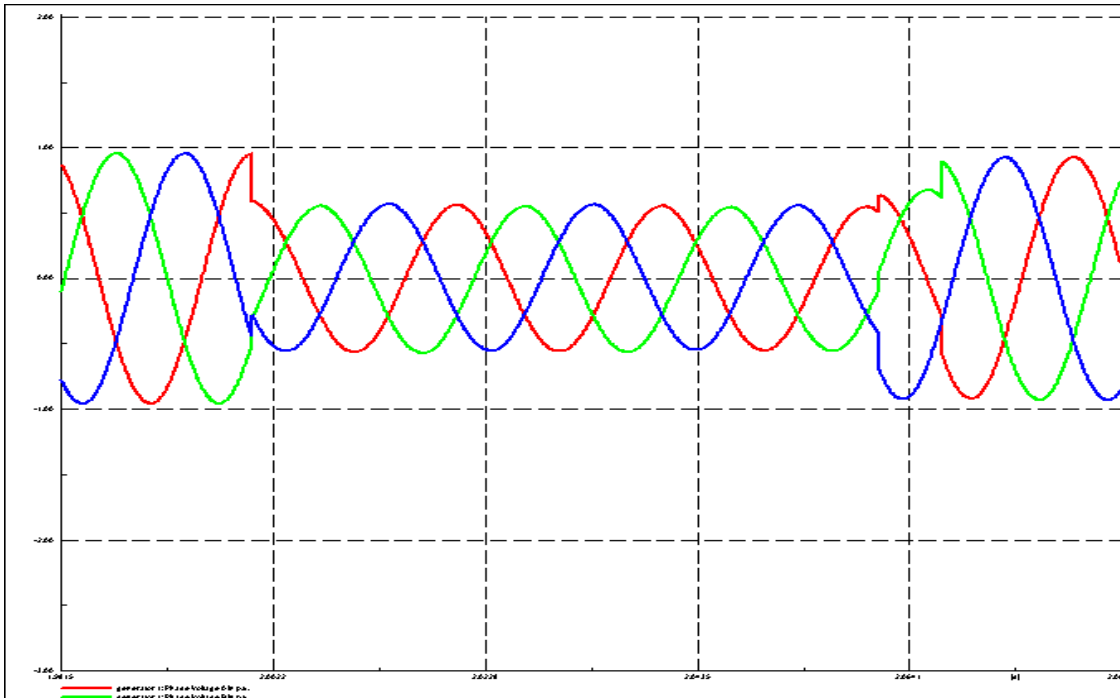


**Figure 3.19 Simulated voltage sag in 11kV bus bar at peedampalli substation**

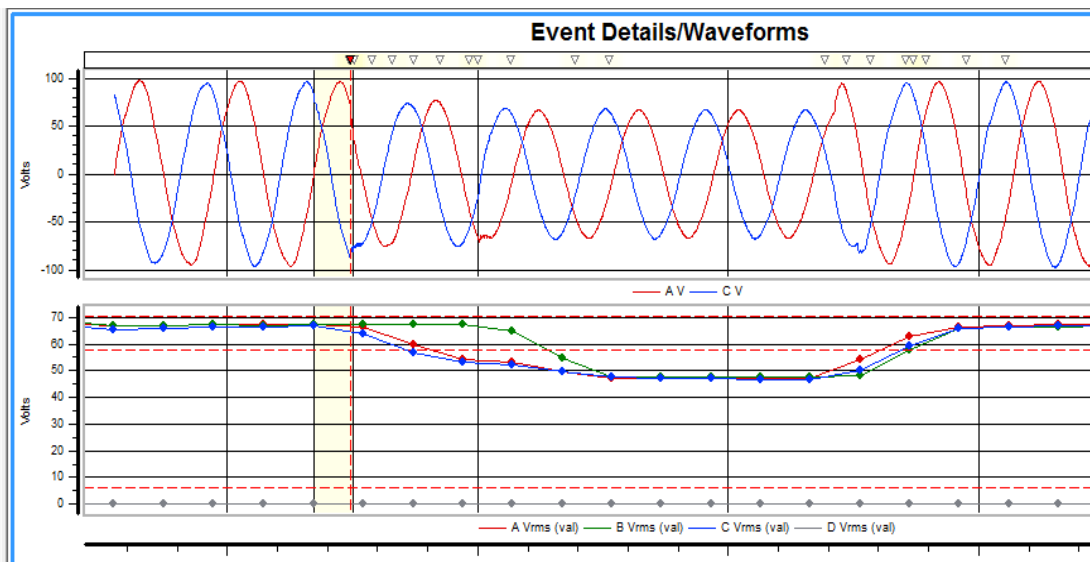


**Figure 3.20 Measured voltage sag at peedampalli sub –station**

### 3.7.2 Transient voltage due to capacitor switching

The network is considered to be in the normal operation before a capacitor is switched into the 11kV bus bar. At the eighth second, the capacitor is switched off. This results in oscillations in the line voltage of the generators 1 and 6 as shown Figures 3.21 and 3.22. A transient-oscillation is noted. It can be seen that the waveforms of Figures 3.21 to 3.23 look alike. Therefore, capacitive switching is considered as one of the cause of the oscillatory transient in the network.

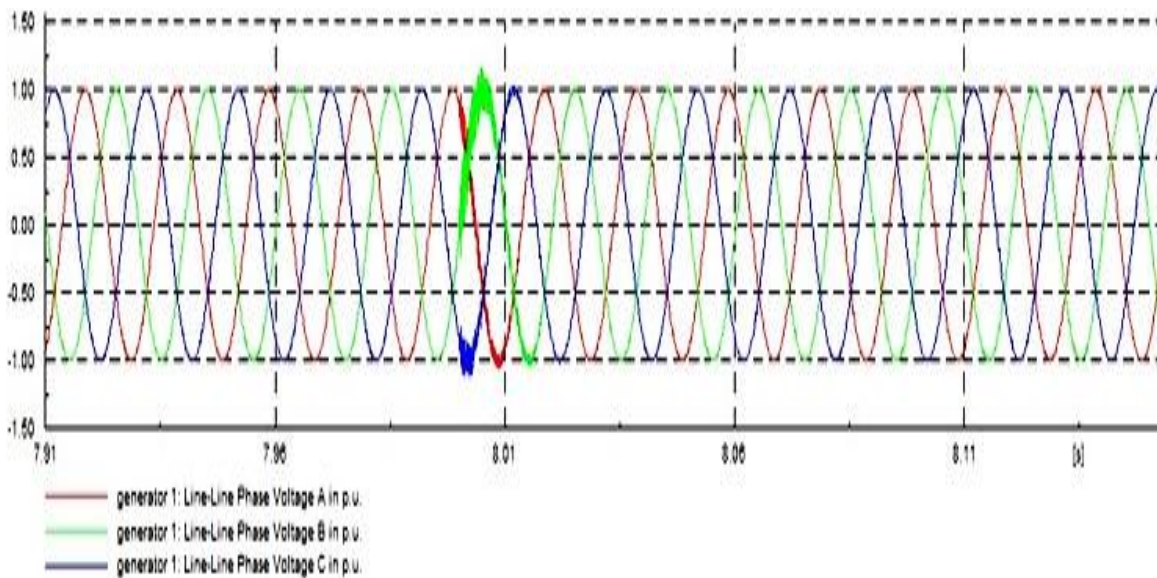


**Figure 3.21 Simulated transient line voltage waveform of generator 1**

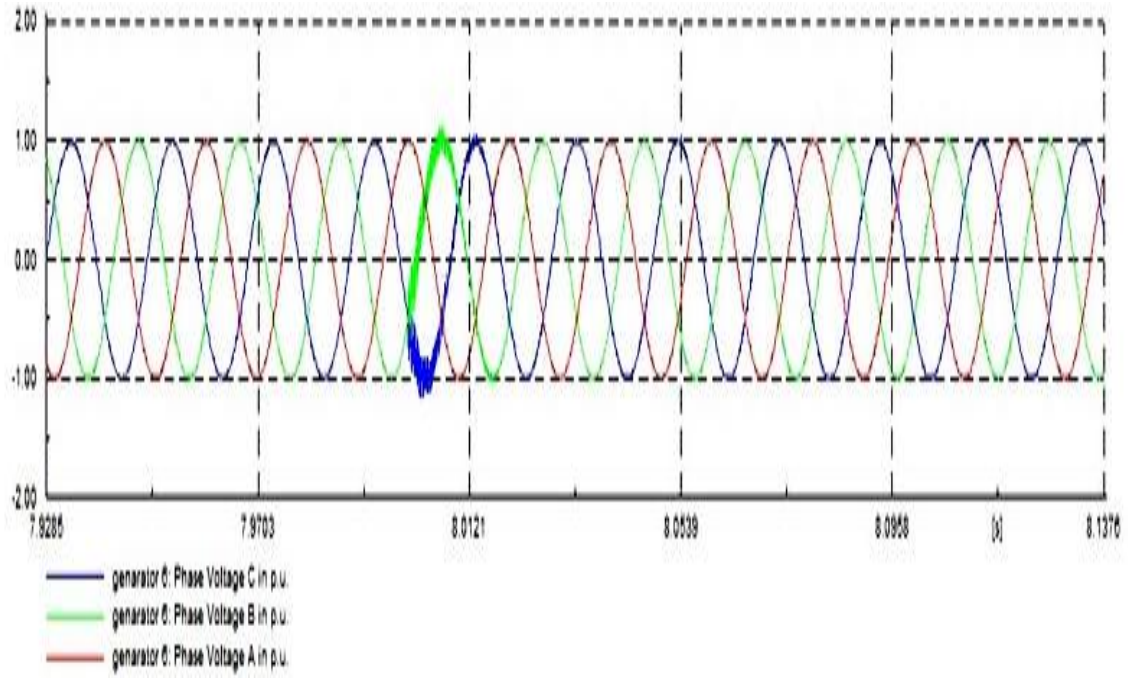


**Figure 3.22 Simulated transient phase voltage waveform of generated 6**

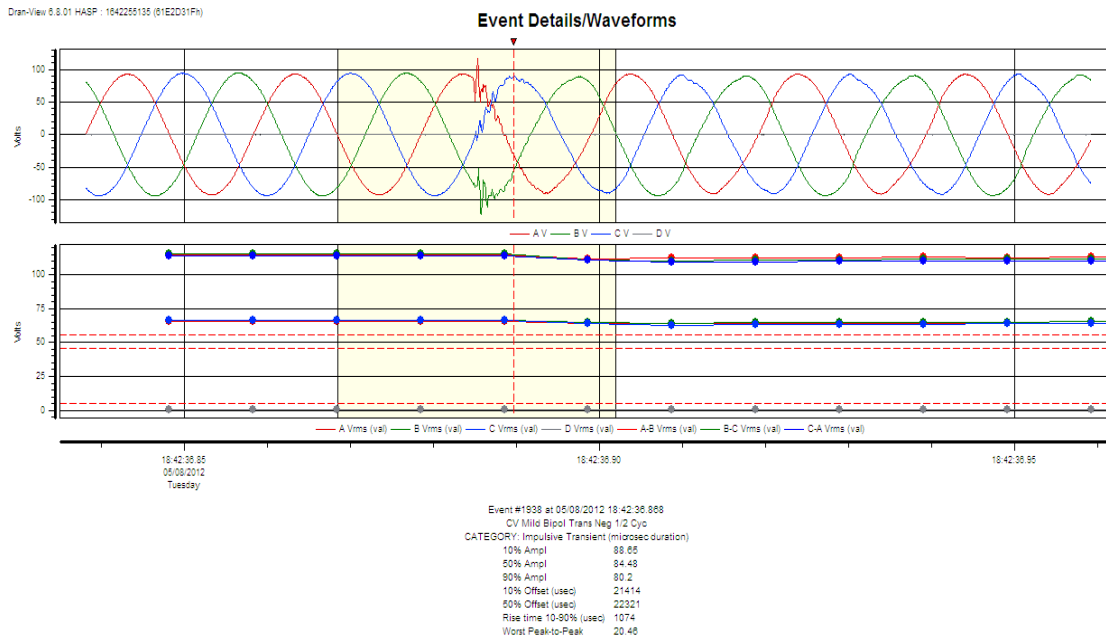


**Figure 3.23 Measured transient voltage waveform of generator in peedampalli**

### 3.7.3 Tripping of the wind generator

The simulation assumes that the generator 1 has been subjected to fault in the wind electric system between the intervals 3 to 4 seconds. Thus, this generator is switched out from the network during the concerned interval. At the fourth second, the fault is cleared and the generator is brought back to the normal operation. The simulation results for such a situation show that the variation in phase voltage as given Figures 3.24.

The noteworthy observations are: The line-to-line voltage of generator 1 suddenly starts decaying and becomes zero at some point in time. It is restored back to the normal operation after the clearance of fault. The Figure 3.25 shows that the measured voltage interruption wave is very similar to the simulated waveform in the DIgSILENT.

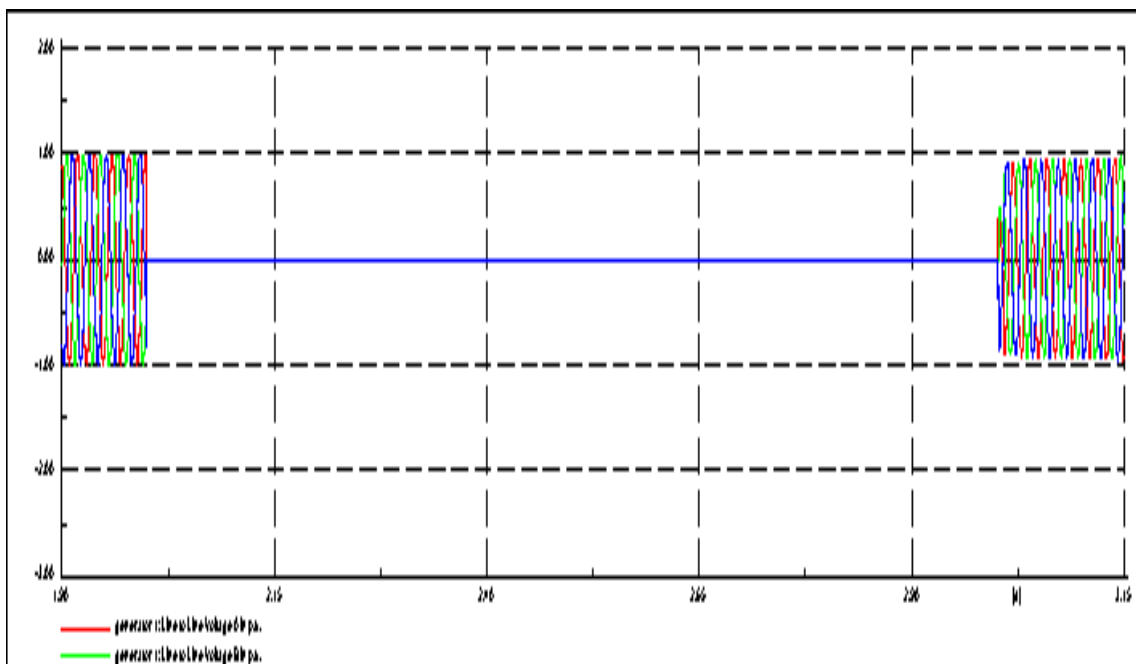


**Figure 3.24: Simulated voltage waveform generators during tripping**

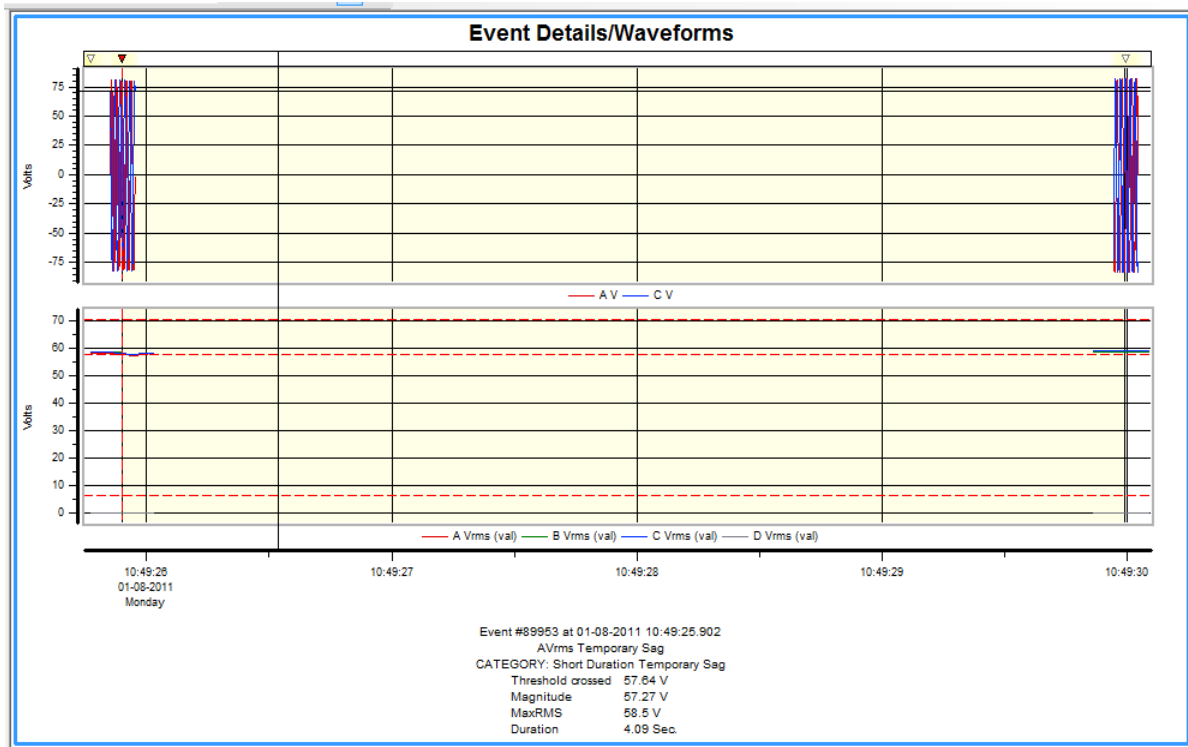


**Figure 3.25: Measured voltage waveform during tripping**

### 3.7.4 Swell

Voltage swell is an increase (between 10% and 90%) in RMS voltage at a power frequency for duration from 0.5 cycles to 1 min. In the designed network, the low voltage loads which are connected to the 11kV bus bar are disconnected. The voltage thus rises from its nominal value of 1 p.u to 1.01 p.u shown in Figures 3.26 to 3.27. The Figure 3.28 shows the measured waveform which is similar to the simulated one.

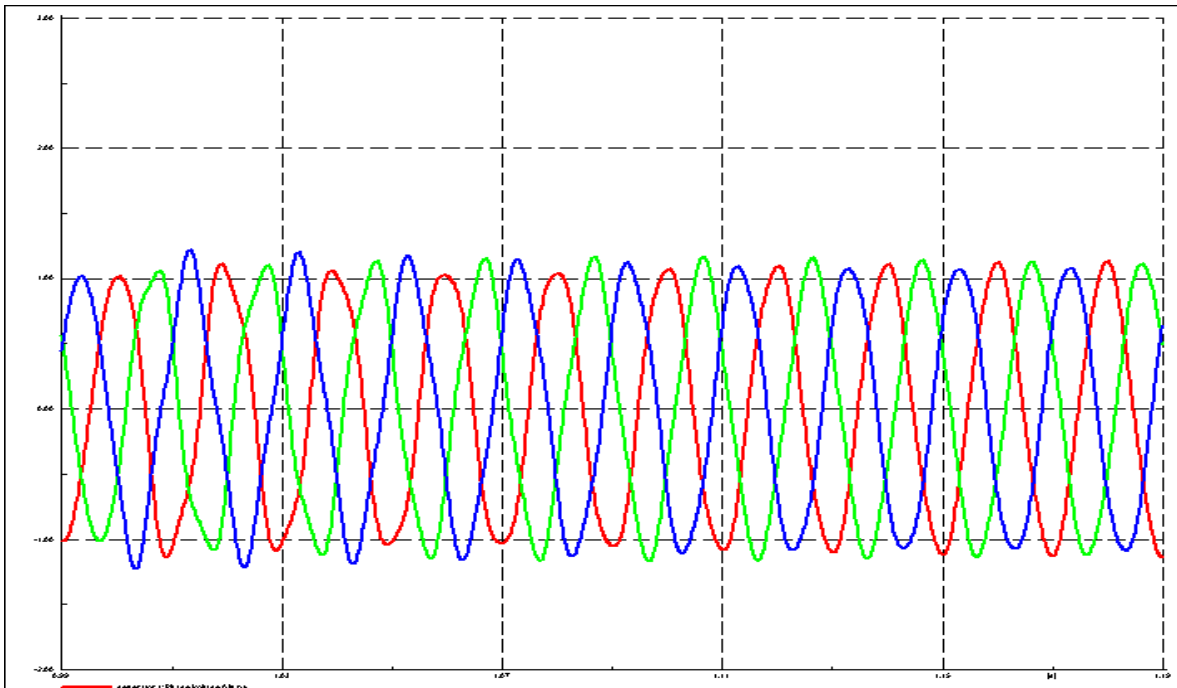


**Figure 3.26** Waveform of simulated voltage swell at generator busbar

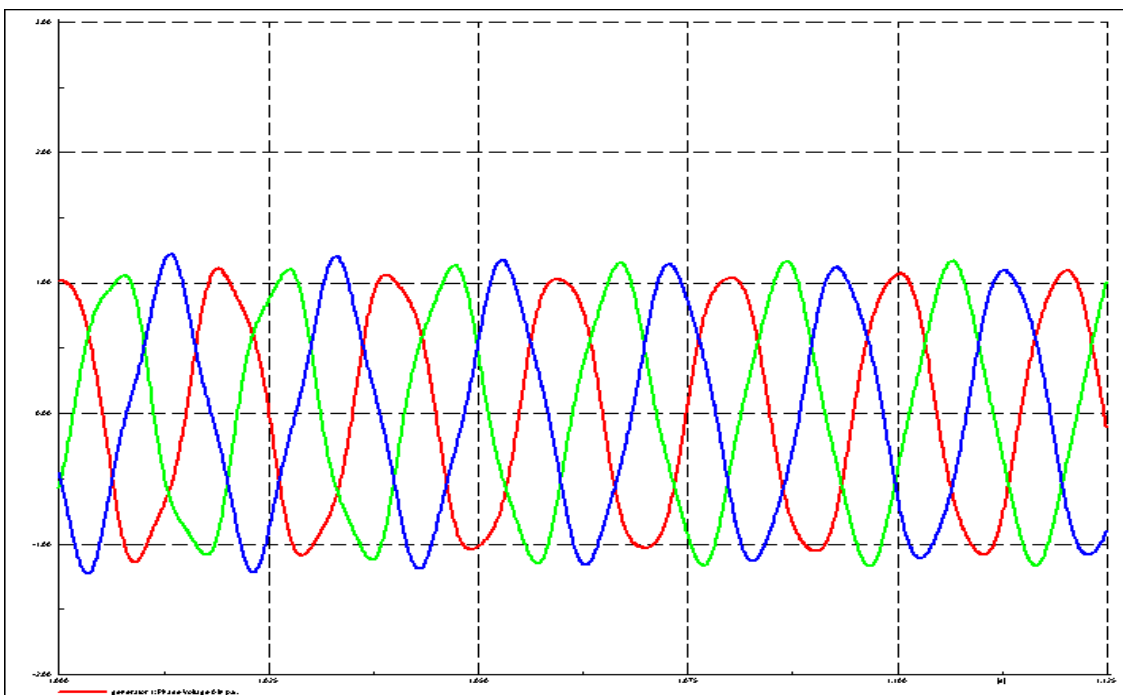


**Figure 3.27** Waveform of simulated voltage swell at transformer busbar

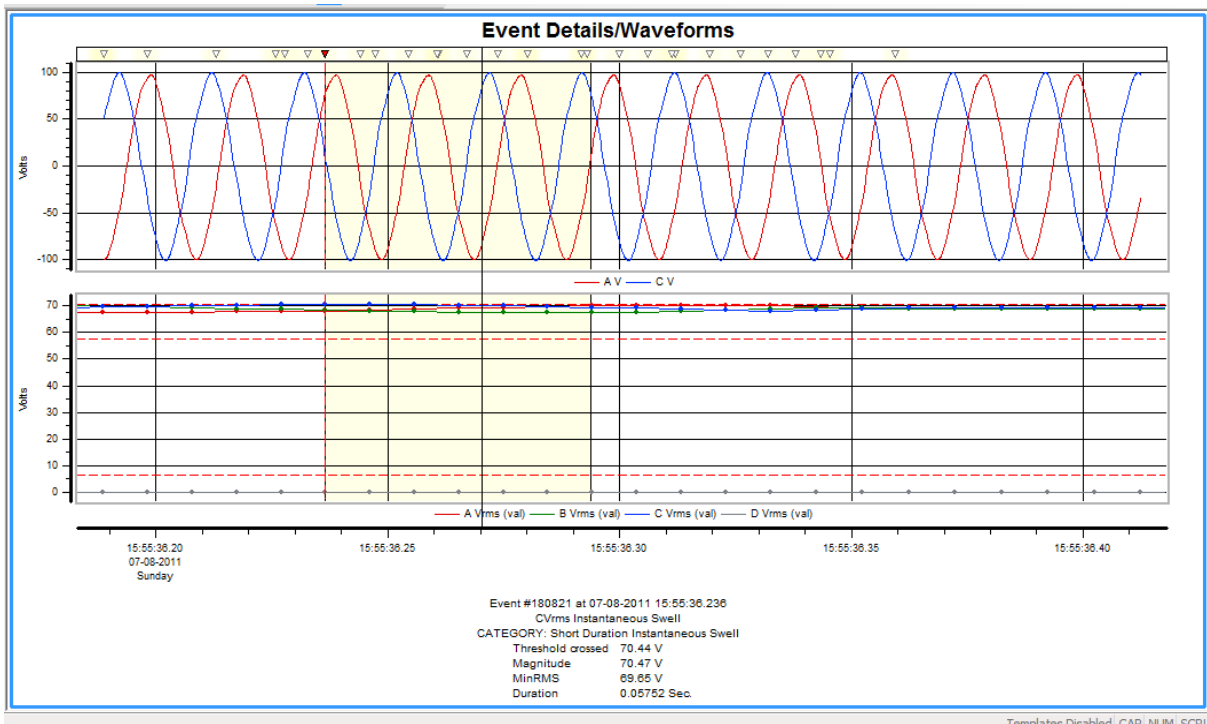


**Figure 3.28 Waveform of measured voltage swell**

### 3.8 Conclusion

The peedampalli wind farm located at Coimbatore district have been taken for the power quality studies. The wind farm contains 6 fixed speed wind turbines each connected to the squirrel cage induction generator which generates 600kW at 690V. The total generated power of the wind farm is 3.6MW. The steady state and dynamic analysis were performed with the help of RMS simulation in DIgSILENT. From the load flow analysis, wind farm total generated power and power demand were identified and the voltage profiles at different feeders are recorded.

Under the steady state analysis, the wind speed is considered as constant. The performances of wind farm are observed under the variations in grid voltage and wind speed. If the wind velocity is decreased below its rated value of 12m/s, the generated power and current of the generator 1 and 6 are reduced. At 3m/s, the induction generator acts as a motor absorbing the real power from the grid. The 110kV grid bus bar voltage is varied in steps. As the grid bus bar voltage is

increased, the generated power remains constant and the current decreases. The generators absorb more reactive power from the grid. If the grid voltage is decreased, the generated real power again remains constant, current increases and reactive power absorption from the grid decreases. The system frequency remains constant with increase or decrease in load demand since the system connected to external grid which behaves like an infinite bus bar.

Under dynamic analysis, wind speed is assumed to vary from cut in speed to cut out speed (3.5m/s to 20m/s). As the wind turbines are a few kilometers apart, the wind speed at individual wind turbines are assumed different values in the simulation. Various scenarios such as Transient stability analysis, three phases Fault, sudden increase of load, load flow harmonics and wind variation were simulated for 600 sec. The wind generator 1 is a few km away from grid bus bar and the generator 6 which is nearer to the grid bus bar are taken for the analysis. The wind generator is pitch controlled to generate constant real power for speeds above the rated value. The three-phase symmetrical fault is applied at 11kV bus bar  $t=5$  sec for the duration of 500ms for the simulation time of 20 seconds. The voltage at 11kV bus bar drops to zero and the other bus bar voltages near to the fault are decreased. At the 11kV bus bar, industrial load was suddenly included for a short span of time about 300 milliseconds. During this interval, there is a sudden 60% dip in the voltage level at 11kV feeder and generator bus bars. The harmonics were injected at the generator bus and its effects were identified at different bus bars with the help of harmonic load flow analysis. The values of  $P_{st}$  and  $P_{lt}$  for continuous and switching operation are calculated using Flicker meter for various impedance angle  $30^\circ$ ,  $50^\circ$ ,  $70^\circ$  and  $85^\circ$  at the point of measurement.

The comparison between the results of the simulations and measurements was carried out to validate the model developed for the peedampalli substation. During this study, power quality issues such as voltage sag, interruption, oscillatory transient and interruption were recorded. The sags are momentary in nature and

they occur due to sudden inclusion of motor at 11kV bus bar. The 30% voltage dip is observed in the simulated and measured result for 5 cycle duration. The capacitive switching is considered as one of the causes of the oscillatory transient in the network. The capacitor is switched off after eight sec, the oscillations in the line voltage of the generators 1 and 6 are observed. The measured and simulated waveforms are well matched with each other. The interruption waveform occurs due to tripping of the generator and the short circuit. The generator 1 is tripped for a short span of time; the line-to-line voltage of generator 1 suddenly starts decaying and becomes zero. It is restored back to the normal operation after the closure of the circuit breaker. The measured voltage during interruption is very similar to the simulated voltage.

## CHAPTER 4

### DATA COLLECTION AND ANALYSIS OF WIND FARM LOCATED AT PETHAPPAMPATTY WIND FARM

#### 4.1 Introduction

The Substation consists of four wind farm feeder namely Pukkulam, SV Patty, Eluppanagaram and Ponneri connected to the 33kV feeder. The station was constructed and commissioned by M/s Gamesa during the year of 2010-11. The wind turbines installed in the wind farm are variable speed doubly fed induction generators (DFIG). The wind farm layout is shown in Figure 4.1

The Pukkulam feeder, consisting of 12 units of variable speed wind turbine connected to doubly fed induction generator with rating 600 kW at 11kV is shown in Figure 4.2. The total capacity of this feeder is 7.2 MW. The DFIG injects the power into the grid from the stator and the rotor with the help of inverter and converter. The voltage generated by the DFIG is directly connected to LV side of the transformer rated at 25MVA at 11/33kV. The HV side of the transformer is connected to the common 33kV feeder.

SV Patty Feeder consists of 17 units of variable speed wind turbine connected to DFIG which generates 600kW at 11kV as shown in Figure 4.3. The total capacity of this wind feeder is 10.2MW. The DFIG is directly connected to the LV side of the 11/33kV transformer. The HV side of the transformer is connected to common 33kV feeder.

Eluppanagaram feeder has 18 units of variable speed wind turbine connected to DFIG as shown in Figure 4.4. The total power capacity of this wind feeder is 10.8MW. The Ponneri feeder consists of 9 units of wind electric system having a total power capacity of 5.4MW. All the DFIG are connected to the LV side of 11/33 kV transformer as shown in Figure 4.5.

All the four wind farm feeders are connected to a common 33kV feeder. The power transformers, 33/110 kV and 110/230kV are used to step up the voltage from 11kV to 230 kV for connecting the wind electric system to the 230kV grid. The Power Quality analyzers were installed at various locations in the Pethappampatty substations from 13/04/2012 to 24/05/2012 (43 days). Three different Power Quality meter was installed: The Fluke 435 meter was installed at wind station connected to Pukkulam feeder using the current transformers. The other Power Quality analyzer manufactured by Dranetz was installed at feeder breaker in Pukkulam substation. The third Power Quality analyzer, HIOKI was installed at 110kV circuit breaker point.

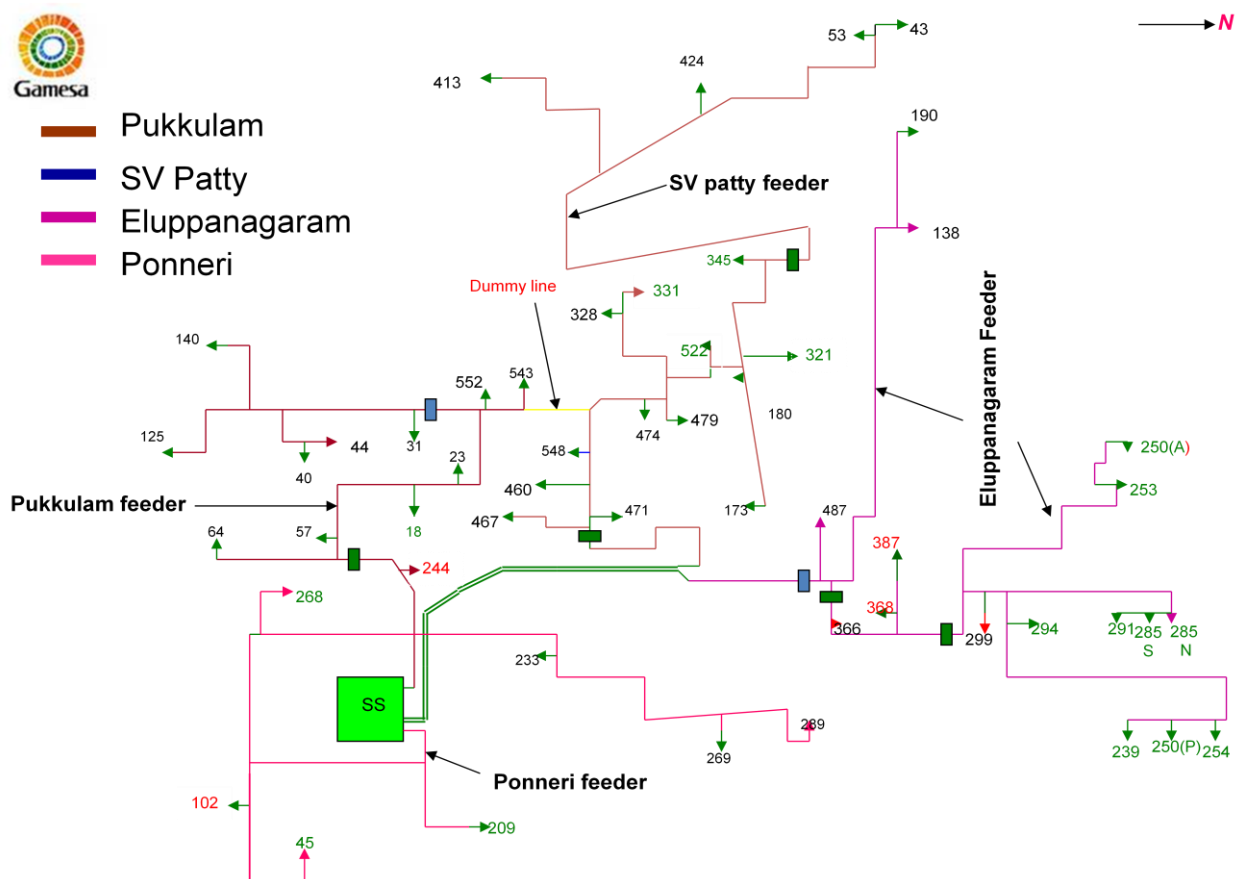


**Figure 4.1: Pethappampatty wind farm layout**

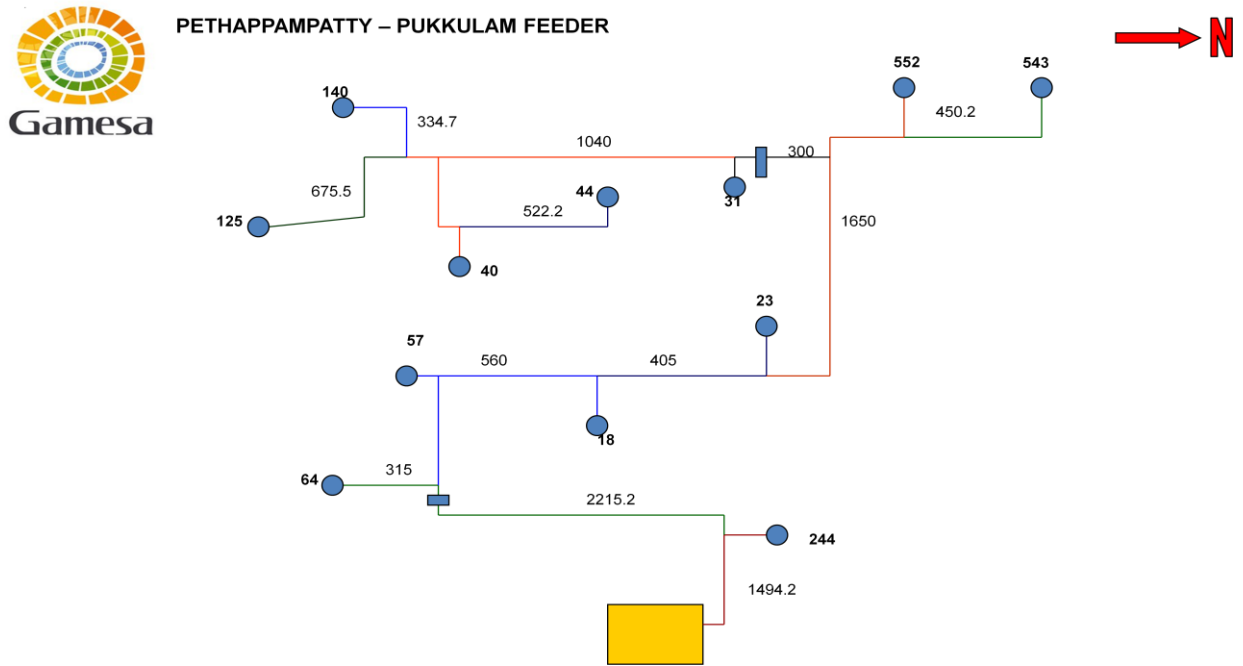


Figure 4.2: Layout of wind farm connected to pukkulam feeder

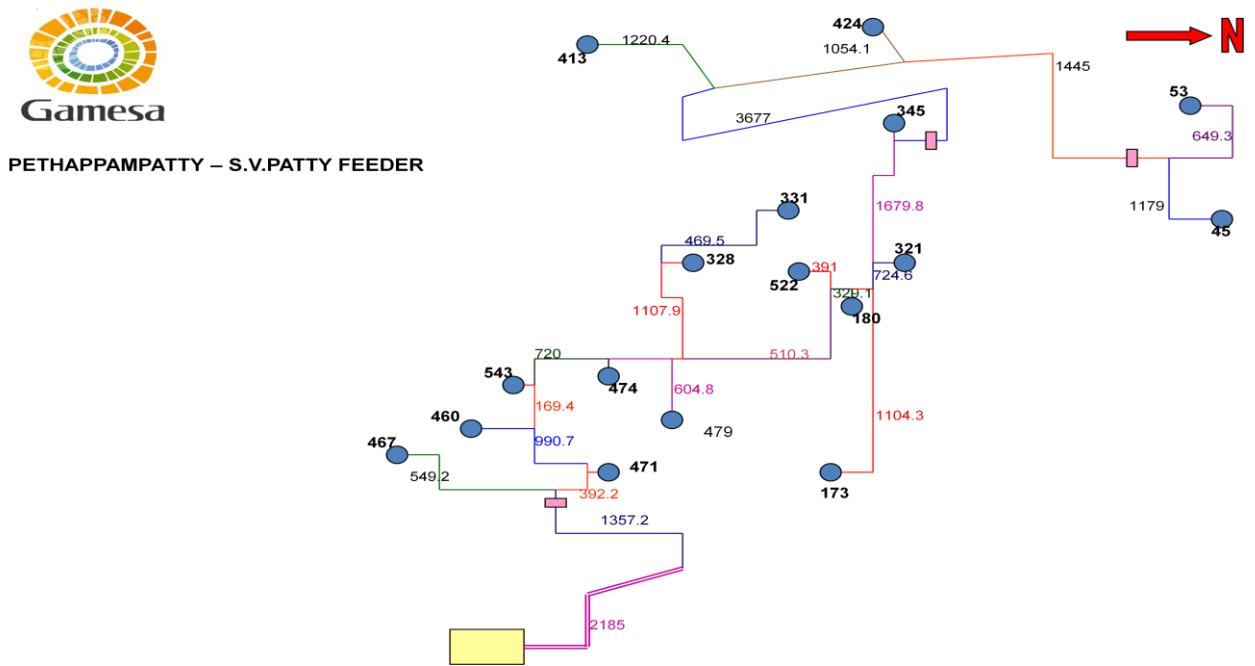
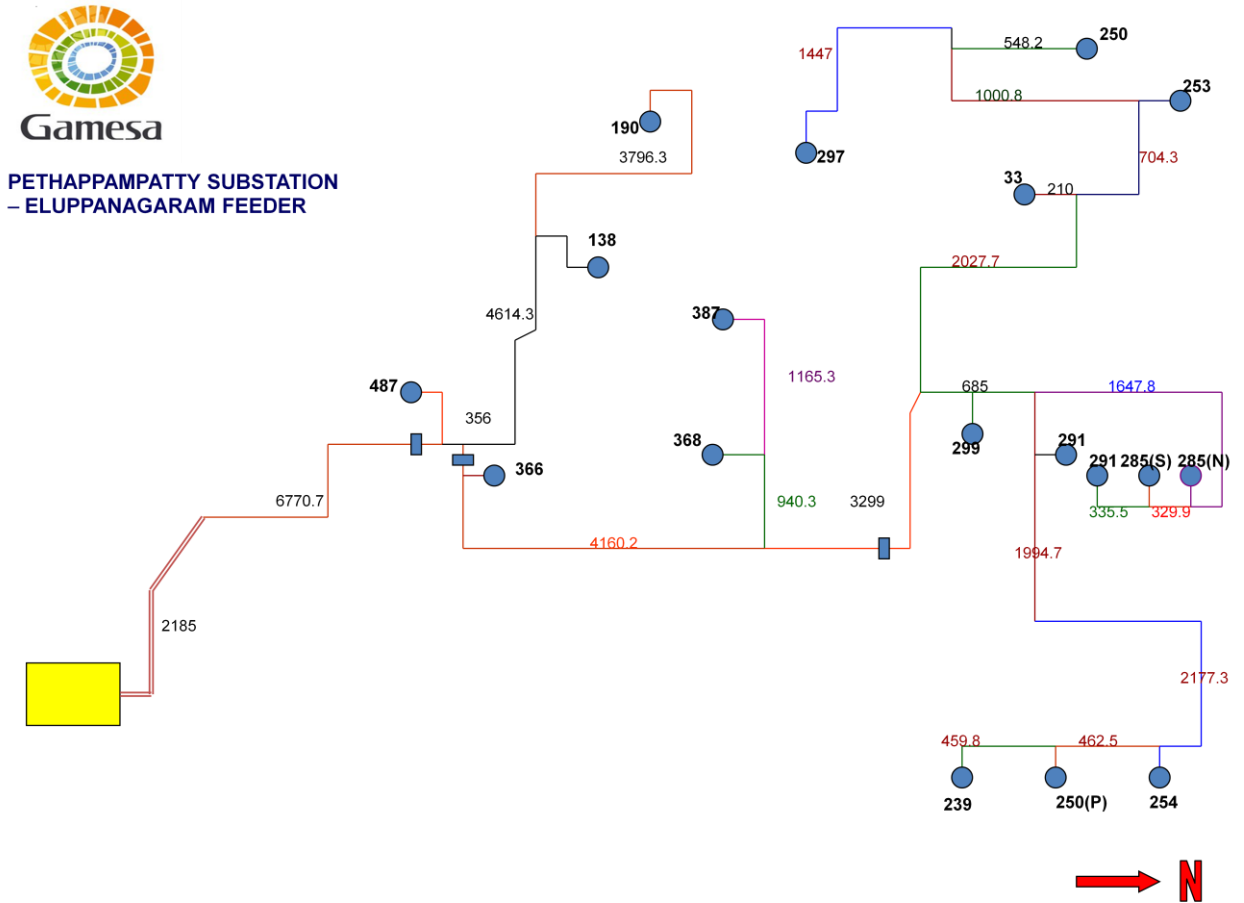
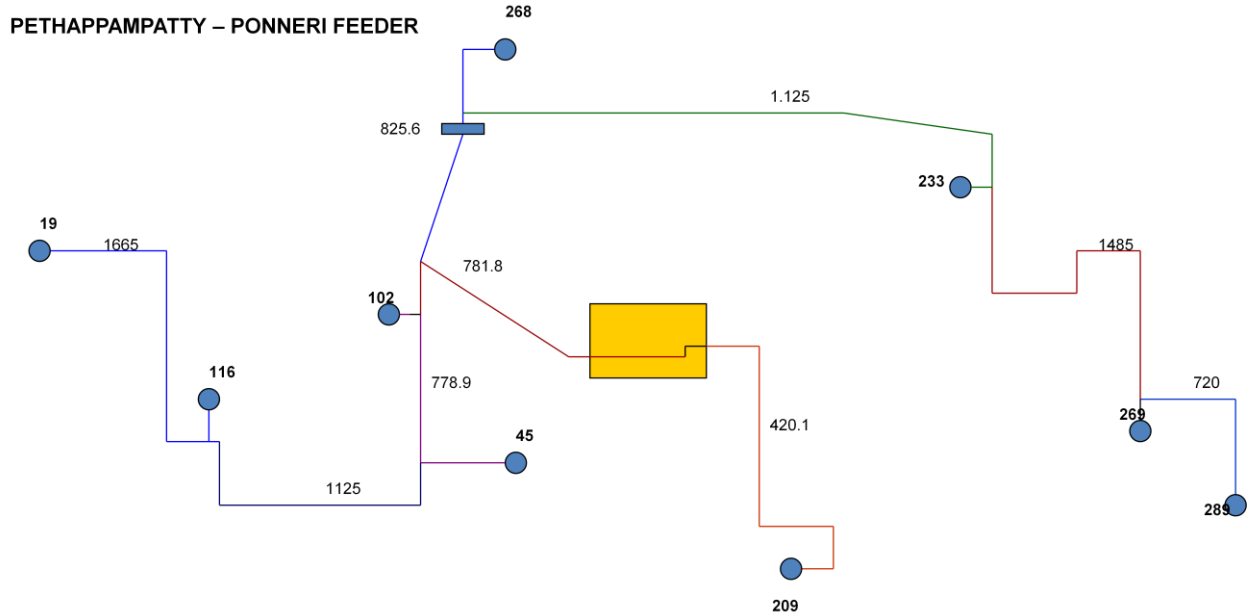


Figure 4.3: Layout of wind farm connected to SV patty feeder



**Figure 4.4: Layout of wind electric generators connected to eluppanagaram feeder**



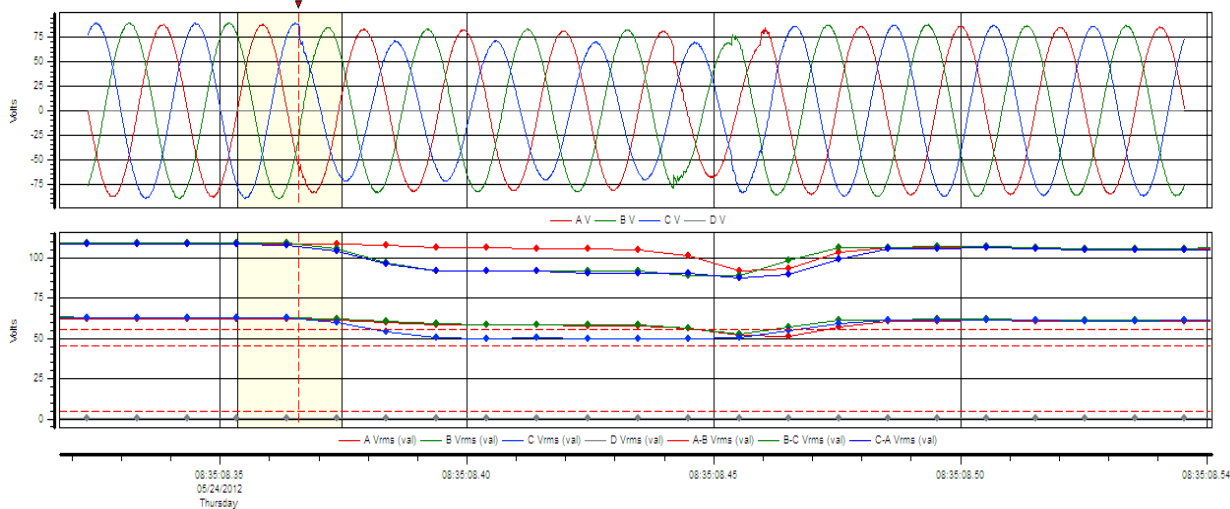
**Figure 4.5: Layout of wind electric generators connected to ponneri feeder**

#### **4.2 Power Quality Analyzer – Dranetz BMI**

Dranetz power quality analyzer was installed at feeder breaker at 33kV Pukkulam substation from 13/04/2012 to 24/05/2012 (43 days). A set of 522 data was recorded during this period. A set of 170 data was taken for analysis as the remaining data were found to be repetitive. Out of 170 data, 88 data are impulsive transients, 24 data are oscillatory transients, 54 data are transients and remaining 4 data are sag and swell. The Figures 4.6 to 4.13 shows the recorded power quality events.

Dran-View 6.8.01 HASP : 1642255135 (61E2D31Fh)

Event Details/Waveforms

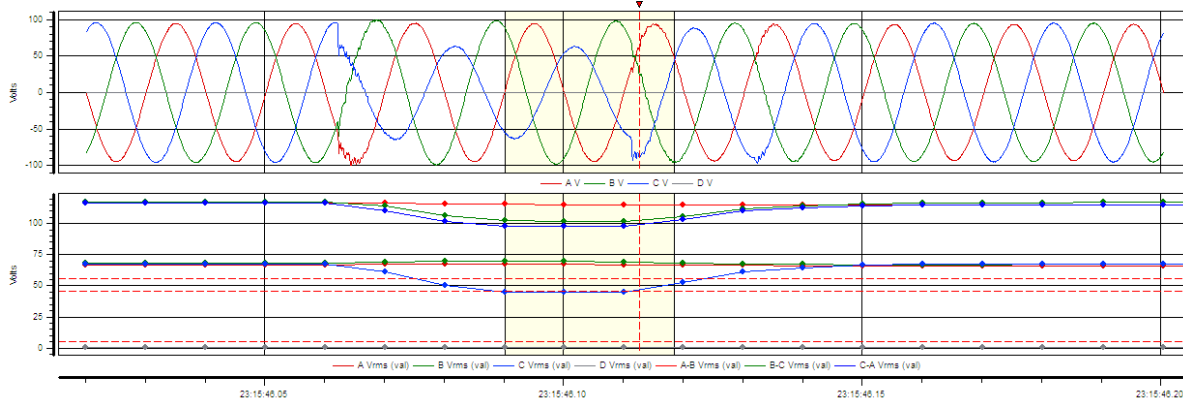


Event #18970 at 05/24/2012 08:35:08.353  
 AV Mild Bipol Trans Pos 1/4 Cyc  
 CATEGORY: Transient  
 10% Ampl: -88.87  
 50% Ampl: -88.91  
 90% Ampl: -88.22  
 10% Offset (usec): 12638  
 50% Offset (usec): 12674  
 Rise time 10-90% (usec): 71.92  
 Worst Peak-to-Peak: 17.98

Figure 4.6: Transient event 18970 on 24-5-12

Dran-View 6.8.01 HASP : 1642255135 (61E2D31Fh)

Event Details/Waveforms



Event #14432 at 05/18/2012 23:15:46.090  
 BV Mild Bipol Trans Neg 1/4 Cyc  
 CATEGORY: Transient  
 10% Ampl: 22.87  
 50% Ampl: 23.01  
 90% Ampl: 23.46  
 10% Offset (usec): 22513  
 50% Offset (usec): 22549  
 Rise time 10-90% (usec): 71.99  
 Worst Peak-to-Peak: 10.83

Figure 4.7: Transient event 14432 on 18-5-12

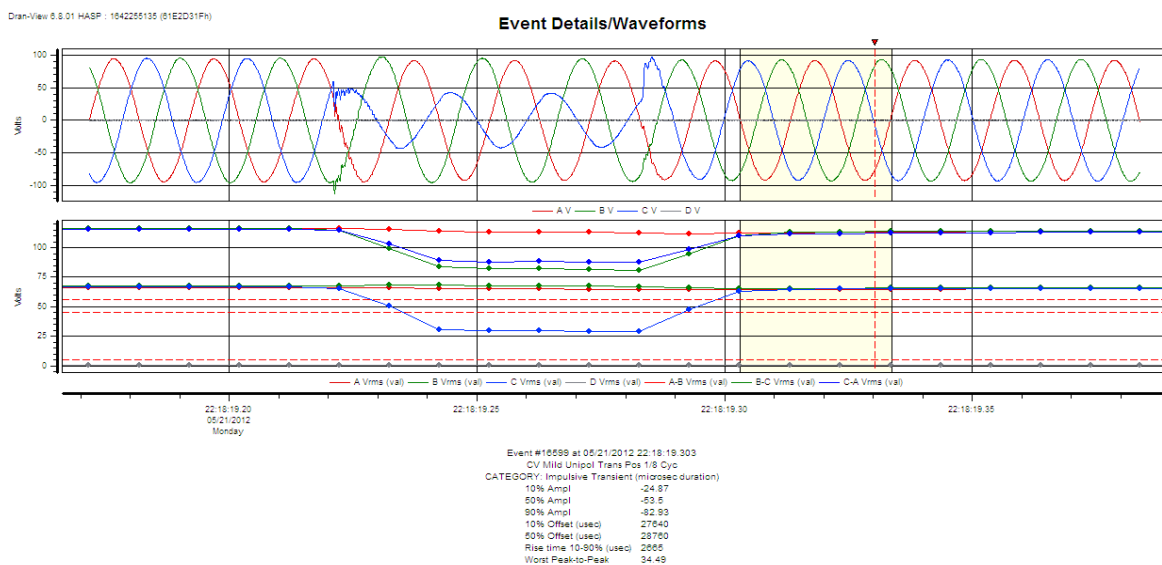


Figure 4.8: Impulsive transient event 16599 on 21-5-12

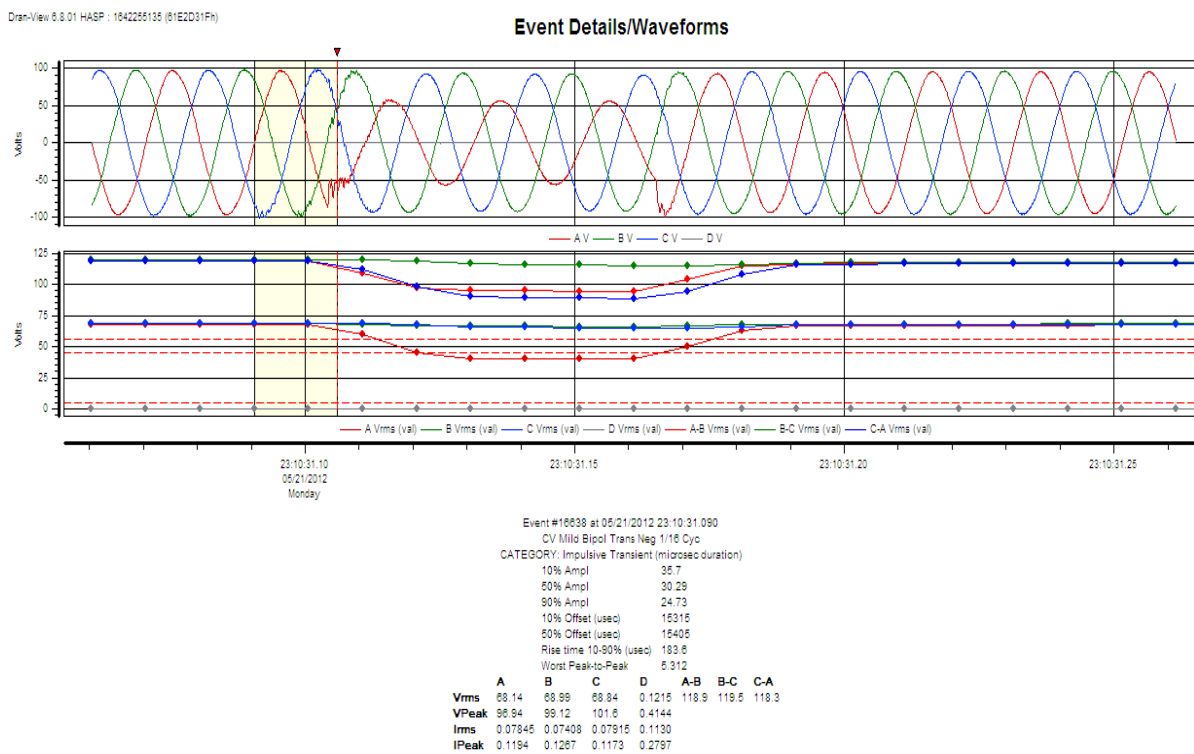
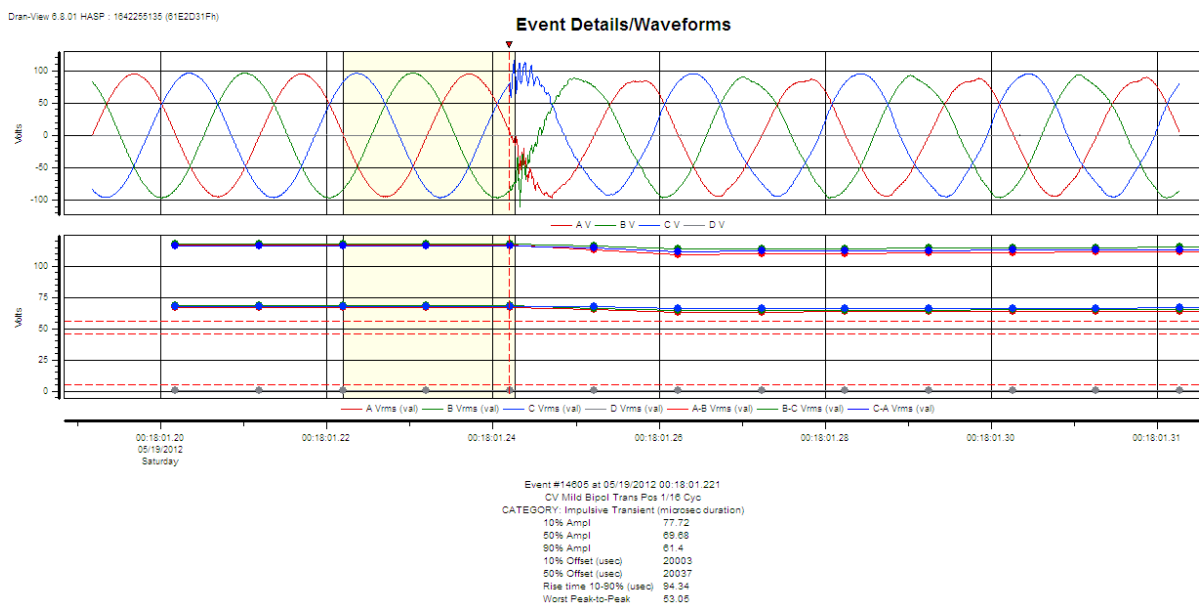
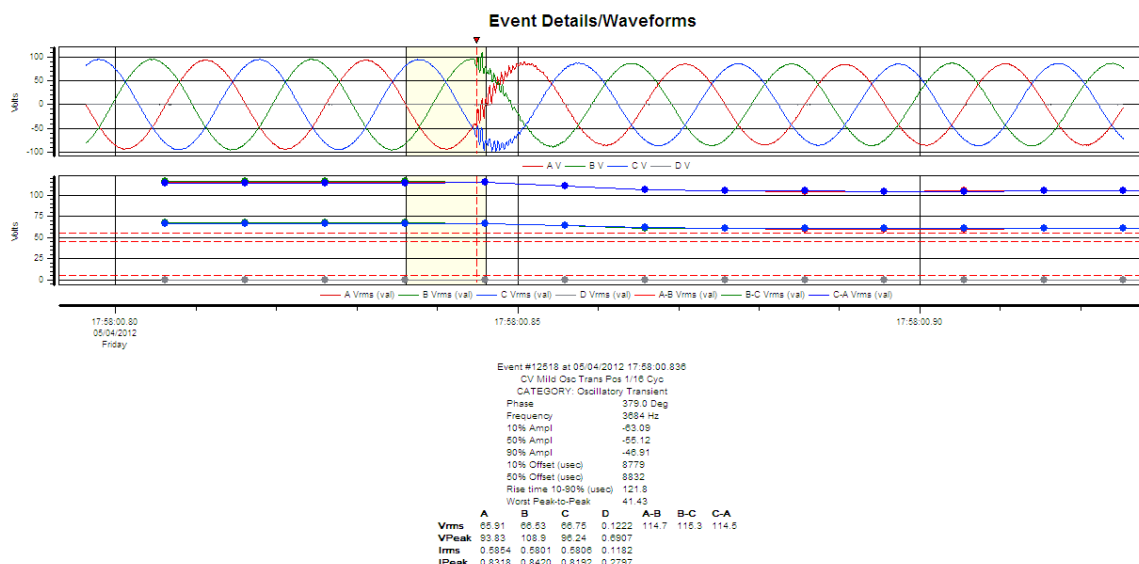


Figure 4.9: Impulsive transient event 16638 on 21-5-12



**Figure 4.10: Impulsive transient event 14605 on 19-5-12**



**Figure 4.11: Oscillatory transient event 12518 on 21-5-12**

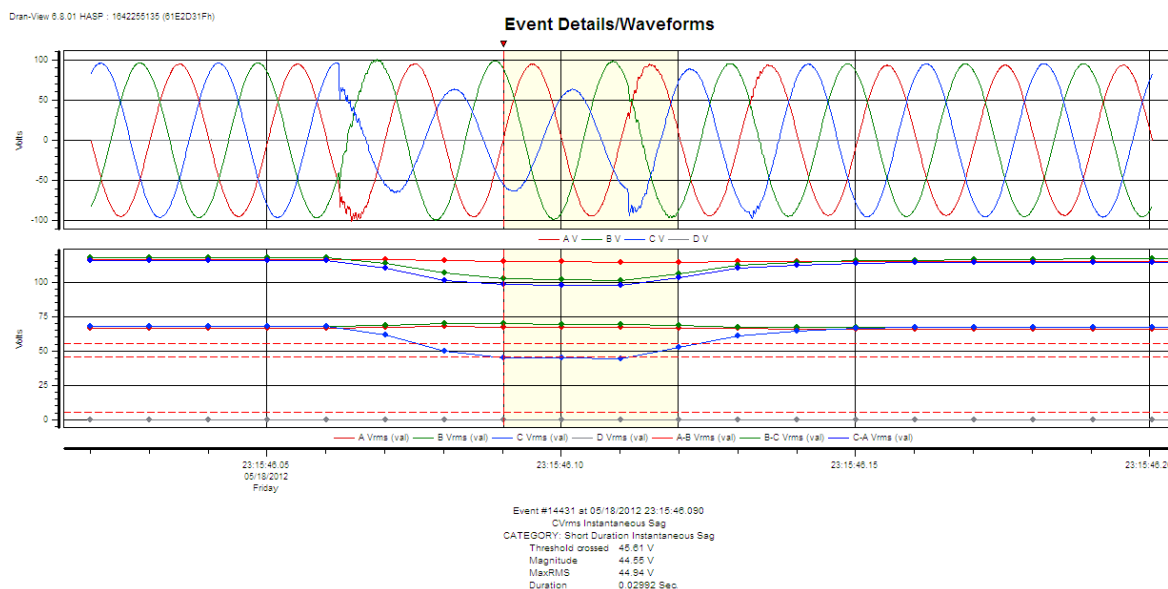


**Figure 4.12: Short duration instantaneous sag event 14431 on 18-5-12**

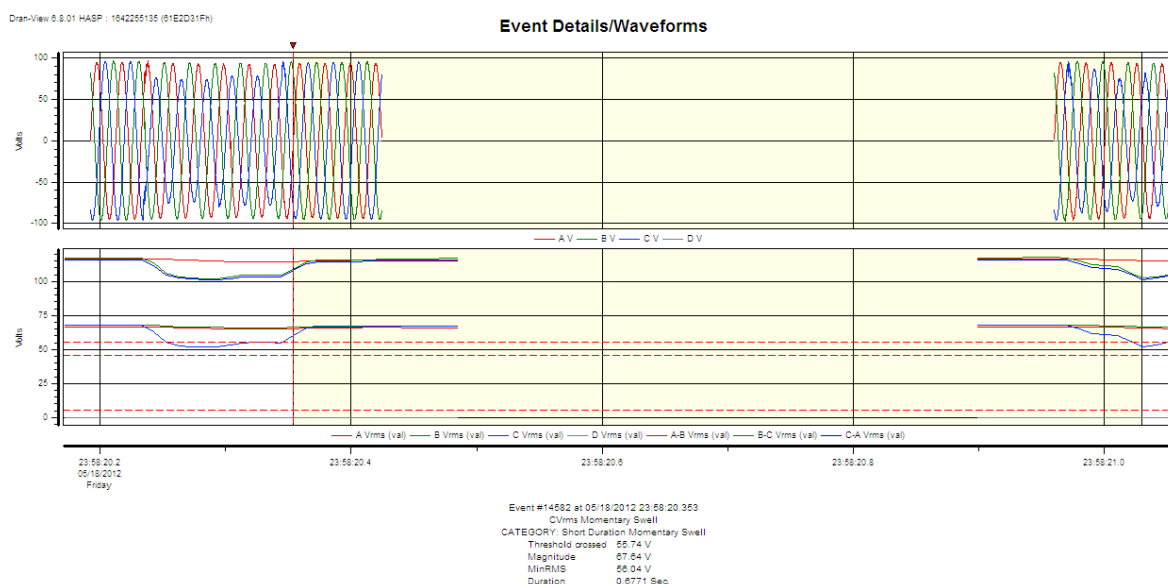


**Figure 4.13: Short duration momentary swell event 14582 on 18-5-12**

### 4.3 Time plot (Pethappampatty)

Dranetz Power Quality Analyzer recorded the time plot for the period of 21.05.12 to 13.04.12 (39 days). The time plots measure the RMS Voltage, Flickering, and Harmonic distortions. The recorded waveform events are shown in Figures 4.14 to 4.15.

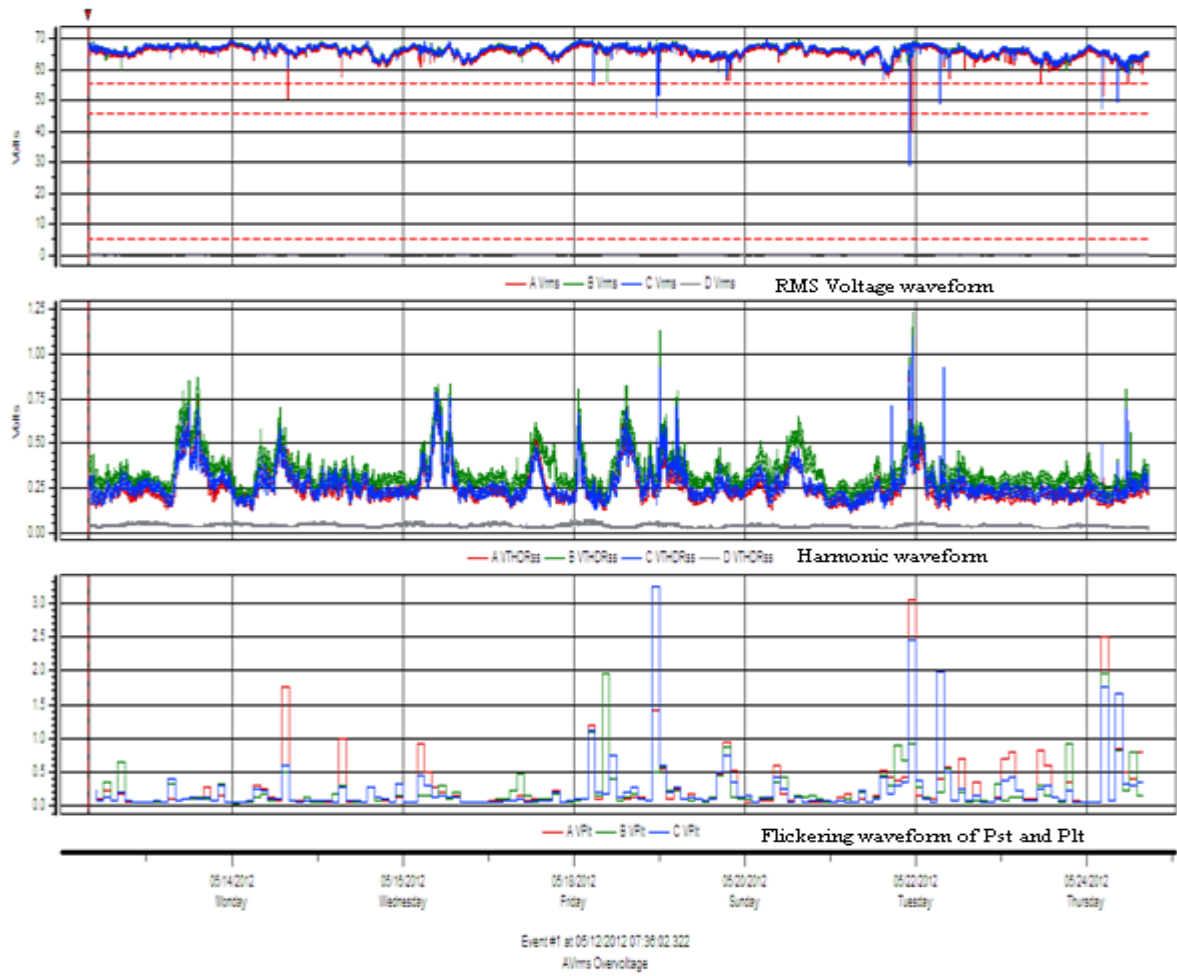


**Figure 4.14: Recorded events from 14.5.12 to 24.5.12**

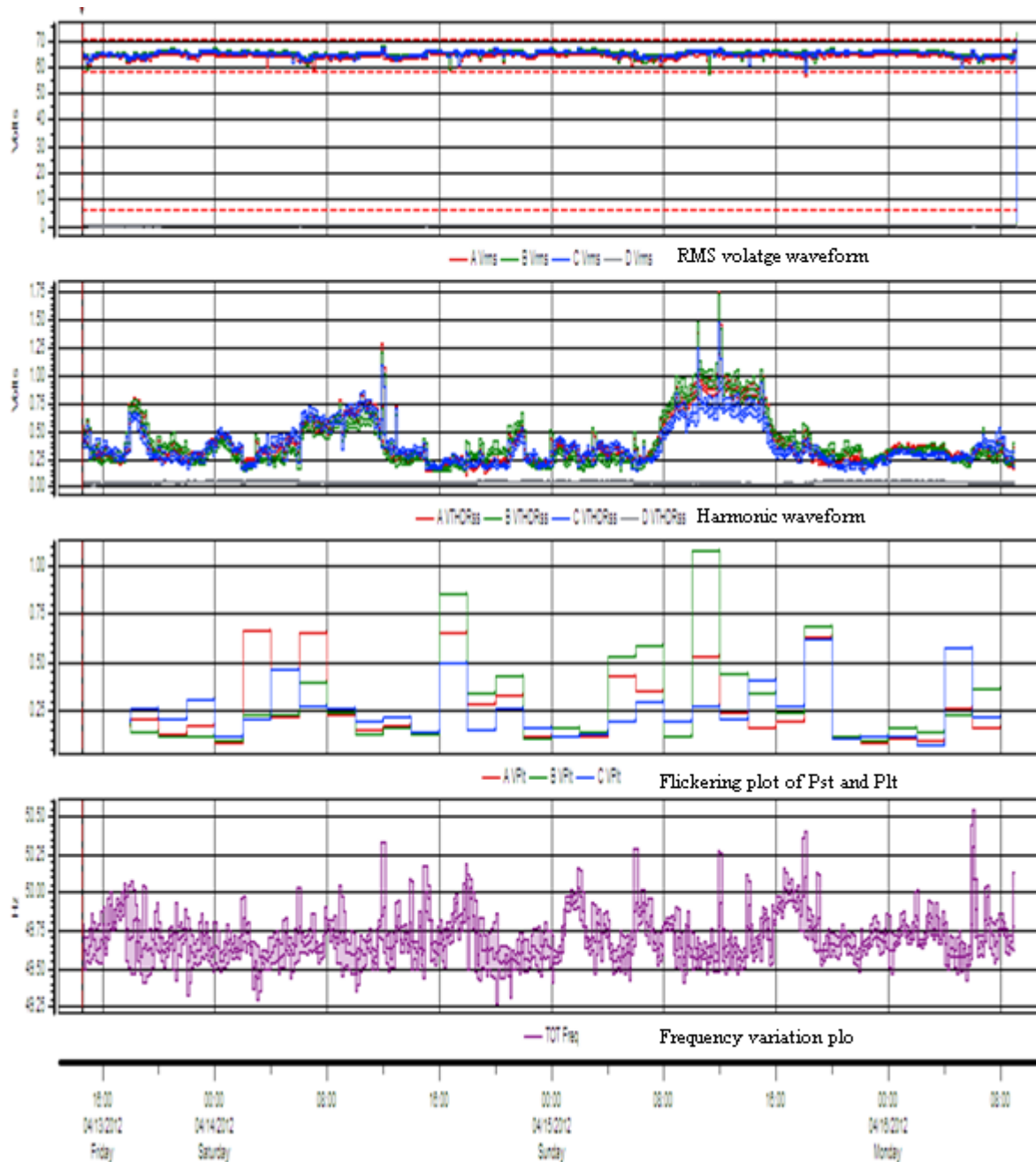


**Figure 4.15 Recorded events from 13.4.12 to 16.4.12**

#### **4.4 Power Quality Analyzer-Fluke 434**

The Fluke Power Quality Analyzer was installed in wind station at Pukkulam wind farm (3 wattmeter connections). From 13/04/2012 to 024/05/2012, the various power quality events such as dip, swell, frequency distortion, current waveform and voltage waveform were recorded. The recorded waveforms are shown from Figures 4.16 to 4.19.

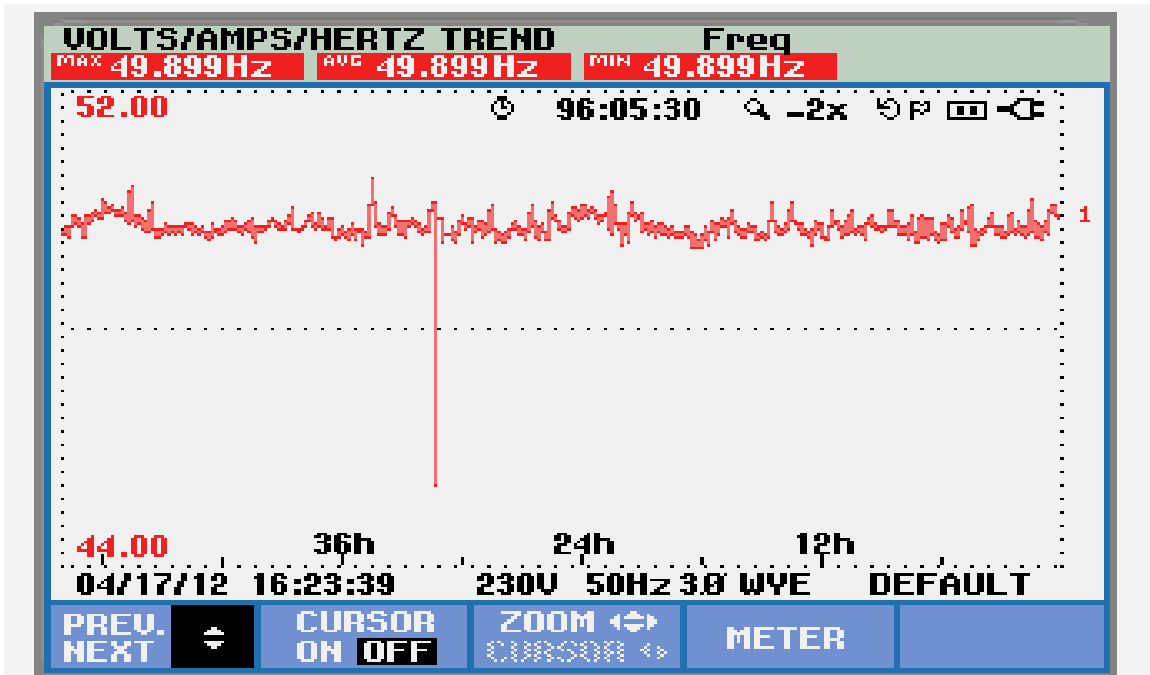


Figure 4.16 Frequency variation plot

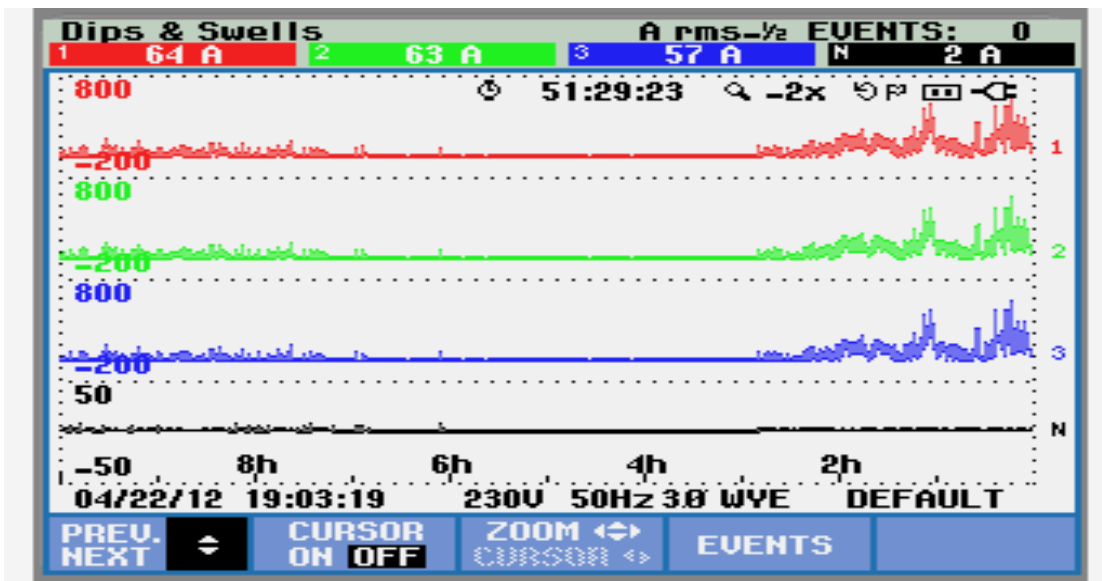


Figure 4.17 Current variation plot

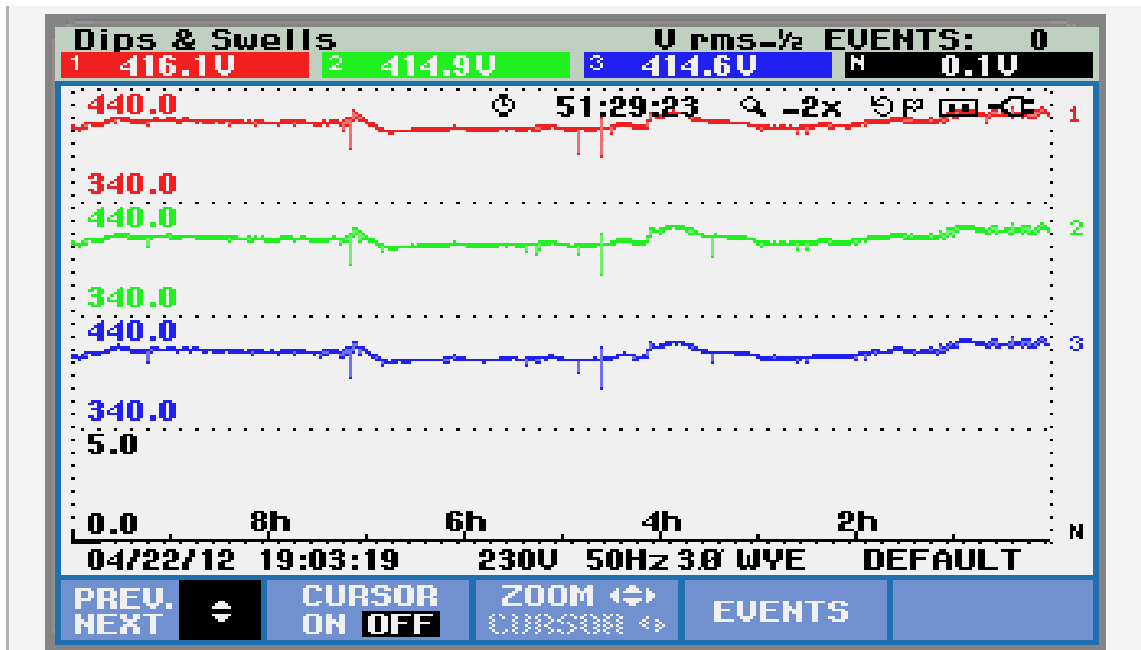


Figure 4.18 Voltage variation plot

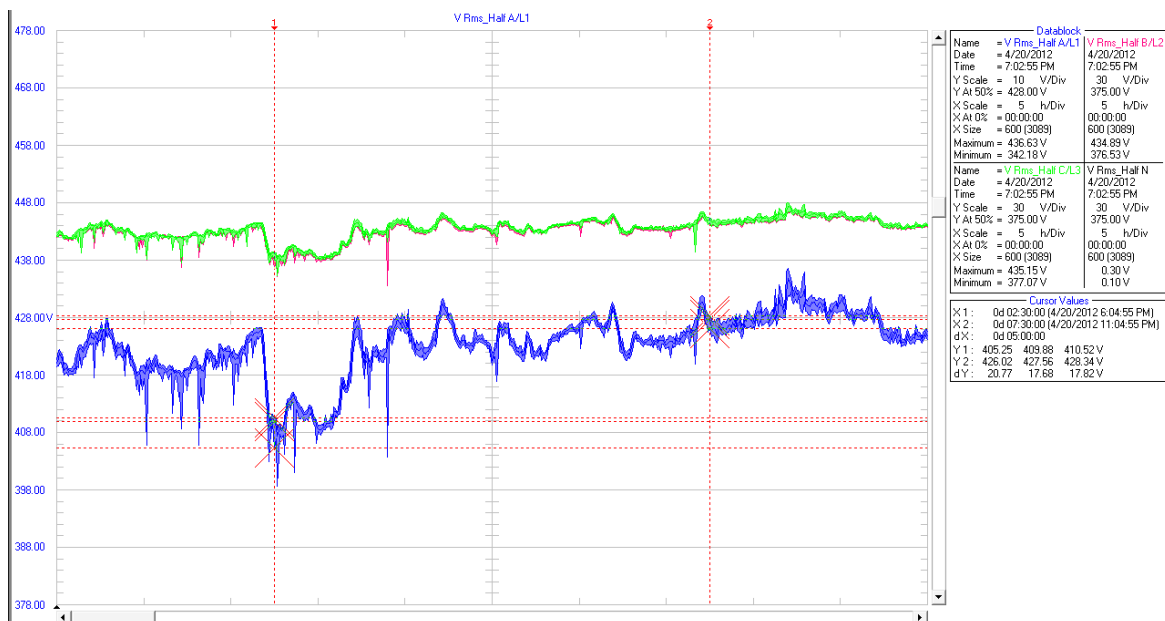
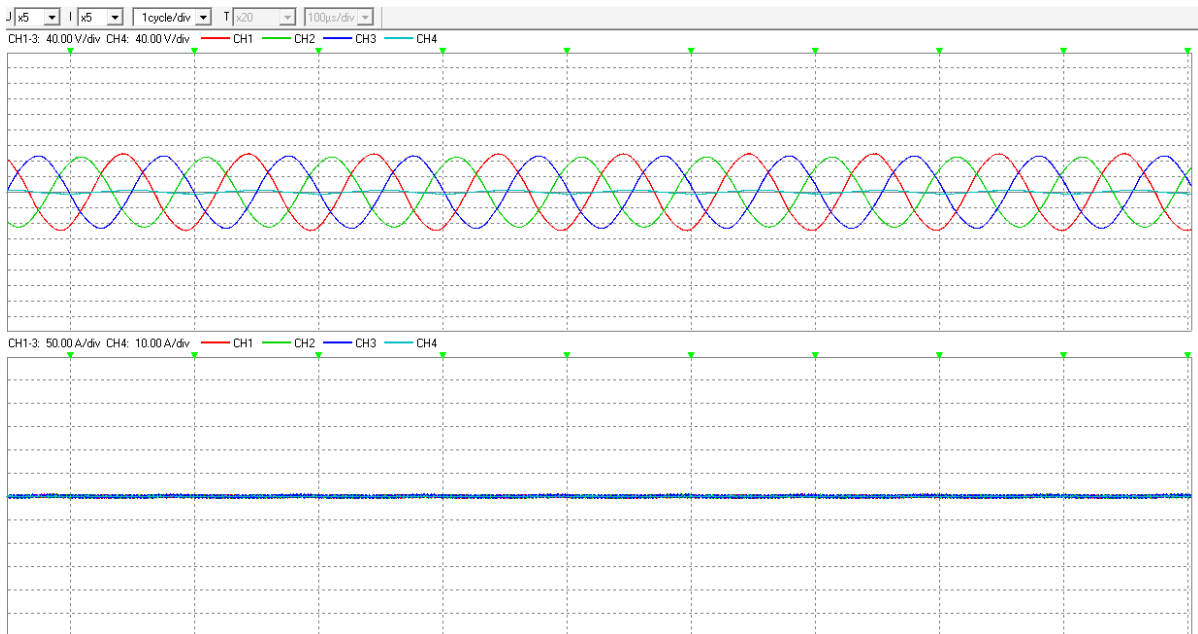


Figure 4.19 Recorded voltage plot on 20/04/12

#### 4.5 Power Quality Analyzer-Hioki 3390

The Power Quality Analyzer manufactured by HIOKI was installed at group control breaker point at 110kV common feeder of Pethappampatty substation with help of step down current transformer. Various power quality issues were recorded such as Voltage, Flickering, and Harmonic in time plot as shown in Figures 4.20 to 4.22.



**Figure 4.20: Voltage and Current waveform**

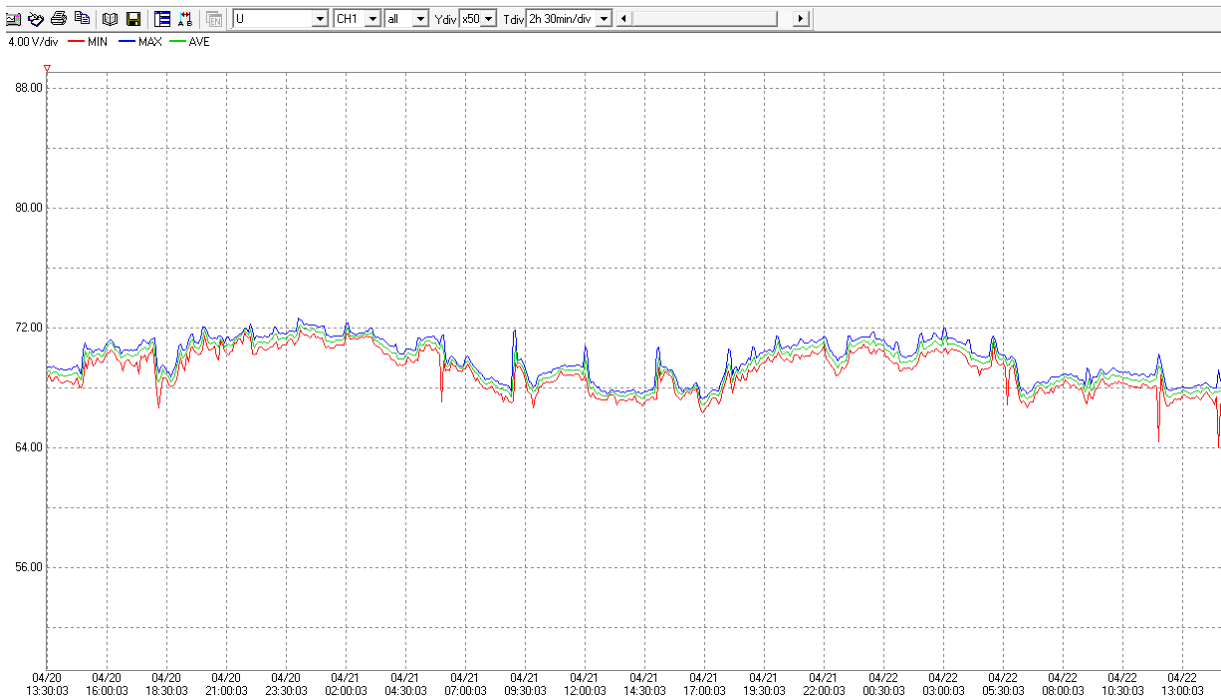


**Figure 4.21: Time plot – Voltage waveform**

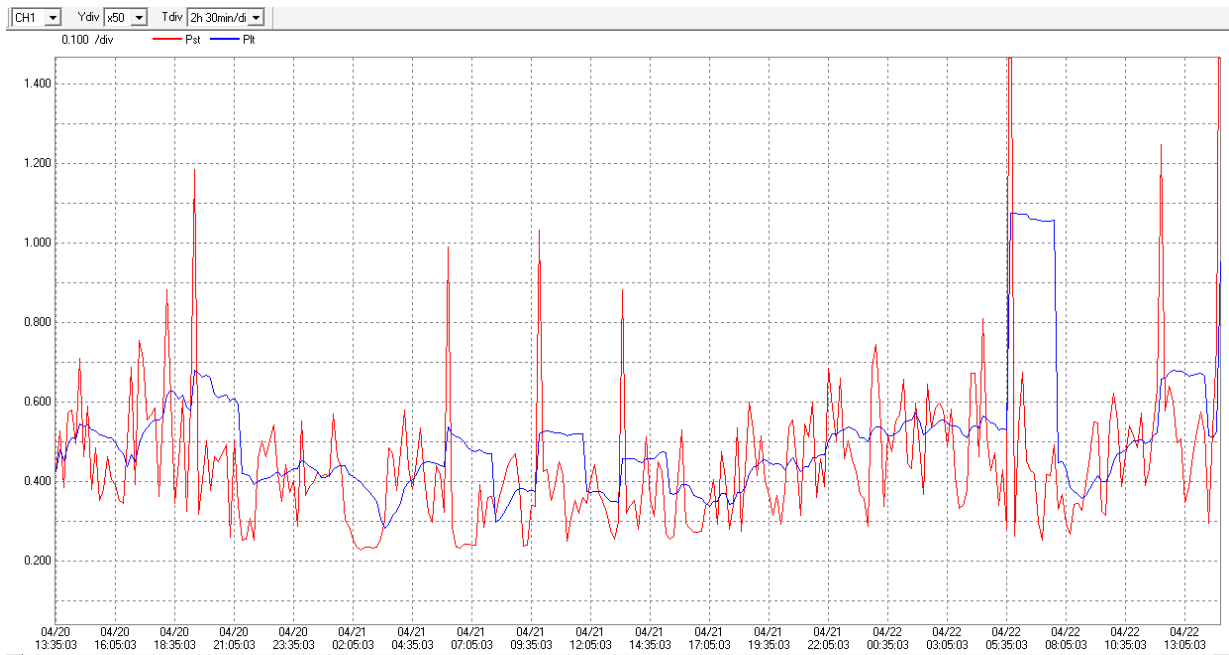


**Figure 4.22: IEC Flicker variation**

## 4.6 Conclusion

The power quality issues related to grid connected wind farm have been recorded and the possible causes are identified. Three power quality analyzers of different manufacturers are used at Pethappampatty Substation, Coimbatore district from 04/13/2012 to 05/24/2012 (43 days). The Power Quality Analyzer, Fluke 435 was installed at individual wind turbine of Pukkulam wind farm with the help of current transformer (3 wattmeter connections). The other Power Quality Analyzer, Dranetz was installed at feeder breaker at Pukkulam substation with the help of step down current transformer. The other Power Quality Analyzer, HIOKI was installed at 110 group control breaker point with help of step down current transformer. About 522 data were recorded during this period and 324 events were found to be repetitive. The remaining 178 events were taken for analysis. Out of 178, about 96 events were Impulsive Transients. About 25 events were Oscillatory Transients, and 53 events were Transients. The remaining 4 events were Sag and Swell. About 96 Impulse transients of time duration of nanosecond to microsecond were recorded. Switching of capacitance, Switching of isolator and Utility fault clearing are the causes for 10% to 20% of voltage spikes. It is observed that the system stability was maintained even with these disturbances. An oscillatory

transient is a sudden change in the steady state condition of the voltage, current or both, at both the positive and negative signal limits, oscillating at the natural system frequency. Only 25 oscillatory transient has been identified. Totally 2 events of Sag and Swell were recorded. The main reason for sag was the sudden increase in the load. It is seen from the recorded graph, voltage drop varied from 40% to 60% of the nominal value. Totally 2 events of Swell due to sudden removal of load and sudden change in wind speed were recorded. Voltage rise was about 10% of nominal value. Two events of Interruption occurred at wind generator station due switching of wind turbine and sudden drop in wind speed for the period ranging from second to minute.

## **CHAPTER 5**

### **DATA COLLECTION AND ANALYSIS OF WIND FARM AT CHINNAPUTHUR SUBSTATION**

#### **5.1 Introduction**

The Chinnaputhur substation was constructed and commissioned by Enercon Pvt Limited in the year 2008 and is located at Dharapuram district. The wind turbines installed in this wind farm are variable speed Permanent Magnet Synchronous Generators (PMSG).

#### **5.2 Substation layout**

The layout of the substation of Chinnaputhur is shown in Figure 5.1. It is seen that the substation has fourteen wind farm feeders (E1- E14) of different rating that are connected to a 22kV bus bar. Each turbine of the wind farm is capable of generating 0.85MW at 0.44kV and is connected to a transformer of rating 0.950MVA, 0.44kV/22kV. This connection is realized with a converter and an inverter control system.

The HT side of the unit transformer of the wind generator is connected to the 22kV bus bar. This 22kV bus bar is connected to 110kV bus bar through the two identical transformers capacity 50MVA, 22/110kV. The capacity of all the 14 wind power feeders (E1- E14) is given in the Table 5.1. The total power generation of the substation is 123.0MW (Table 5.1).

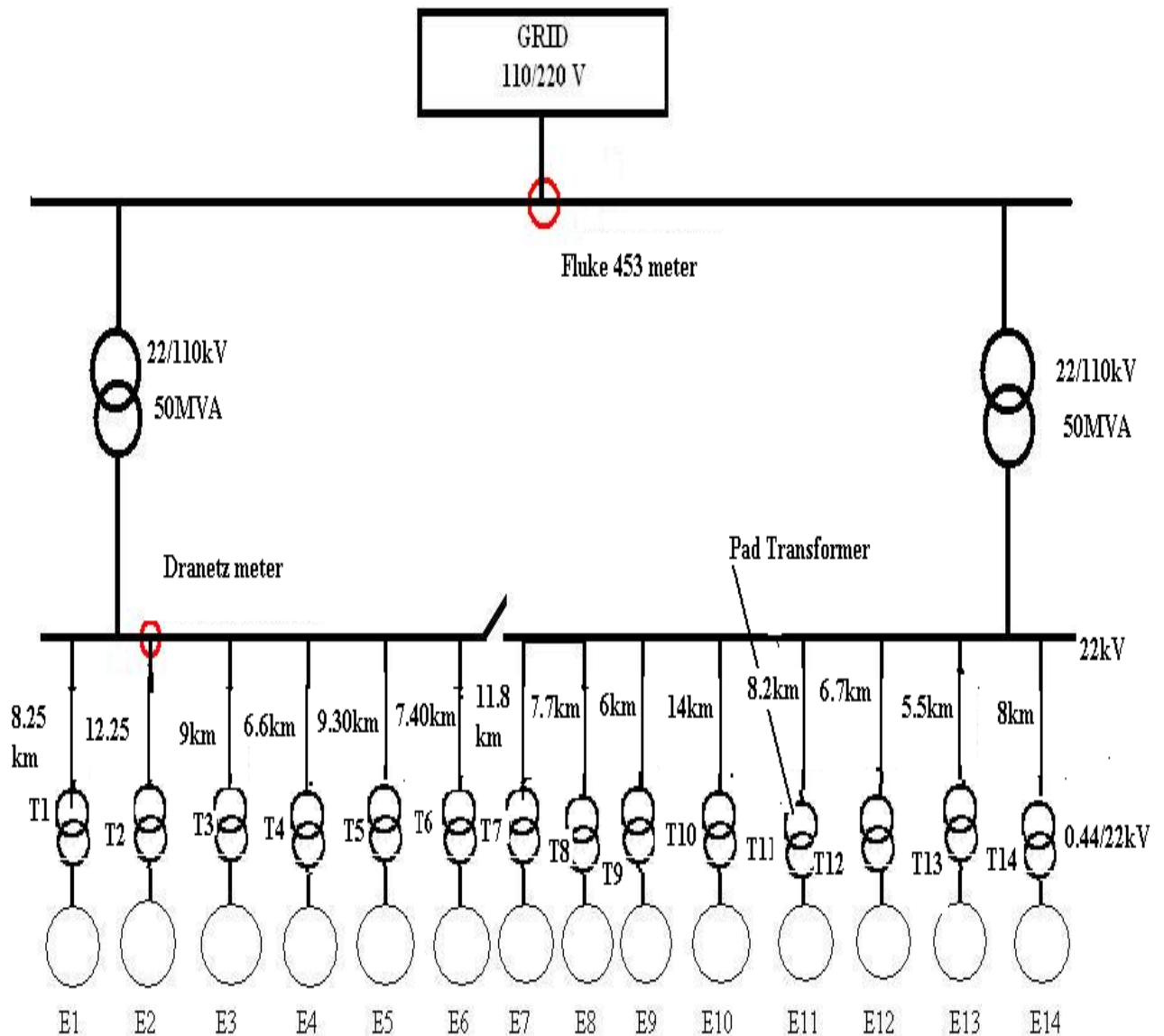


**Figure 5.1: Substation layout of Chinnaputhur**

**Table 5.1: Feeder capacity of the wind farm (E1-E14)**

Si.No	Name of the feeder	Location of equivalent generator from SS (KM)	Capacity of individual wind turbine MW	No of wind turbine	Total capacity MW
1.	E1	8.25	0.85	12	10.2
2.	E2	12.25	0.85	11	9.35
3.	E3	9	0.85	10	8.5

4.	E4	6.6	0.85	10	8.5
5.	E5	9.30	0.85	14	12
6.	E6	7.40	0.85	10	8.5
7.	E7	11.80	0.85	11	9.35
8.	E8	7.75	0.85	7	5.95
9.	E9	6	0.85	10	8.5
10.	E10	14	0.85	12	10.2
11.	E11	8.2	0.85	9	7.65
12.	E12	6.7	0.85	7	5.95
13.	E13	5.5	0.85	10	8.5
			0.30	5	1.5
14.	E14	8	0.85	10	8.5
				<b>Total</b>	<b>123.00MW</b>

In order to analyze the power quality disturbances in the grid connected wind farm, two power quality analyzers namely Fluke 435 and Dranetz meters were installed in the substation from 16/07/13 to 24/08/13 (40 days). The Dranetz was installed at the 22kV feeder E2 and fluke 435 meter was installed at the group control breaker of the 110kV bus bar. The specification as well as the connection details of the both the power quality analyzers were clearly explained in the previous reports 2 and 3. The various power quality events such as sag, swell, transient, interruption, flickering and harmonics were found to occur during the measurement period.

### **5.3 Analysis of recorded events**

Analysis is carried out for the data recorded by the Power Quality measurement instruments. The events recorded are classified as transients, sag, swell and interruption

### 5.3.1 Transients

The various transient events recorded are shown in Figures 5.3- 5.4. The 15% of dip in the voltage occurs during the transient period for the duration of 0.01ms.. The transient occurs due to the switching operation of isolator switch and generator.

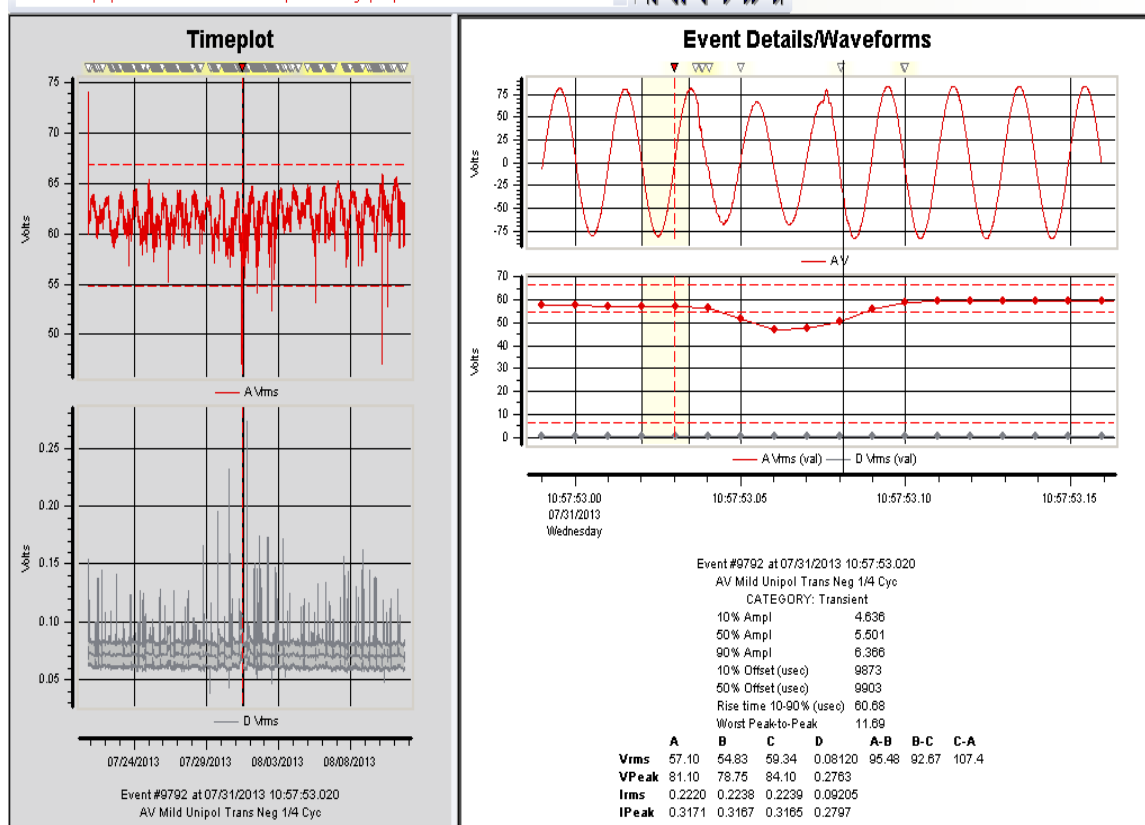


Figure 5.3: Transient Event 9792 on 31/7/13

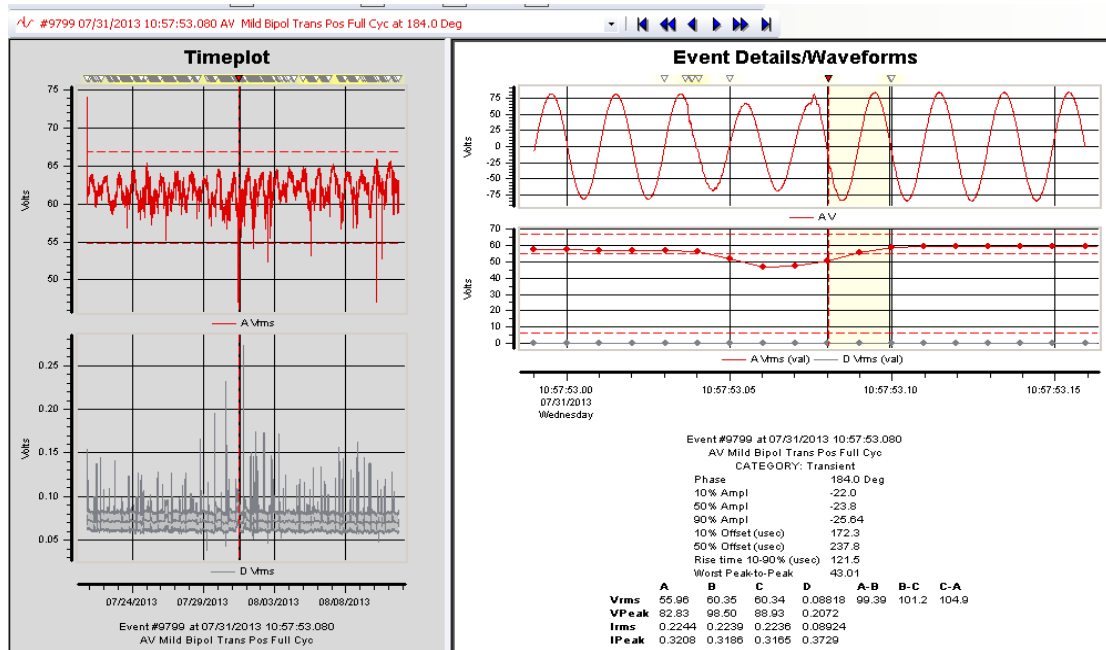


Figure 5.4: Transient Event 9799 on 31.7.13

### 5.3.2 Impulsive transients

The ten Impulsive transient events recorded are shown in Figures 5.5- 5.6. The impulse transient occurs for the duration less than 50usecs due to switching of capacitor and isolator switch.

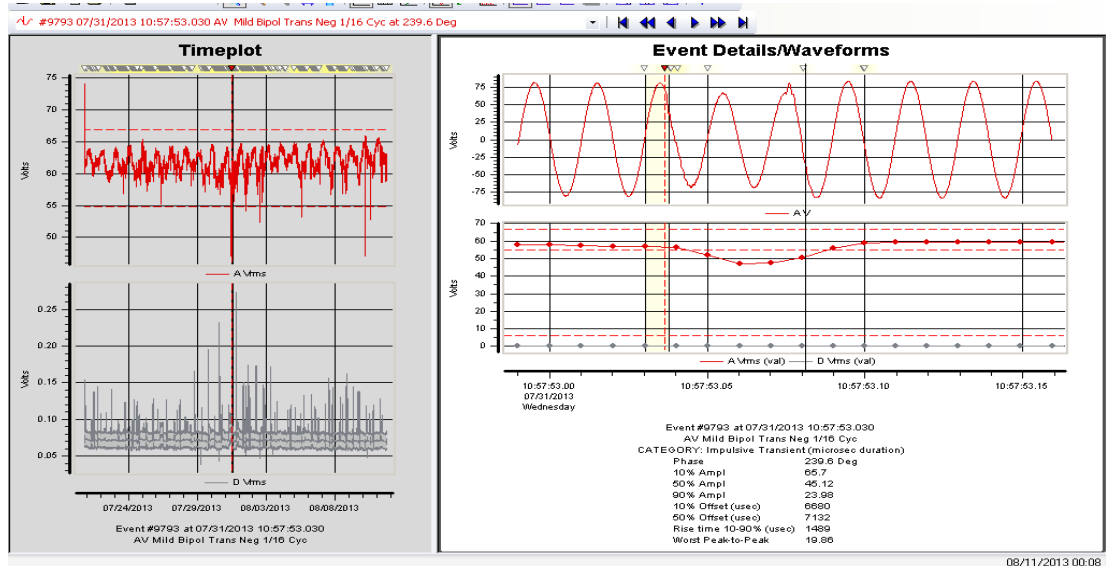
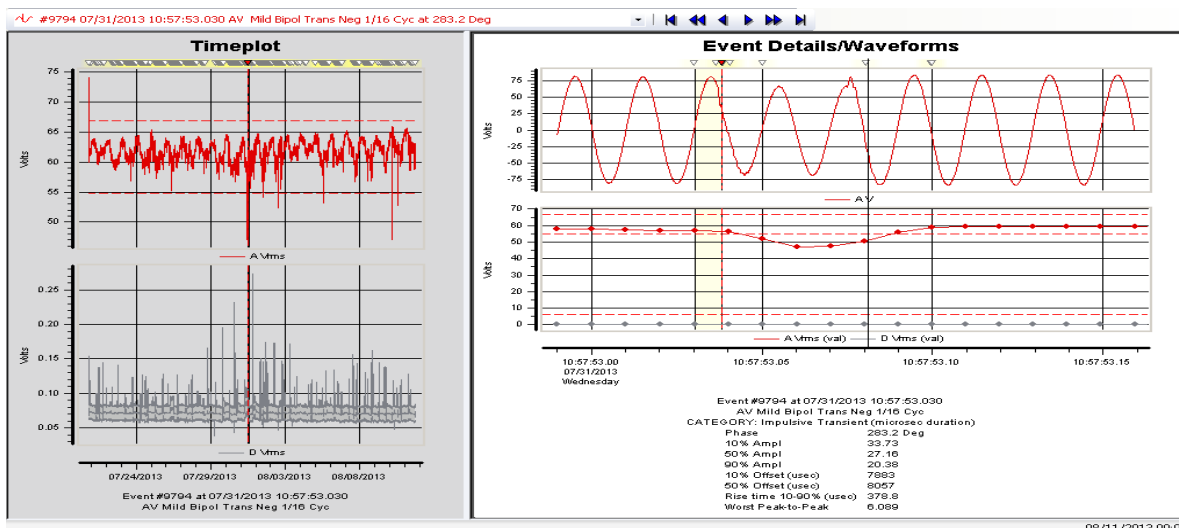


Figure 5.5: Impulsive Transient Event 9793 on 31.7.13



**Figure 5.6: Impulsive Transient Event 9794 on 31.7.13**

### 5.3.3 Sag

The six sag events recorded is shown in Figure 5.7. The instantaneous sag occurs for the duration of two to four cycles due to the symmetrical or unsymmetrical fault at the substation level.

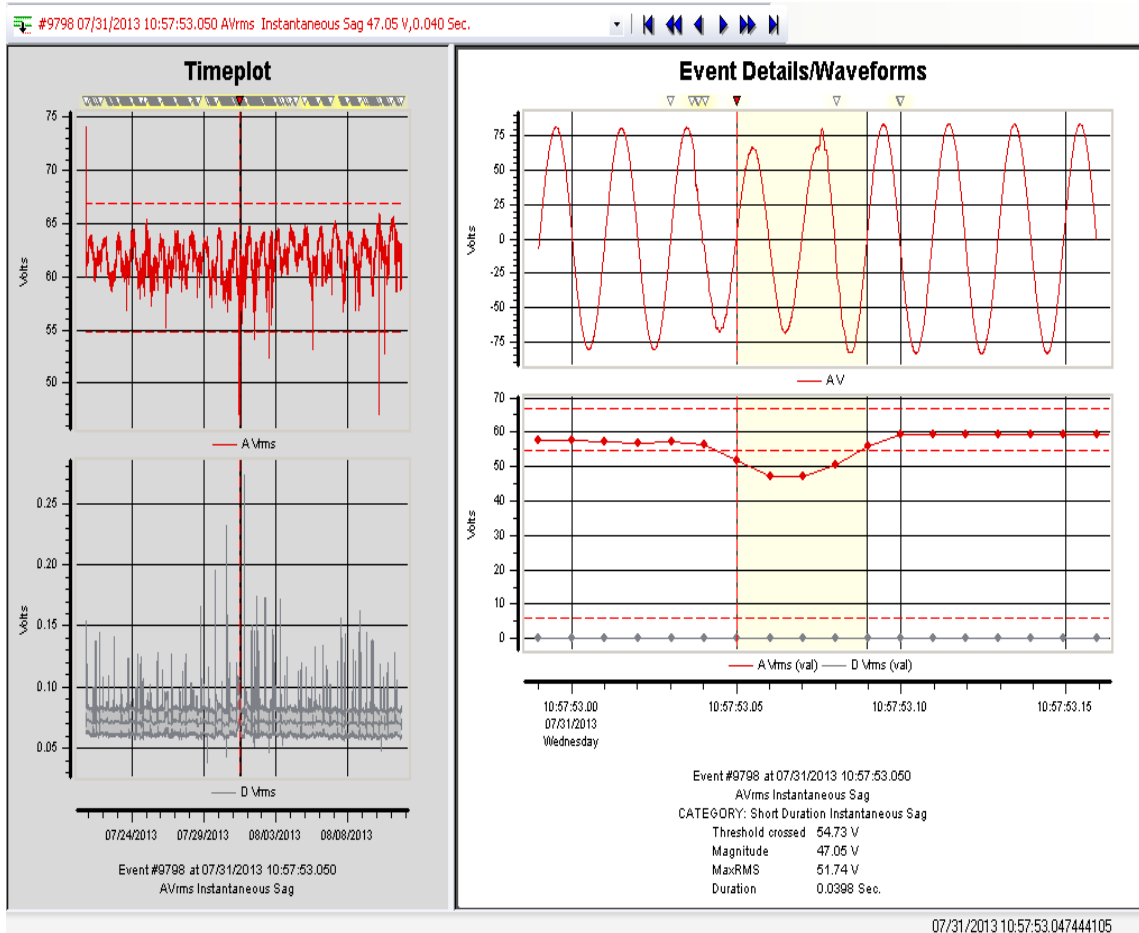


**Figure 5.7: Short duration instantaneous sag event 9798 on 31.7.13**

### 5.3.4. Swell

The only swell event recorded is shown in Figure.5.8. The swell may occur due sudden removal of load for the duration of 0.09 sec.

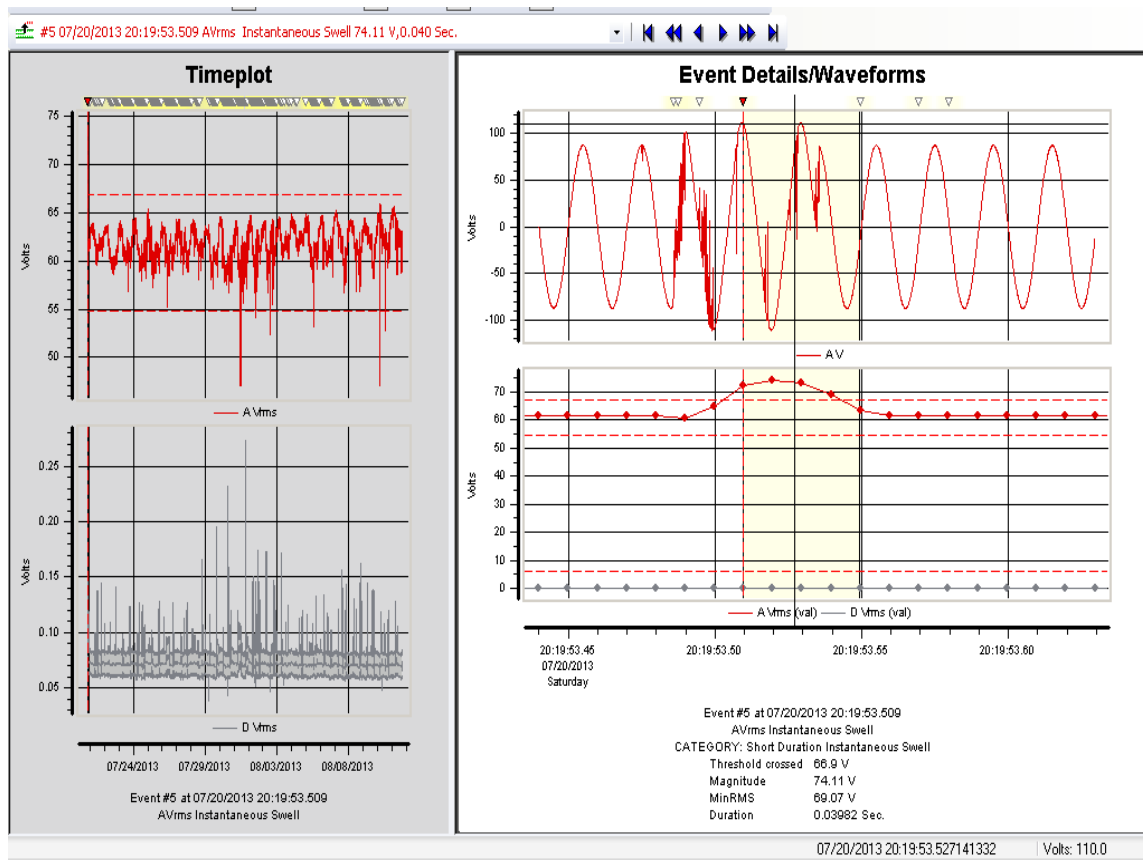


**Figure 5.8: Instantaneous Swell event 03 on 20.7.13**

## 5.4 Analysis of overall recorded events

The overall power quality events are generated using the Dranetz software. The report specifies the variation of the magnitudes of voltage for events such as Transients, Sag and Swell. The variation in magnitude of the current, flickering and harmonics are also given.

### 5.4.1 Voltage time plot

The Figures 5.9 and 5.10 show the variation of voltage magnitude for the observation period as specified according to EN50160 standard. The nominal voltage is identified as 62V. The dotted red line above and below the nominal

voltage specifies the upper voltage and lower voltage limits whose values are 67V and 55V respectively.

During forty days of observation, the magnitude of voltage decreases below the lower limit for six times and increases above the upper limit only once. The drop in voltage below the lower voltage limit is called as Sag and the increase in the voltage above the upper limit is called as Swell. As per the compliance report EN50160 standard, the sags have sustained for the duration of 10 to 100 milliseconds and a swell have sustained for the duration of 10 milliseconds. The occurrence of sag is due to the varying power demand and a fault in the substation and swell may occur due to the removal of load at the distribution level.

There was no interruption during the period of study. Nineteen transient events were observed which might have been caused due to the switching of capacitor bank or isolator.

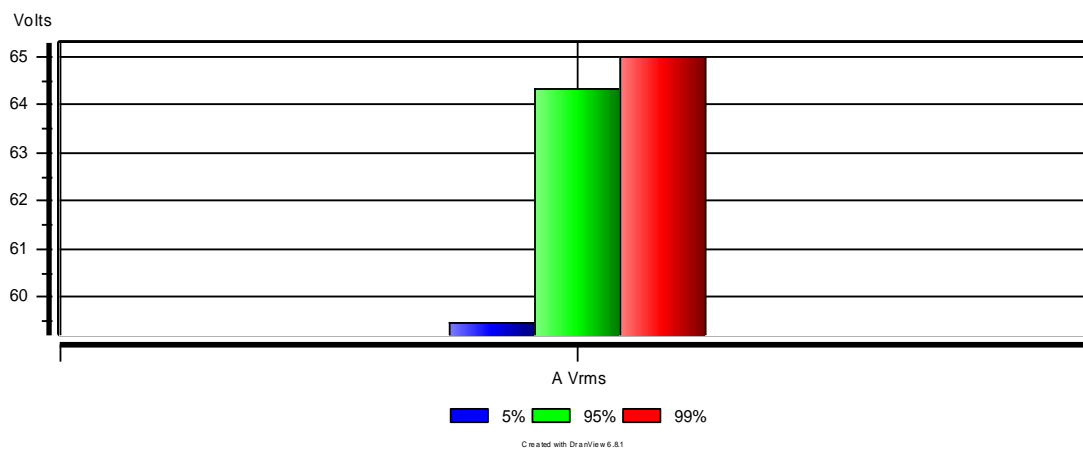


**Figure 5.9: Bar chart of phase voltage, A**

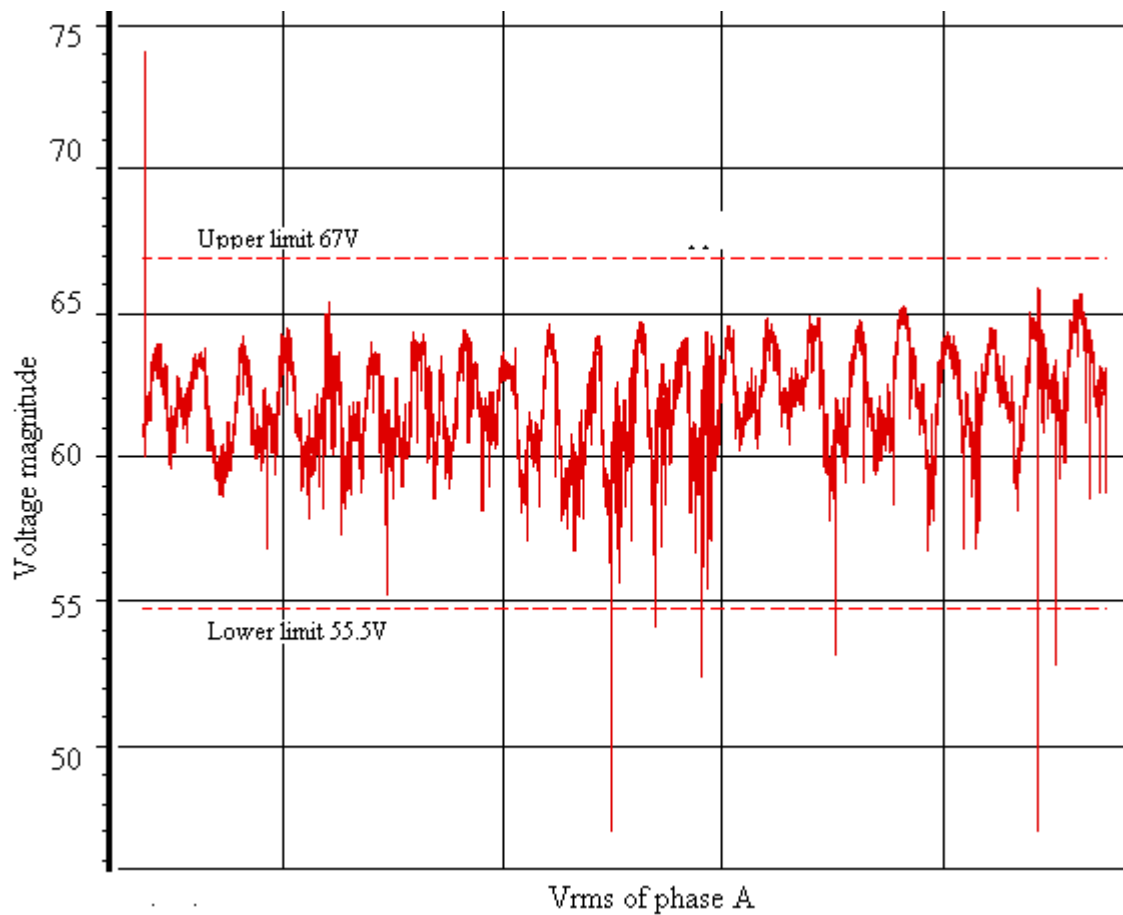


**Figure 5.10: Time plot of phase A voltage magnitude**

#### 5.4.2 Time plot of current

The Figure 5.11 shows the variation of current magnitude during the observation period in compliance with EN50160 standard. The current value rises above 0.75A four times during the period of study and this increase is predicted due to the occurrence of sag.

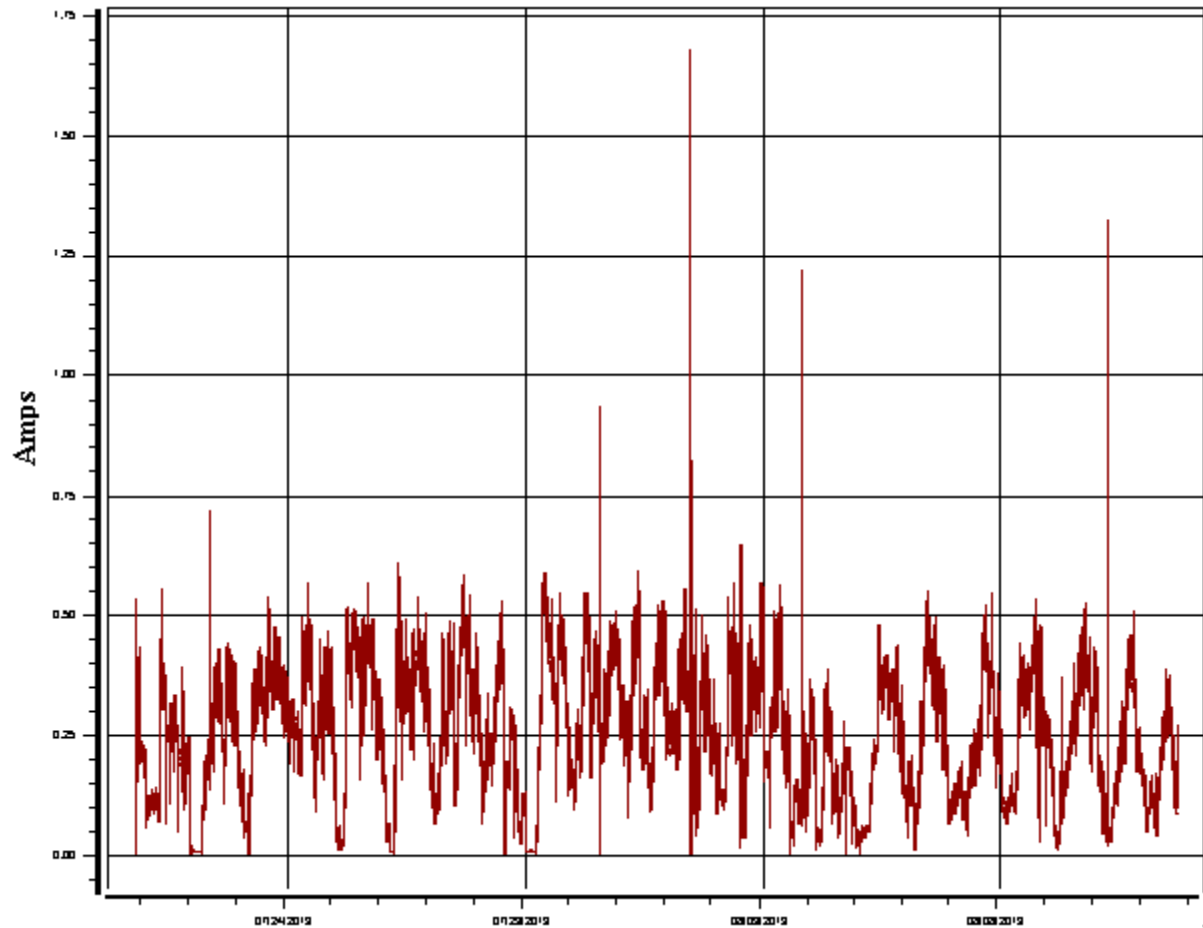


**Figure 5.11: Variation of Current Magnitude**

### 5.4.3 Flickering

The low frequency fluctuation in voltage is referred as flickering. Short term flickering and long term flickering may occur due to the continuous and switching operations in the substation. The acceptable fluctuation limits  $P_{st}$  and  $P_{lt}$  is less than one. The Figure 5.12 shows the flickering events. The  $P_{st}$  and  $P_{lt}$  values increase above one for six times during the observation period.

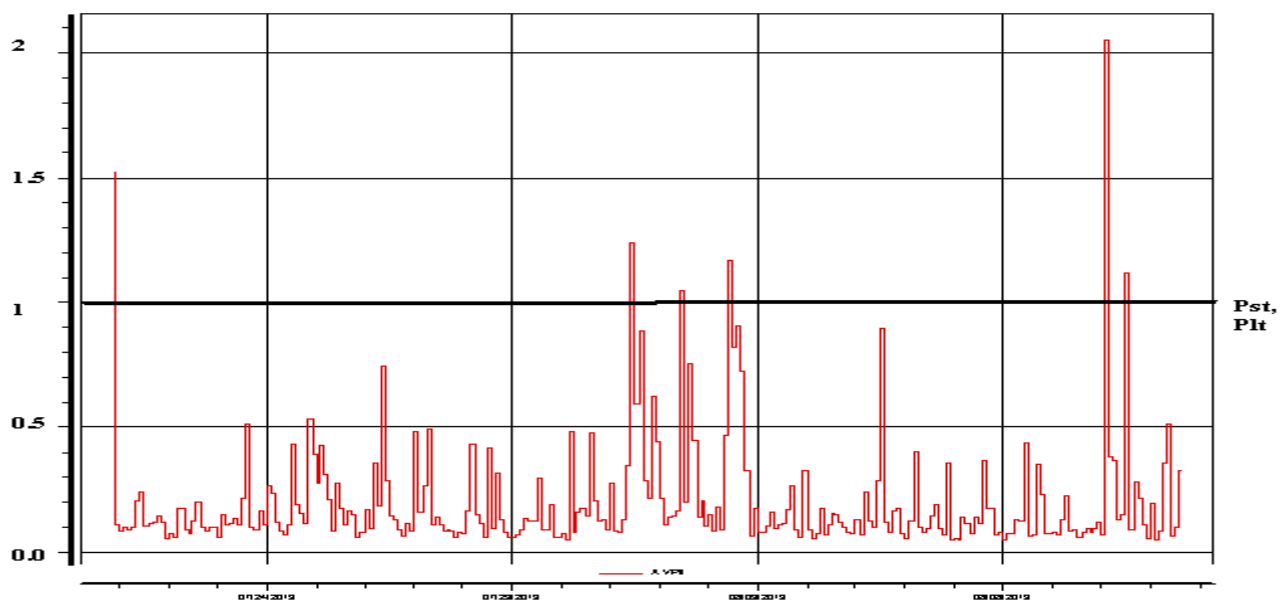


**Figure 5.12: Variation of flickering values**

#### 5.4.4 Frequency

The Figure 5.13 shows the bar chart which depicts the consistency of frequency during the period of study. It was found that 99% of the duration the frequency is maintained below 50.4Hz and 5% of the duration the frequency is below 49.8Hz which may be due to increase in demand.

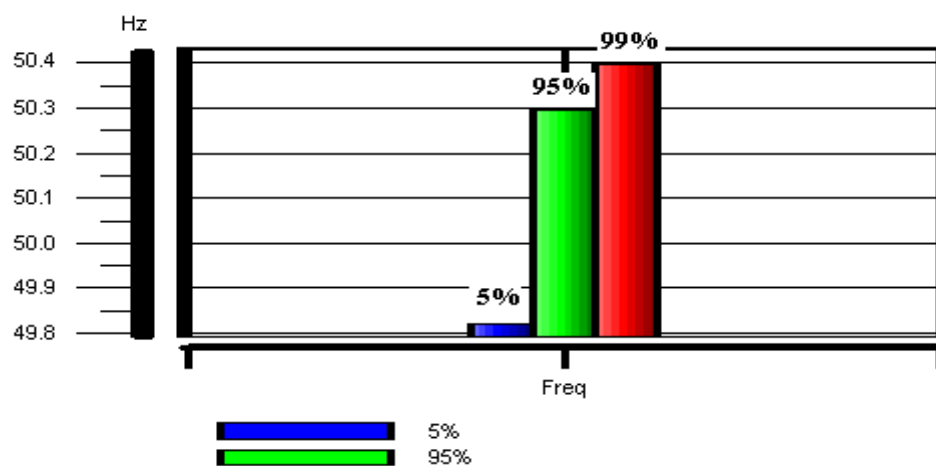


**Figure 5.13: Bar diagram of frequency variation**

## 5.5 Conclusion

The various power quality events of variable speed permanent magnet synchronous generator are analyzed. The Chinnaputhur substation located at Coimbatore district consist of variable speed wind turbines. It has fourteen (E1-E14) wind farms feeders of different capacity which are connected at 22kV bus bar. To analyze the power quality disturbances in grid connected wind farm, two power quality analyzers namely Fluke 435 and Dranetz meters were installed from 16/07/13 to 24/08/13 (40 days). The meter Dranetz was installed at the feeder E2 of wind farm and fluke 435 was installed at the group control breaker of the 110kV bus bar. The various power quality events such as Sag, Swell, Transient and interruption and Flickering were recorded according to EN51620 standard. Totally 22 events were recorded out of which 6 events were sag, 1 event was swell and the remaining events were transient events. The flickering occurs due to continuous and switching operation of the wind turbines. The recorded flickering graph shows the Pst, Plt values are less than 1 for most of the time and it exceeded the value unity almost six times during the measuring period. Therefore, variable speed generator produces less flickering. From the recorded report, the variable speed generator has less number of power quality events than the fixed speed generator.

## CHAPTER 6

### MODELLING AND CONTROLLING CONCEPT OF THE VARIABLE SPEED WIND TURBINE WITH PMSG IN DIgSILENT

#### 6.1 General

A comprehensive dynamic simulation model of the PMSG wind turbine is implemented in the power system simulation software DIgSILENT Power Factory and a control strategy for the entire turbine system is developed. The general structure of the variable speed wind turbine type with full-scale converter is shown in Figure 6.1.

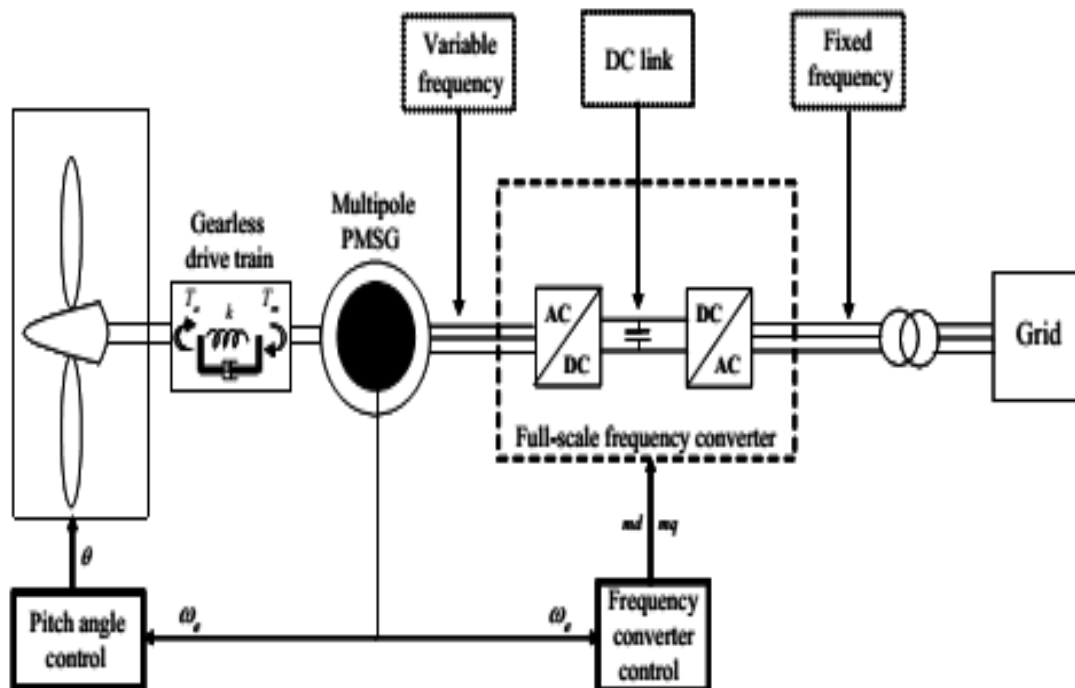


**Figure 6.1: Variable speed multi-pole PMSG wind electric system**

#### 6.2 Simulation tools

The models of the wind speed, the mechanics, aerodynamics and the control systems of the wind electric system are written in the dynamic simulation

language (DSL) of the DIgSILENT. The DSL makes it possible for the users to create their own blocks either as modifications to the existing models or as completely new models. These new models can be collected into a library, which can be easily used further in the modeling of other wind farms and wind turbines. The DIgSILENT provides a comprehensive library of models of electrical components in power systems. The library includes models of generators, motors, power electronic controllers, dynamic loads and various passive network elements such as lines, transformers, static loads and shunts. Therefore, in the modeling, the grid model and the electrical components of the wind turbine model are taken from the standard components in the existing library.

The Figure 6.2 shows the modeling scheme of the PMSG wind turbine and its control concept. The whole model includes the models for both the aerodynamical and mechanical system as well as for the electrical system and its control structure. The built-in models for all the electrical components (generator model, converter models, transformer model, grid model) are provided in the DIgSILENT library and they are marked by the yellow blocks. The models for all mechanical components (wind, aerodynamics, drive train model) and for the total control system developed by the user are marked in Figure 6.2 by the grey blocks.

The frequency converter control of the PMSG is divided into two types: a control for the grid side converter and a control for the generator side converter. The frequency converter control is coordinated with the pitch angle control of the rotor blades.

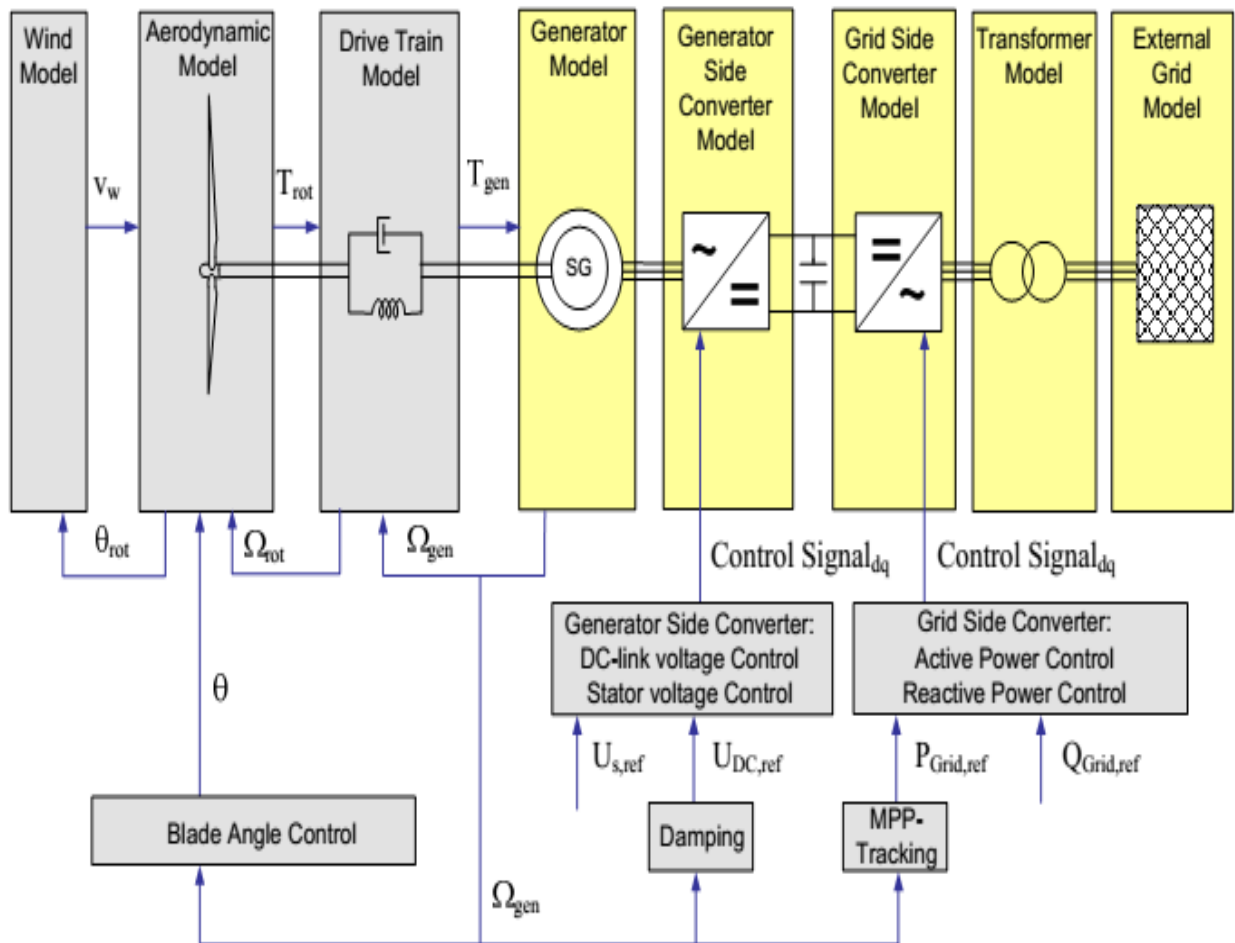


**Figure 6.2: Modelling scheme and control concept of the variable speed wind turbine with PMSG**

$V_w$ - Wind Velocity

$\Omega_{rot}$ -Angular velocity of the Turbine rad/sec

$\Omega_{gen}$ - Angular velocity of the Generator rad/sec

$P_{grid}$  – Real power at the Grid side

$Q_{grid}$ - Reactive power at the Grid side

$U_s$ - Stator voltage of the generator

$T_{rot}$ -Wind Turbine Torque

$T_{gen}$ -Generator Torque

The DIGSILENT has the ability to simulate load flow, RMS fluctuations and transient events in the same software environment. It provides models on different levels of the detailing. It combines the models of electromagnetic transient simulations of the instantaneous values with the models of the electromechanical simulations of RMS values. This makes the models useful for the studies of grid fault, the power quality and control issues.

The developed model will be able to support the analysis of the interaction between the mechanical structure of the wind turbine and the electrical grid both during normal operation of the wind turbine and during the transient grid fault events. The dynamic interaction between a wind turbine/wind farm and a power system are simulated by using RMS simulation in the DIgSILENT. In the recent years, the trend has been moved from the installations of a few wind turbines to the large wind farms with several hundred MW of capacity. This situation means that future wind farms must be able to replace conventional power stations, and thus be active controllable elements in the power supply network. In other words, wind farms must develop power plant characteristics. The TNEB utility which is responsible for the transmission systems in Tamil Nadu has issued requirements that focus on the influence of wind farms on the grid stability and the power quality and on the control capabilities of the wind farms.. The E2 wind power feeder of Chinnaputhur substation is simulated to study the various power quality issues and their causes.

### **6.3 Simulation model of individual blk using dsl**

In this simulation model, mechanical side control and converter side control of variable speed PMSG are modeled independently. The mechanical side control consists of wind speed blk, shaft blk, pitch angle control blk, speed measurement blk and machine blk and are connected together to generate the electrical energy. The generated electrical energy is controlled with help of generator side converter. The converter side control consists of converter blk, inverter blk, maximum power point tracking blk, grid side controller blk and generator side controller and they are connected together. The converter system controllers generate a constant stator voltage, real power and necessary reactive power at all the power system condition such as load variation and fault. In this section, modeling of individual blocks in the DSL and their interconnection together are explained.

### 6.3.1 Modeling of mechanical side block

The mechanical side control consist of wind speed blk, shaft blk, pitch angle control blk, speed measurement blk and synchronous machine blk. The model of wind speed blk, shaft blk, and pitch angle blk were explained in the report 4 already submitted. With the help of frame model, the individually developed blk are integrated together. The composite model is used connect the wind electric system to the grid.

#### 6.3.1.1 Speed measurement

The speed measurement block definition is included in this model to measure the speed of the generator. This speed variable is used as the input data for the maximum power point tracking control. In this block the variable, speed\_gen represents the rotor speed of generator and hpi represents the rotor angle and these variables are the input signals to the speed measurement blk. The signal, speed is the output variable as shown in Figure 6.3. The parameter variable  $f_{nom}$ , nominal frequency of the generator, is also entered.

The screenshot shows the 'Block Definition' dialog box for a block named 'Speed Measurement'. The dialog is divided into several sections:

- Basic Data:** Name is 'Speed Measurement', Title is empty, and Level is 'Level 3: Level 2 + lim()-function precise in time'. There is a warning message: 'Caution: Changing level of already used models requires adaptation of all dependent models!'. The 'Automatic Calculation of Initial Conditions' checkbox is unchecked.
- Classification:** The 'Linear' checkbox is checked, while 'Macro' and 'Matlab' are unchecked.
- Upper Limitation:** Fields for 'Limiting Parameter' and 'Limiting Input Signals' are present. The 'Parameter Name' is 'sUpLimPar'.
- Lower Limitation:** Fields for 'Limiting Parameter' and 'Limiting Input Signals' are present.
- Variables:**
  - Output Signals: speed
  - Input Signals: speed\_gen, hpi
  - State Variables: (empty)
  - Parameter: fnom
  - Internal Variables: (empty)

On the right side of the dialog, there are buttons for 'OK', 'Cancel', 'Contents', 'Equations', 'Macro Equat.', 'Check', 'Check Inc.', 'Pack', 'Pack->Macro', and 'Encrypt'.

**Figure 6.3: Speed Measurement block for defining the variable**

The mathematical equations developed for the speed measurement block are entered in the block definition as shown in Figure 6.4.

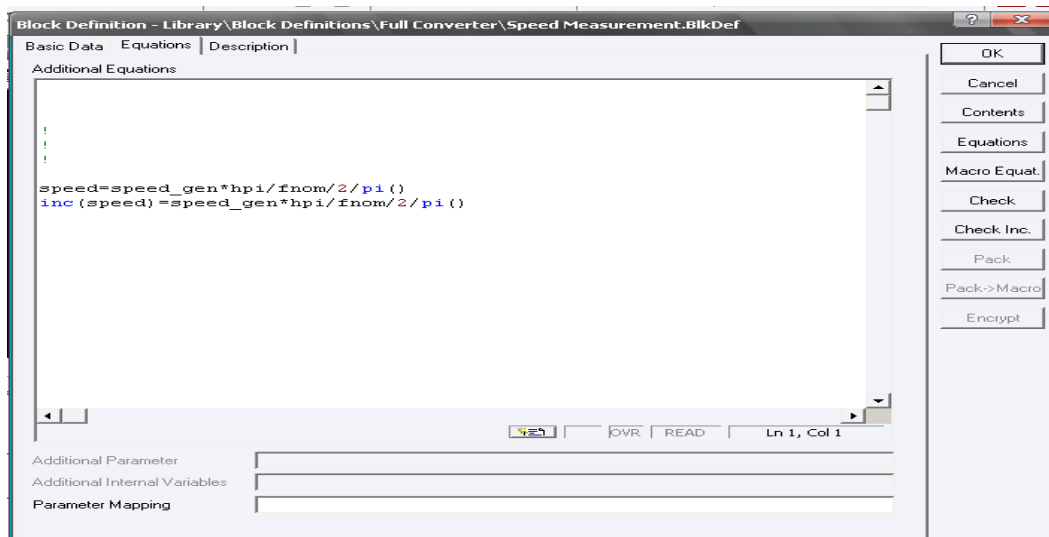


**Figure 6.4: Speed Measurement block for entering the equation**

### 6.3.1.2 Synchronous Generator Model

The synchronous generator namely, Sym Elm blk, available in library has been selected for the wind electric generator. The synchronous generator is modeled in the DIgSILENT using the models described in the literature (Kundur P., 1994). The synchronous generator parameter data such as steady state reactance, sub transient reactance and transient reactance values are entered as shown in Figure 6.5. The acceleration time constant value is used to control the rotor damping. In this SymElm blk (synchronous machine block),  $P_t$ , turbine power and  $v_e$ , the excitation voltage are given as the input and  $x_{speed}$ , the speed of machine in p.u and  $h_{pi}$ , the rotor angle, are taken as the output.

**Synchronous Machine Type - Library**

State Estimator	Reliability	Generation Adequacy	Tie Open Point Opt.	Description
Basic Data	Load Flow	VDE/IEC Short-Circuit	Complete Short-Circuit	
ANSI Short-Circuit	IEC 61363	RMS-Simulation	EMT-Simulation	Harmonics
				Optimization

**Inertia**

Acceleration Time Const. (rated to Pgn)  s

Mechanical Damping  p.u.

**Stator Resistance/Leakage Reactances**

rstr  p.u.

xl  p.u.

xrl  p.u.

**Rotor Type**

Salient pole

Round Rotor

**Synchronous Reactances**

xd  p.u.

xq  p.u.

**Transient Time Constants**

Td0'  s

**Transient Reactances**

xd'  p.u.

**Subtransient Time Constants**

Td0''  s

Tq0''  s

**Subtransient Reactances**

xd''  p.u.

xq''  p.u.

Main Flux Saturation

**Figure 6.5: Synchronous machine windows for setting the generator parameter**

### 6.3.1.3 Frame

A Frame is a type of block definition which includes a number of slots for integrating the various blocks defined. The variable speed wind electric system is developed with generator PMG and PWM converter frames. The PWM converter frame connects the power electronic component blk, grid side and generator side controller blks. The Generator PMG frame connects the built in blocks from the wind source to generator side. All the individual blocks such as Turbine blk, Shaft model blk, Pitch angle controller blk, built in model of synchronous Machine (Sym blk) are connected together as shown in Figure 6.6. When a slot in the frame definition is selected the project block gets opened where in the number of functional block already defined are displayed.

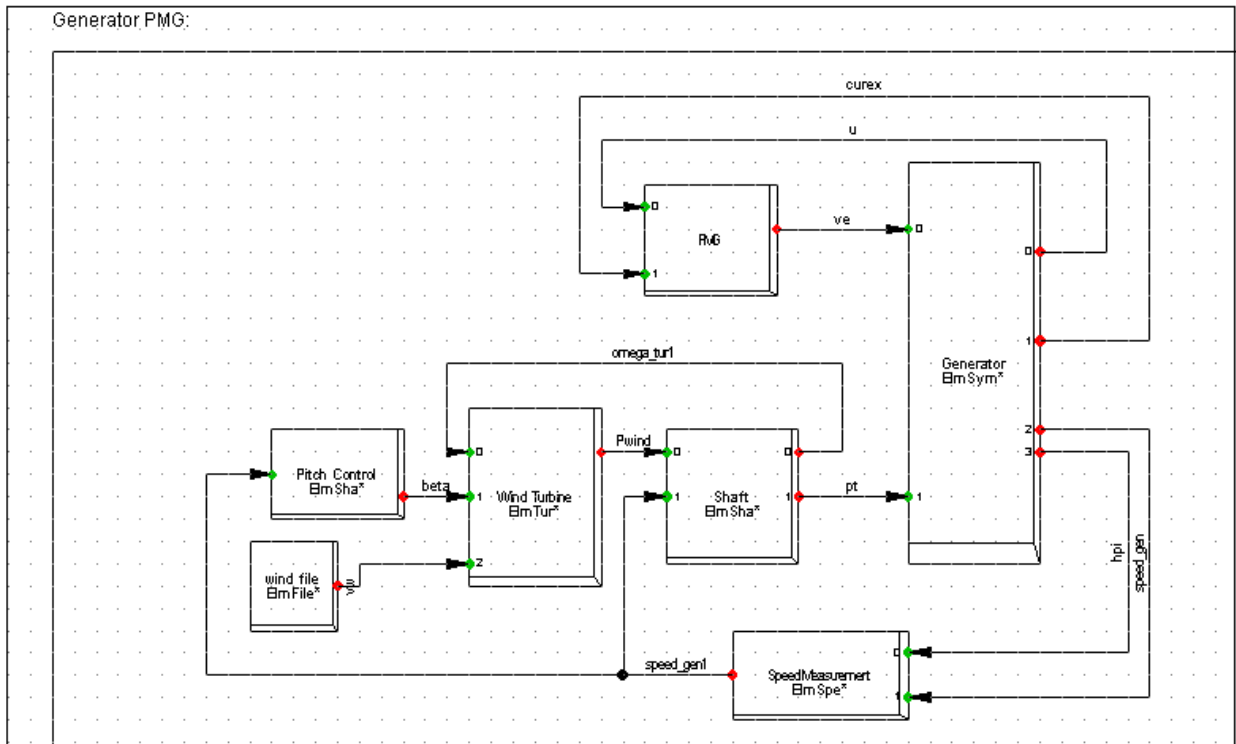


**Figure 6.6: Frame definition to form slots to integrate the Generator PMG blocks**

#### 6.3.1.4 Composite model

In the frame definition, the wind electric generator system is modeled to integrate all the blocks that have been discussed in the previous section. In order to connect the wind electric system to the grid, the composite model is used. In the composite model a frame is selected for linking the individual slots to the variables of the common model. The various slots and their linking to the common block variables are shown in Figure 6.7.

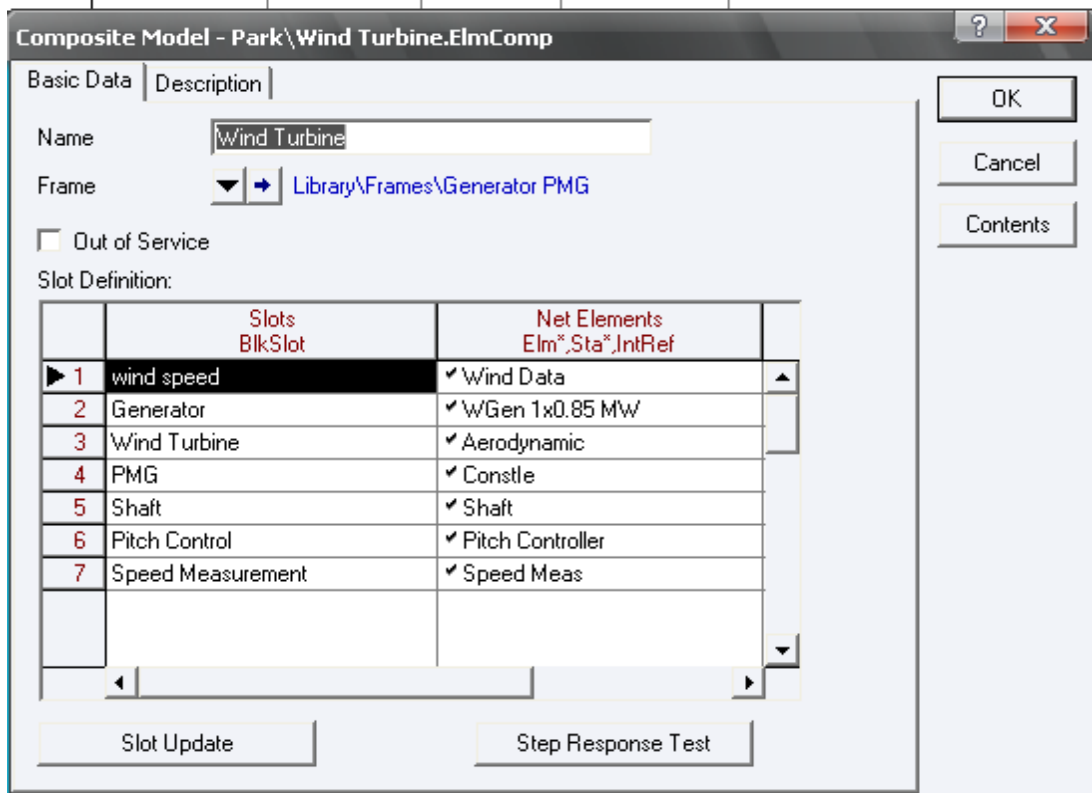


**Figure 6.7: Composite model of Generator PMG**

### 6.3.2 Modeling of frequency converter

The PWM converter frame consists of converter blk, inverter blk, maximum power point tracking blk, grid side controller blk and generator side controller. The individual built in blk are integrated together with help of frame. The Figure 6.8 shows the overall grid side and generator side controller block.

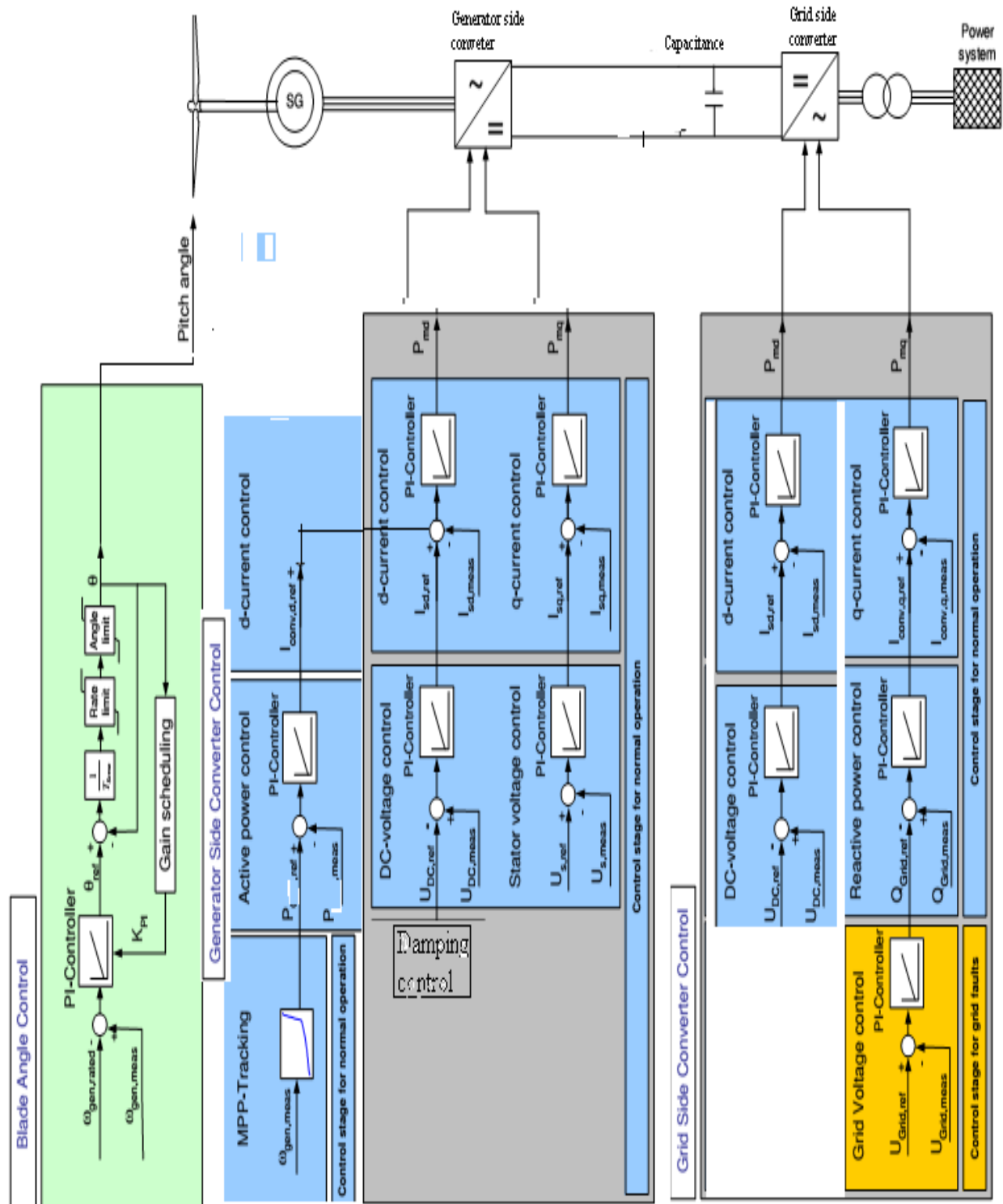
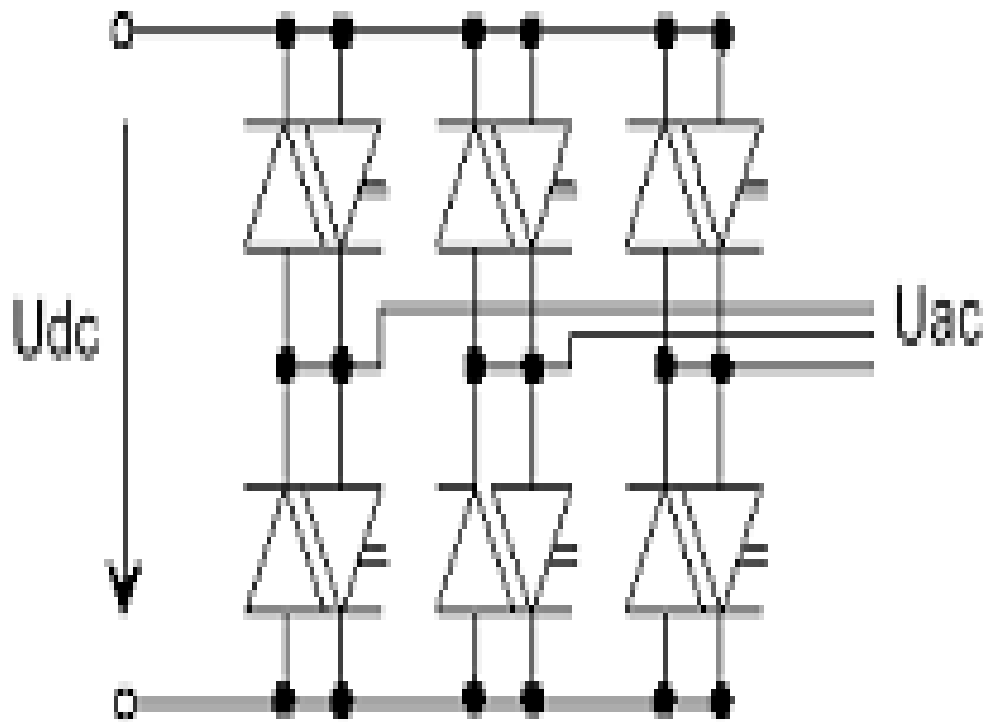


Figure 6.8: Grid and Generator side controller block in DigSILENT

### 6.3.2.1 Frequency converter

The power converters used in wind turbine application are usually realized by self commutated pulse-width modulated circuits. The voltage source AC/DC converter equivalent circuit is shown in Figure 6.9.



**Figure 6.9: Generic PWM converter model**

These circuits are built with six switches with turn-off capability and six anti parallel diodes. The switches are typically realized by IGBTs because they allow for higher switching frequencies than the classical devices. The general model of the PWM converter that usually operated as a voltage source converter is illustrated in Figure 6.10.

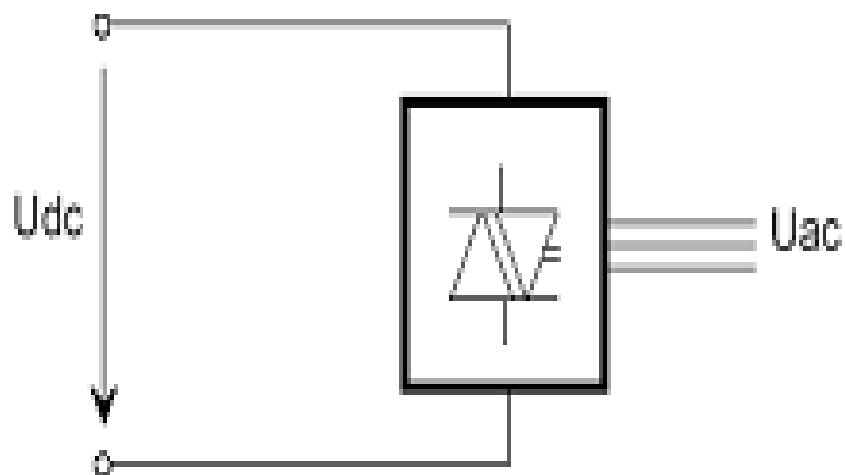


**Figure 6.10: PWM converter –General model**

In load flow analysis, the PWM converter model supports several control conditions.

The supported control conditions are as follows:

- Vac-phi – Specifies magnitude and phase of the AC terminal voltage. It is typical control mode is for the motor-side converters in variable speed applications.
- Vdc-phi – Specifies the DC-voltage and the AC-voltage phase. No specific application.
- PWM-phi – Load flow setup without control. The PWM index and phase are directly set.
- Vdc-Q – Specifies DC-voltage and reactive power. Typical applications: STATCOM, UPFC, grid-side converter for doubly-fed induction machine.
- Vac-P - Specifies AC-voltage magnitude and active power. This mode is equivalent to a PV characteristic of synchronous generators. Typical applications: Grid-side converter control driven synchronous machines and VSC.
- P-Q – Specifies P and Q at the AC-side. This control is equivalent to a PQ characteristic of synchronous machines. Typical applications: Grid-side control of converter driven synchronous machines, VSC.

Since the model is based on the fundamental frequency approach, the load flow calculations will assume always a frequency as defined in the external grid. Then, the voltage angle for each bus bar is calculated with respect to the global reference. For all the control conditions in the load flow analysis the frequency is not a controlled variable.

The control variables for the stability model are defined in 4 ways depending on the applications (DIgSILENT, 2006):

- A.  $P_{mr}$ ,  $P_{mi}$ – Real and imaginary part of the PWM index. The reference system in this case is the global reference frame, which is usually defined by a reference-machine, external network, voltage source or a PWM converter. This set of inputs must be always used in combination with phase measurement devices e.g. Phase Locked Loop (PLL) and transformation between reference frames.
- B.  $P_{md}$ ,  $P_{mq}$ ,  $\cos\text{ref}$ ,  $\sin\text{ref}$ – This set of input is used in grid connected applications. The PWM Index-vector is specified with reference to a reference system, which is defined by  $\cos\text{ref}$  and  $\sin\text{ref}$ . For example the outputs from the current controllers are connected to  $P_{md}$  and  $P_{mq}$  while the voltage is measured using a PLL and its output gives the  $\cos\text{ref}$  and  $\sin\text{ref}$  signals.
- C.  $P_{m\_in}$ ,  $d\phi_{iu}$  – magnitude and phase of the PWM Index. This representation is equivalent to  $P_{mr}$ ,  $P_{mi}$ . The phase of PWM Index  $d\phi_{iu}$  is expressed with reference to the global reference frame.
- D.  $P_{m\_in}$ ,  $f_0$  (50Hz) –  $P_{m\_in}$  is the magnitude of the PWM index and  $f_0$  permits varying the frequency of the output voltage. The control variable  $f_0$  defines the frequency in p.u., the base value 50Hz. This input pair “is especially useful in variable speed-drive applications, in which a PWM converter is used for driving an induction machine.

### 6.3.2.2 Generator side controller

The stator voltage of the generator and the voltage of the DC-link with respect to real power are regulated. The controller is equipped with fast current loop. The current reference values are derived from the voltage regulators as indicated in Figure 6.11.

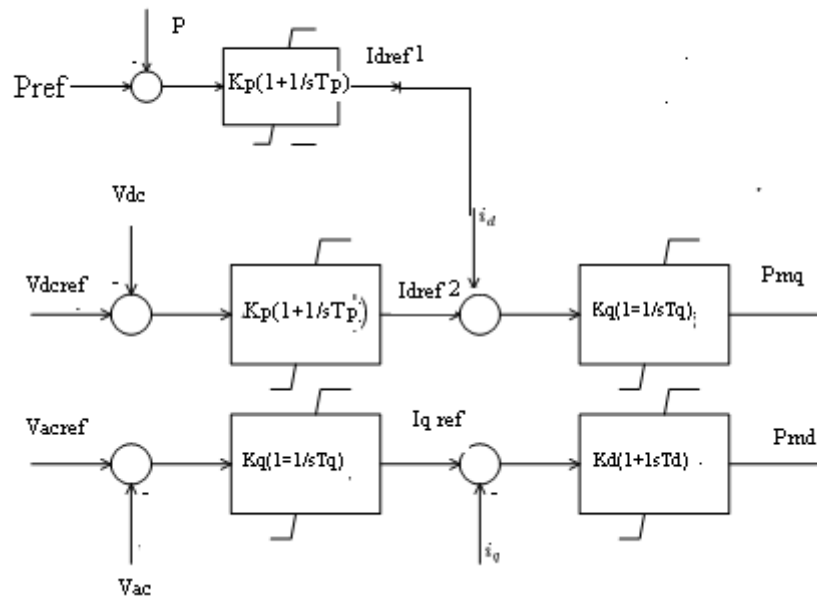


**Figure 6.11: Model of generator side converter controller in DIGSILENT**

The generator controller blocks are built with block definition to control the real and reactive power generation. The input signals are  $V_{dc}$ ,  $V_{ac}$ ,  $V_{dc\_ref}$  and  $V_{ac\_ref}$ , The output signals are  $id\_ref$  and  $iq\_ref$ . The parameters are:  $T_{fp}$ ,  $T_{fVac}$ ,  $T_{fVdc}$ ,  $T_p$  and  $K_p$ . The internal variables are:  $I_{max}$ ,  $I_{min}$ ,  $\Delta V$ ,  $dV_{ac}$ ,  $dV_{dc}$  and  $id\_ref$  as shown in Figure 6.12. The sub blocks of the generator controller model are MeasFlit blk, PI controller blk, absolute blk as shown in Figure 6.13.

The DC voltage ( $V_{dc}$ ) measured at the DC busbar,  $V_{dc\_ref}$  voltage measured from system damping and  $P_{ref}$  measured from look table of MPT block, the real power ( $P$ ) is measured at the generator busbar with help of in-built power measurement blk are connected to the PI controller through the summing point to track the  $V_{dc}$ . The AC voltage ( $V_{ac}$ ) is measured at the generator busbar and  $V_{ac\_ref}$  voltage are connected to the PI controller through the summing point to track the  $V_{ac}$ . The outputs of the PI controllers are  $id_{ref}$  and  $iq_{ref}$  and are connected to the converter. The modulation indices  $P_{md}$  and  $P_{mq}$  are varied and these depend on the error signals.

Basic Data	Equations	Description
Name	<input type="text"/>	
Title	<input type="text"/>	
Caution: Changing level of already used models requires adaptation of all dependent models!		
Level	Level 3: Level 2 + lim()-function precise in time	
<input type="checkbox"/> Automatic Calculation of Initial Conditions		
Classification		
<input checked="" type="checkbox"/> Linear		
<input type="checkbox"/> Macro		
<input type="checkbox"/> Matlab		
Upper Limitation		
Limiting Parameter	<input type="text" value="i_Max,iMax"/>	
Limiting Input Signals	<input type="text"/>	
Lower Limitation		
Limiting Parameter	<input type="text" value="i_Min"/>	
Limiting Input Signals	<input type="text"/>	
Variables		
Output Signals	<input type="text" value="id_ref,iq_ref"/>	
Input Signals	<input type="text" value="Vac,Vac_ref,Vdc,Vdc_ref,sw"/>	
State Variables	<input type="text" value="xVac,xVdc,xVac_ref,xVdc_ref"/>	
Parameter	<input type="text" value="Kp,Tp,KVac,Tp,deltaVdc"/>	
Internal Variables	<input type="text" value="Imax,Imin"/>	

**Figure 6.12 Definition of variables in Generator side controller**

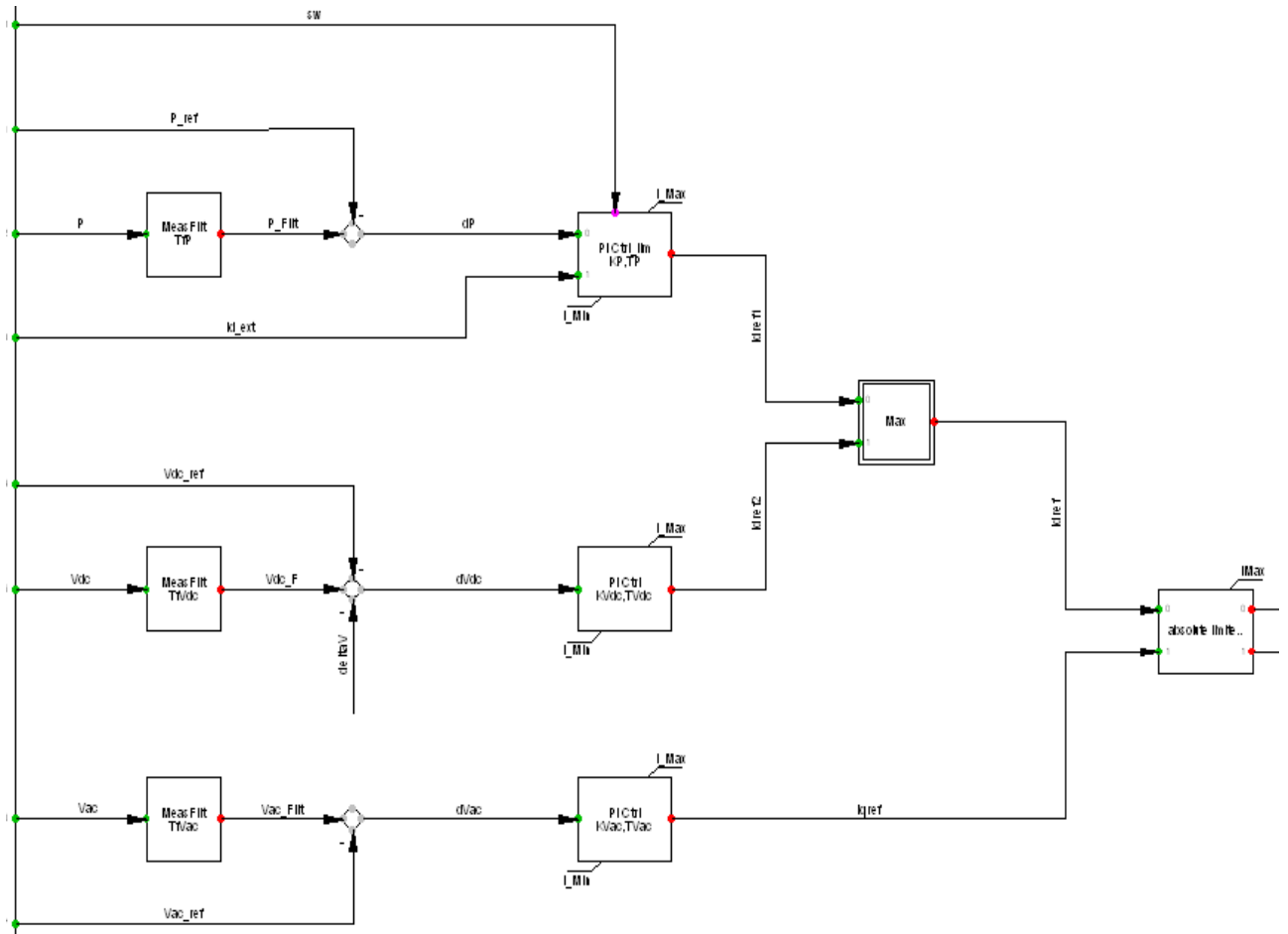


**Figure 6.13** Block definition of Generator side controller

### 6.3.2.3 Grid side controller

The DC voltage and reactive power at the grid terminal are controlled by grid side controller is shown in Figure 6.14. The block definition are built with the input signals are  $V_{dc}$ ,  $Q_{ref}$ ,  $V_{dc\_ref}$ ,  $V_{ac\_ref}$ ,  $P_{ref}$  and  $P$ . The output signals are  $P_{md}$  and  $P_{mq}$ . The parameters are  $T_{fp}$ ,  $T_{fVac}$ ,  $T_{fVdc}$ ,  $T_p$  and  $K_p$ ,  $i_{max}$ ,  $i_{min}$ . The internal variables are  $I_{max}$ ,  $I_{min}$ ,  $\Delta V$ ,  $dV_{ac}$ ,  $dV_{dc}$ ,  $i_{dref}$ ,  $i_{qref}$  and  $i_q$  as shown in Figure 6.15.

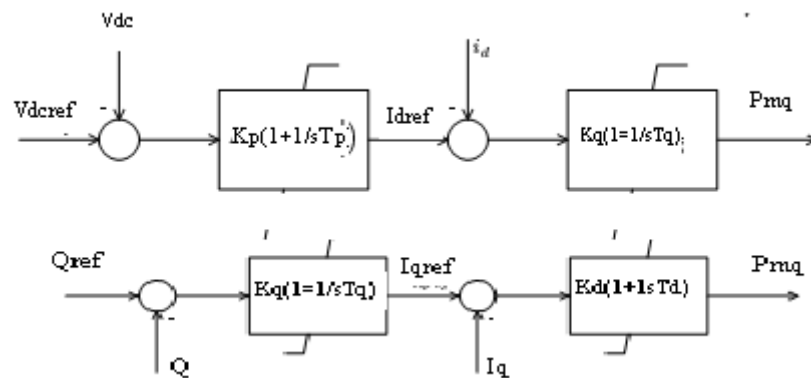


**Figure 6.14: Model of Grid side converter controller in DIgSILENT**

The sub blocks of the grid controller model are MeasFlit blk , PI controller blk, absolute blk as shown in Figure 6.16.

The reactive power ( $Q$ ) is measured at the grid bus bar with help of power measurement .The variables  $Q$  and  $Q_{ref}$  are connected to the PI controller through the summing point to control the reactive Var. The  $V_{dc}$  is measured at the capacitance busbar and  $V_{dc\_ref}$  are connected to the PI controller through the summing point to reduce the steady state error. The output of the PI controllers is  $i_{dref}$  and  $i_{qref}$  is connected to the rectifier, where the modulation indices  $P_{md}$  and  $P_{mq}$  vary with the error signals.

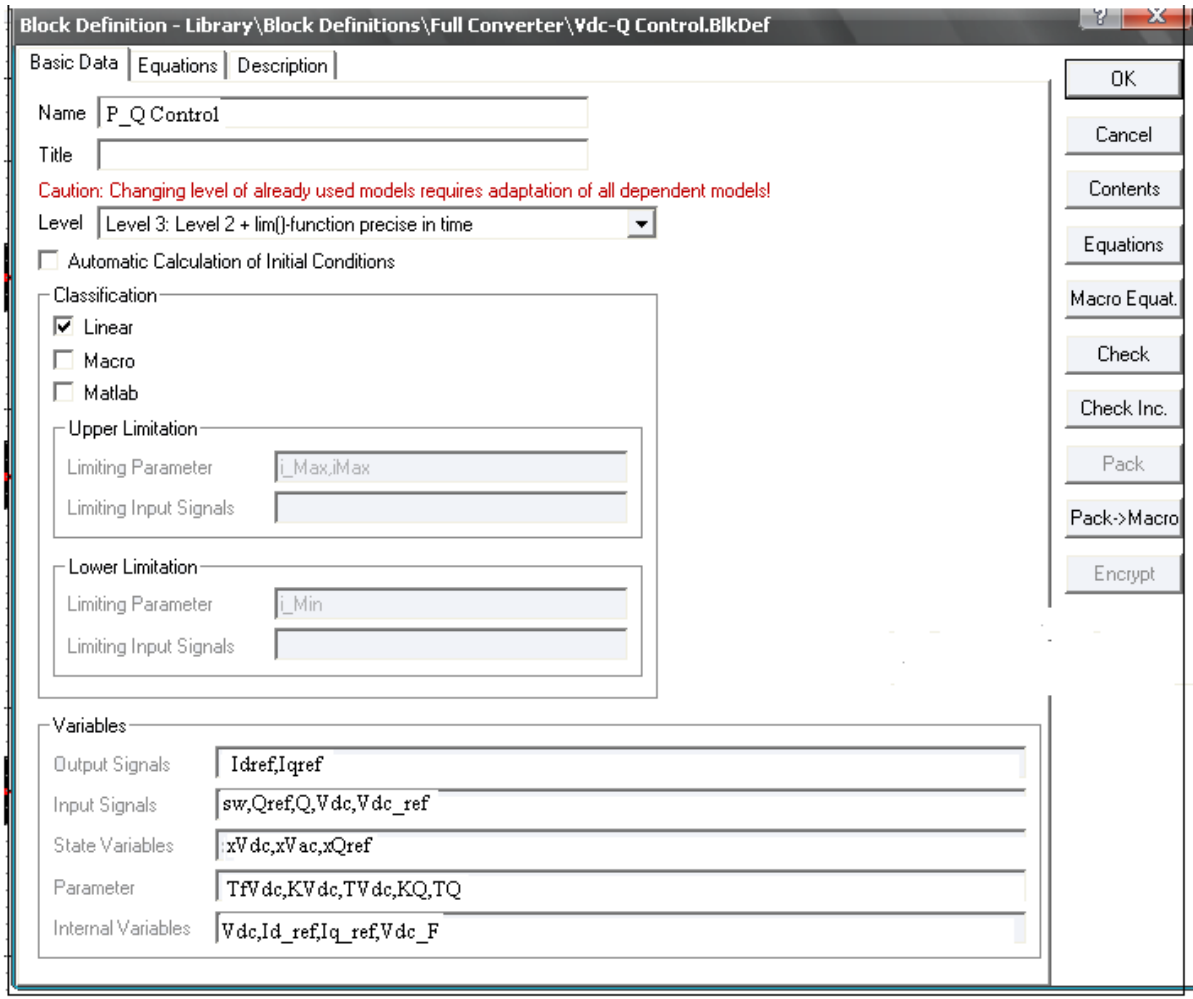


**Figure 6.15: Definition of variables in Grid side controller**

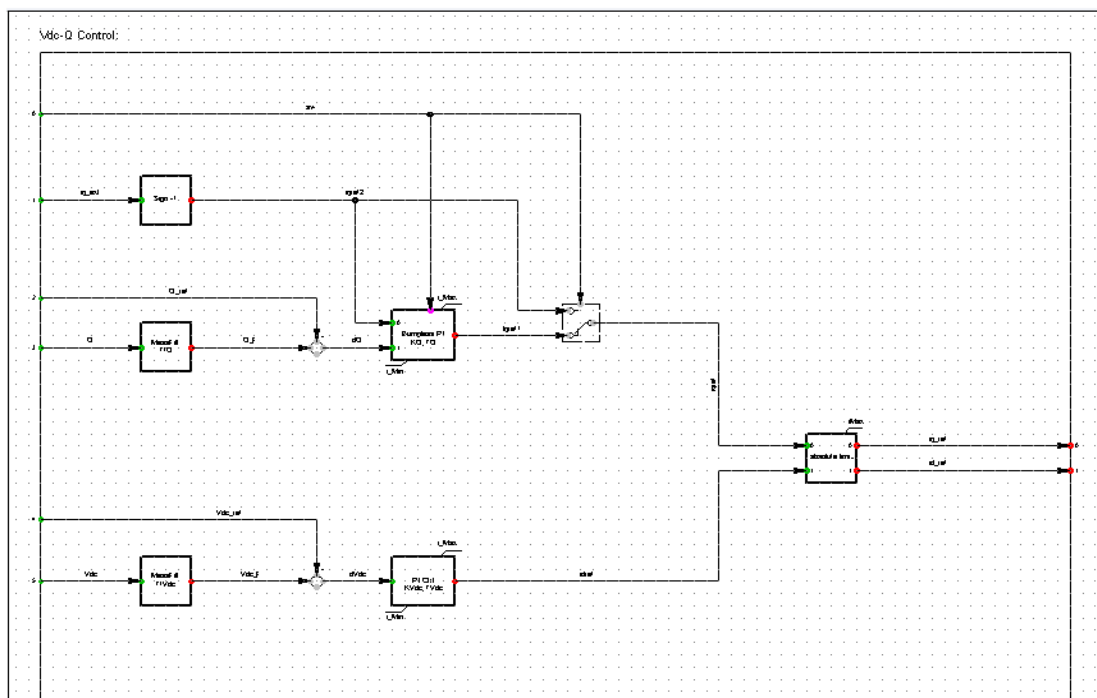


**Figure 6.16: Block definition of Grid side controller**



the individual slots to the variables of the common model. The various slots and their linking to the common block variables are shown in Figure 6.18.

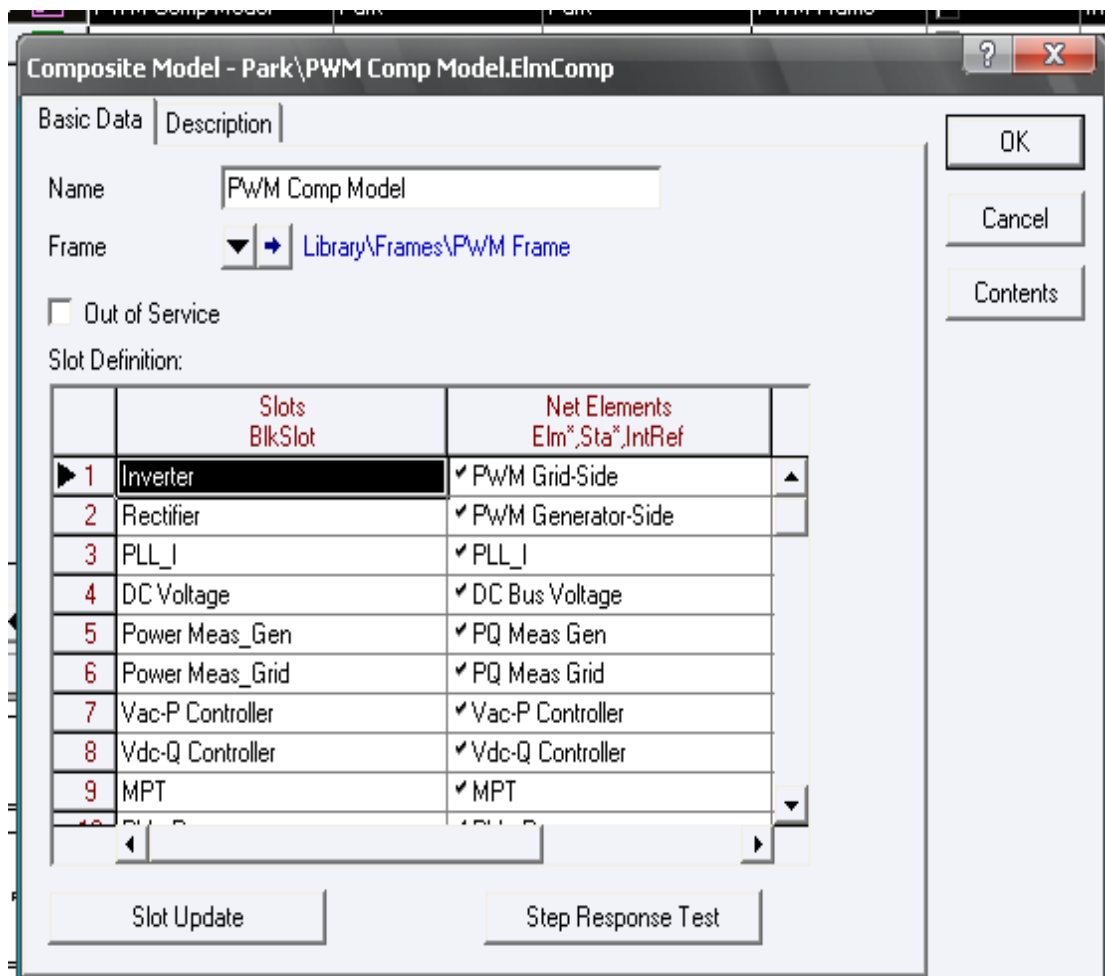


**Figure 6.18 PWM Composite models**

#### 6.4 Grid connection

The DIGSILENT consists of inbuilt power system components like transformer, cable (power cable, underground, overhead cable), feeder, bus bar, terminal, current transformer, voltage transformer, power electronics component (Inverter and Converter) and consumer load. The grid connected wind electric system is modeled with the help of these components as shown in Figure 6.19. The wind turbine is connected to the variable speed synchronous generator unit and it is connected to the grid through the frequency converter. To regulate the variable power and variable frequency, a shunt capacitor is connected across the converter and inverter. The filter circuit (LC) is connected at the DC bus bar to remove the

ripple content. The generator power is synchronized to the grid through the step up transformer and underground cable.

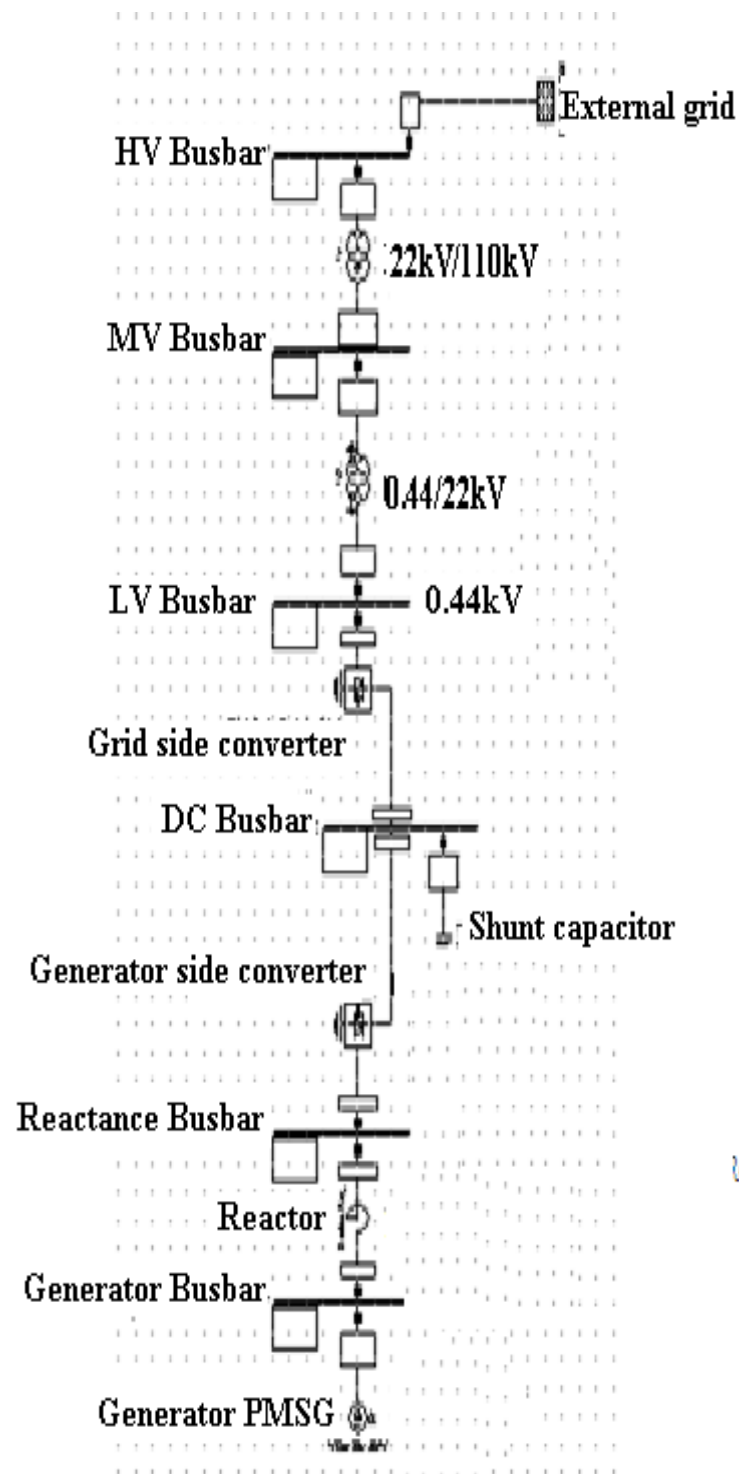


**Figure 6.19: Simulation model of variable speed wind electric system with PMSG**

## 6.5 Conclusion

With a view to getting a better understanding of the variable speed wind electric system, a generic model was introduced, where the various independent elements of a wind turbine and their interaction are explained. The individual blocks such as turbine BlkDef (block), shaft BlkDef, pitch angle control BlkDef, Grid side controller BlkDef, Generator side controller BlkDef, MPT BlkDef were designed using the mathematical model in DSL. All the individual blocks were connected together with help of frame definition block including the built-in model of SYM BlkDef and Converter BlkDef .The values of the parameter variable in each block are entered using common model. The composite model (ElmComp) connects the frame slot and common model. Finally, the simulation model of the grid connected variable speed wind turbine was built with the help of power system component such as bus bar, transformer, cable, feeder etc from the software. The generator side converter controls the stator voltage and optimal power generation with respect to the speed of the machine. The grid side controller controls the real power and reactive power at the grid bus bar.

## CHAPTER 7

### ANALYSIS AND SIMULATION OF E2 WIND FARM FEEDER IN CHINNAPUTHUR SUBSTATION

#### 7.1 Introduction

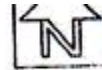
The E2 wind farm feeder has eleven individual variable speeds PMSG of same rating of 0.85MW. The total generated power capacity is 9.45MW. The generators are located at 8.25KM to 12.25KM away from the substation. The Figure 7.1 shows the layout of E2 wind farm feeder. The Table 7.1 shows the distance of generators from the grid 110kV. The E2 feeder layout is modeled with the help of DIgSILENT software to analyze the various power quality issues. The generator in the left hand side of the layout is considered as G1 which is far away from the grid and G11 near to the grid in this simulation. The power quality analyzer, Dranetz 431 was installed at E2 wind farm feeder. The power quality events as per EN50160 standard were recorded.

The electromechanical transient (RMS) simulation is performed for 600sec under steady state and dynamic state conditions. The various power quality events such as Sag, Swell and Transient are simulated.

**Table 7.1 Distance of generators from grid for E2 feeder**

Generator	G1	G2	G3	G4	G5	G6	G7	G8	G9	G10	G11
Location from the grid in KM	12.25	12.5	12.00	11.86	9.68	9.46	9.42	8.9	8.78	8.57	8.23

# CHINNAPUTHUR E-2 FEEDER



12.25.16 PD.

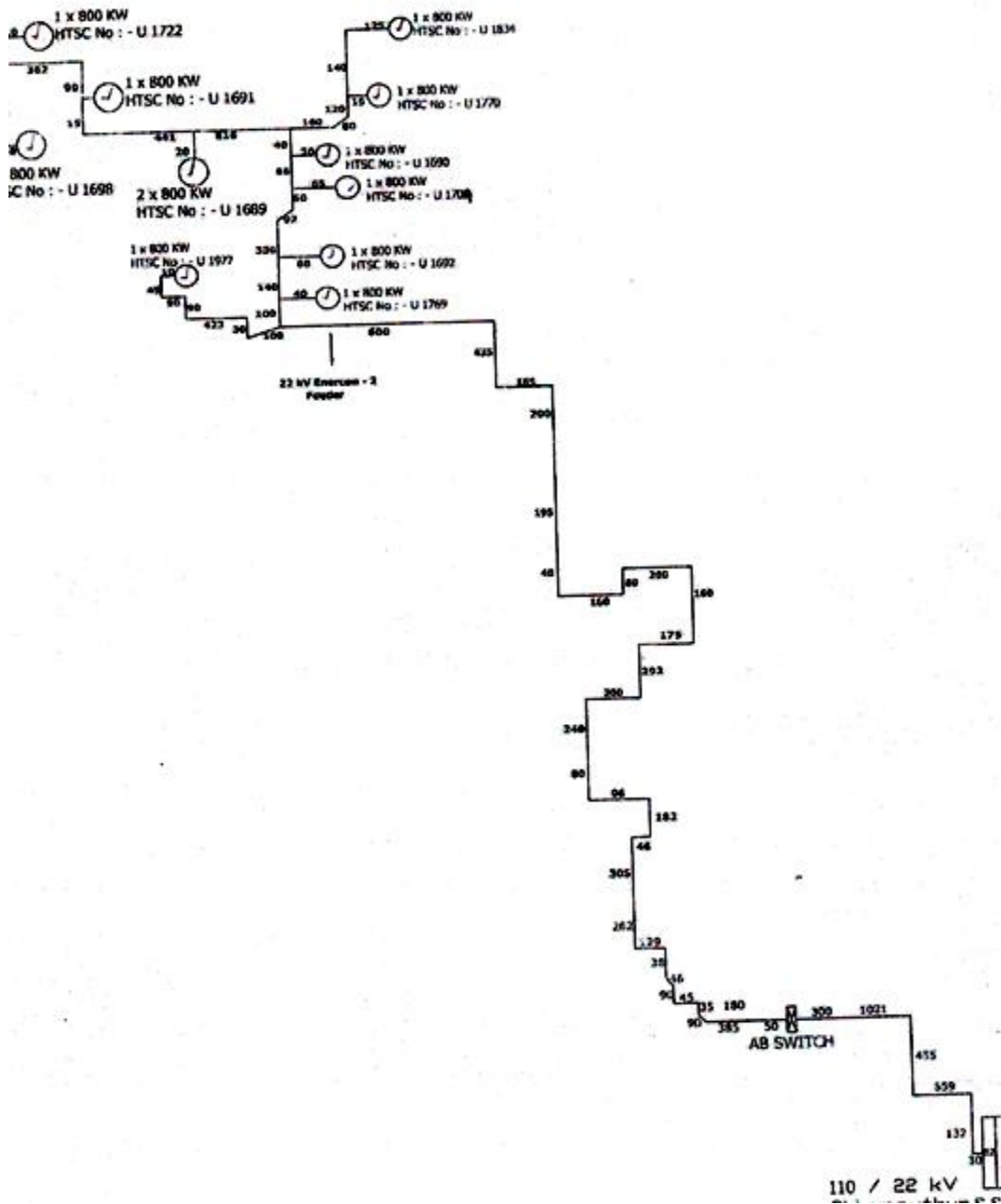


Figure 7.1: Substation Layout of E2 feeder

## 7.2 Load flow studies

The power flow or load flow analysis of the grid connected PMSG helps us to calculate the Real power generation, Reactive power consumption, Current and the Voltage values at PCC and different bus bars. This wind farm feeder consists of eleven individual wind turbines of same rating 0.85MW, 0.44kV connected to a transformer of rating 0.95MW,0.44/22kV through the converter and inverter controller. The HT side is connected to 22kV bus bar through the underground cable of capacity 22kV. The specification of the components of all the wind turbines are of the same rating. The performance of the individual wind turbine is shown in Table 7.2.

**Table 7.2: Load flow study of E2 feeder**

Si. No	Power system component	Load flow measurement
1	Generator	0.85MW,0.088Mvar,1.18kA
3	Generators bus bar	0.44kV
4	Generators side converter	0.85MW,0.0Mvar,1.18kA
6	DC bus bar	0.71kV
7	Grid sides converter	0.85MW,0.08Mvar,1.18kA
8	LV bus bar	0.44kV
9	MV bus bar	22kV
10	HV bus bar	110kV

The simulation model of the E2 wind farm feeder using DigSILENT software is shown in Figure 7.1.

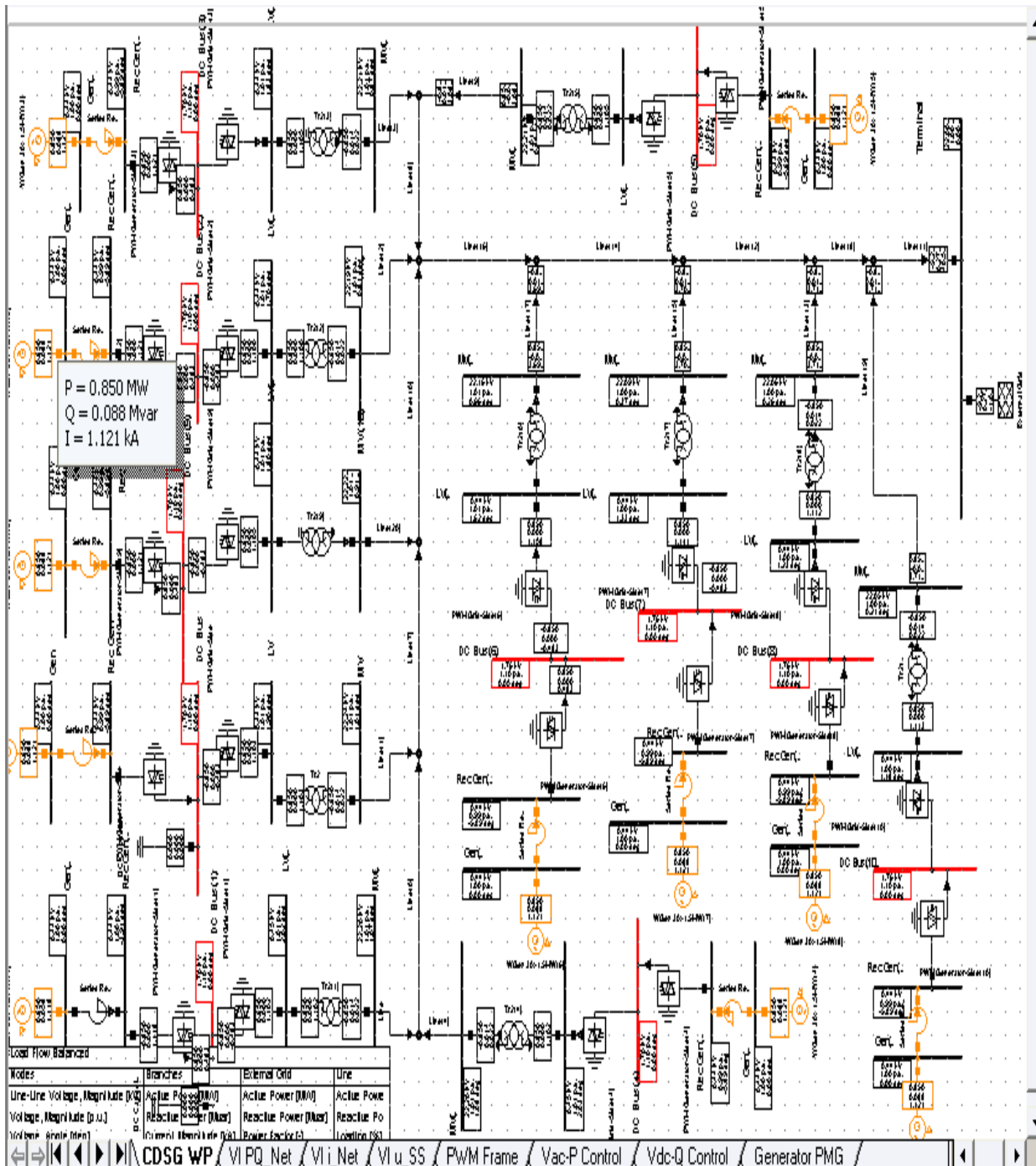


**Figure 7.2 Simulation model of E2 feeder**

### 7.3 Steady state simulation of the E2 feeder connected to the grid

The steady state analysis of the grid connected wind farm helps us to analyze the system performance under the constant wind speed and load conditions. The system behavior is analyzed under the variation in the grid voltage, frequency and wind speed conditions.

### 7.3.1 Simulation of E2 feeder system for various bus bar voltages

There are situations where the grid bus bar voltage may increase or decrease depending upon the load and symmetrical fault. Hence, it becomes significant to study the system behavior under various bus bar voltages. The grid voltage is increased by 10% of its nominal value and the performance of G1 which is far away from the grid bus bar is shown in Table 7.3. The Table 7.4 shows the performance of the G11 generator which is very near to the grid bus bar HV or PCC. It is observed that the generators near and away from the grid bus bar are affected similarly. The generators current of the E2 feeder is decreased when the grid voltage is increased. The grid voltage is decreased by 10% of its nominal value and the results are shown in Table 7.5. It is observed that the current increases when the grid bus bar voltage varies, the generator controller regulates the generator bus bar voltage and DC bus bar voltage at constant values as per the set values. The Figures 7.3 and 7.4 show the bar chart of bus bar voltages for the increase and decrease in the grid voltage.

**Table 7.3: Grid bus bar voltage increased from 110kV to 121 kV at wind velocity of 12m/s**

Si. No	Power system component	Real power flow MW	Reactive power flow Mvar	Voltage kV	Current kA
1.	Generator G1	0.85	0.08	0.44	1.122
2.	Generator side converter	0.85	0.08	0.44	1.122
3.	Grid side converter	0.85	0.12	0.44	1.01
4.	Generator bus bar			0.44	
5.	DC bus bar			0.702	
6.	LV bus bar			0.44	
7.	MV bus bar22			24.5	
8.	HV bus bar 110kV			121	

**Table 7.4: Grid bus bar voltage increased from 110kV to 121 kV at wind velocity of 12m/s**

Si. No	Power system component	Real power flow MW	Reactive power flow Mvar	Voltage kV	Current kA
1.	Generator G11	0.85	0.08	0.44	1.122
2.	Generator side converter	0.85	0.08	0.44	1.122
3.	Grid side converter	0.85	0.12	0.44	1.01
4.	Generator bus bar			0.44	
5.	DC bus bar			0.702	
6.	LV bus bar			0.44	
7.	MV busbar22			24.5	
8.	HV bus bar 110kV			121	

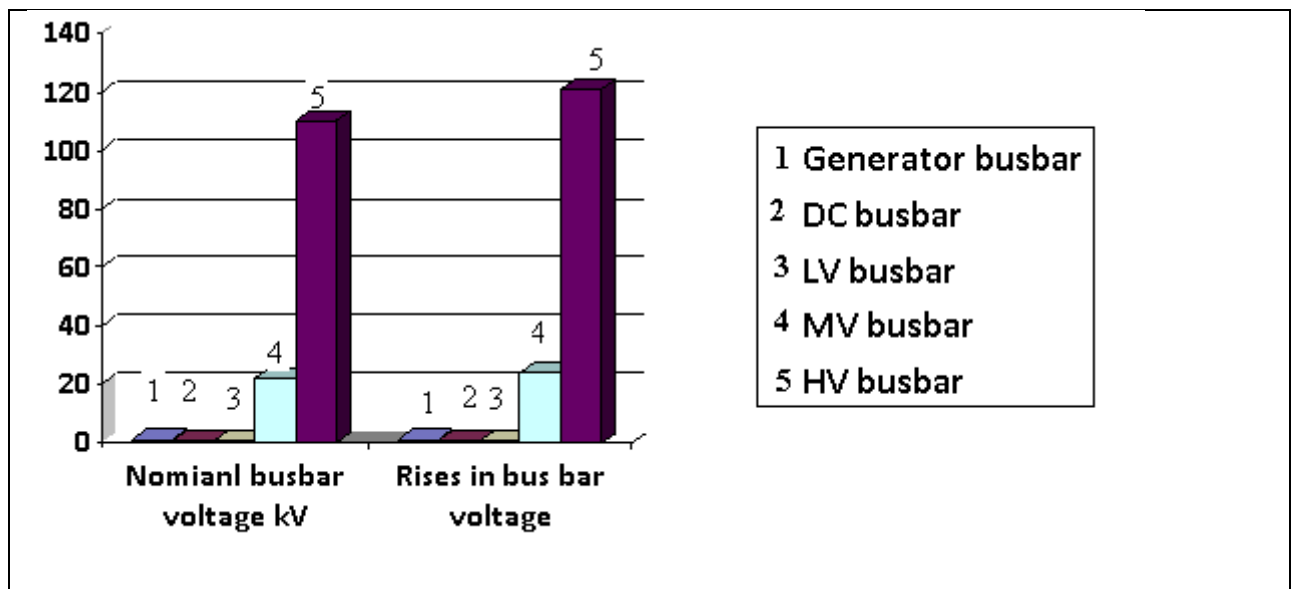


**Figure 7.3: Bar chart for rise in bus bar voltage for the Generator G11 far away from the grid**

**Table 7.5: Grid bus bar voltage decreased from 110kV to 99kV  
at wind speed of 12m/s**

Si. No	Power system component	Real power flow MW	Reactive power flow Mvar	Voltage kV	Current kA
1.	Generator G1 and G11	0.85	0.088	0.44	1.122
2.	Generator side converter	0.85	0.088	0.44	1.122
3.	Grid side converter	0.85	0.12	0.44	1.32
4.	Generator bus bar			0.44	
5.	DC bus bar			0.702	
6.	LV bus bar			0.44	
7.	MV bus bar 22			18.36	
8.	HV bus bar 110kV			99	
9.	Grid power	0.85	0.02		1.32

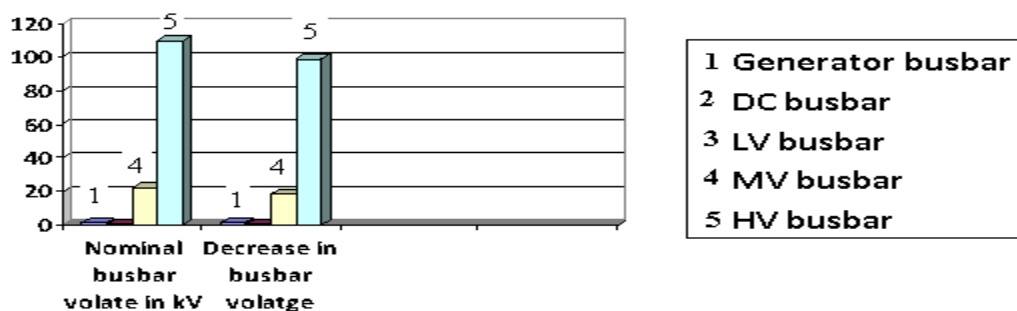


**Figure 6.4: Decrease in grid busbar voltage**

### 7.3.2 Frequency variations

The variations in the frequency occur due to the variation in the speed of the generator. But the speed of generator depends upon the real power demand and wind speed variation. The generator side converter controller controls the stator voltage and DC voltage under variable wind speeds. The generator frequency

remains constant for wind speeds above the rated value and decreases gradually below the rated wind speed from 11m/s to cut-in speed of 5m/s. The grid side converter controller controls the real and reactive power flow to the grid under the variable load conditions. Therefore, the system frequency is almost maintained constant under all the load conditions.

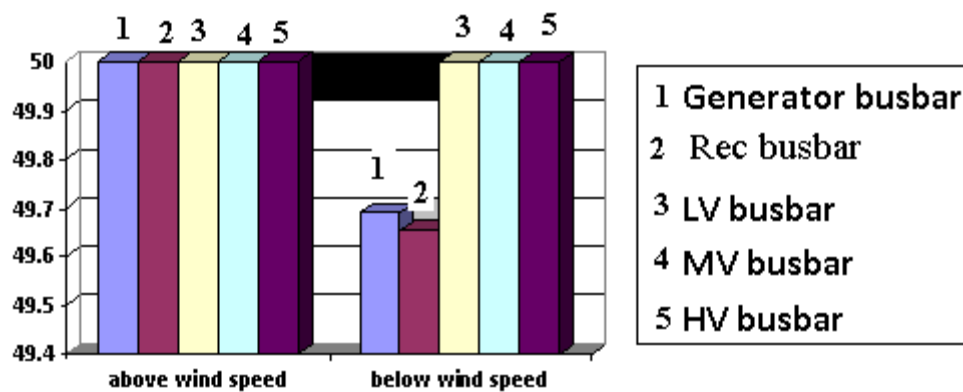
The Table 7.6 shows the constant frequency for the wind speed condition above the rated value. The Table 7.7 shows the variation in the frequency for the speeds below the rated wind speed. The generator and reactance bus bar frequencies are varied but the grid side converter controller maintaining the constant grid bus bar frequency. The Figure 7.5 shows the bar chart of generator and grid frequency under change in wind speed.

**Table 7.6: Constant frequency above the rated wind speed at 19m/s**

	Name	Grid	Electrical Frequency Hz	Nominal Frequency Hz
✓	HV	Chinnaputhur ss	50.	50.
✓	Gen	Chinnaputhur ss	50.	50.
✓	Rec Gen	Chinnaputhur ss	50.	50.
✓	LV	Chinnaputhur ss	50.	50.
✓	MV	Chinnaputhur ss	50.	50.
✓	DC Bus	Chinnaputhur ss	0.	0.
✓	LV(1)	Chinnaputhur ss	50.	50.
✓	MV(1)	Chinnaputhur ss	50.	50.
✓	Gen(1)	Chinnaputhur ss	50.	50.
✓	DC Bus(1)	Chinnaputhur ss	0.	0.
✓	Rec Gen(1)	Chinnaputhur ss	50.	50.
✓	HV (1)	Chinnaputhur ss	50.	50.
✓	LV(2)	Chinnaputhur ss	50.	50.
✓	MV(2)	Chinnaputhur ss	50.	50.
✓	Gen(2)	Chinnaputhur ss	50.	50.
✓	DC Bus(2)	Chinnaputhur ss	0.	0.
✓	Rec Gen(2)	Chinnaputhur ss	50.	50.

**Table 7.7: Variation of the frequency below the rated wind speed at 8m/s**

	Name	Grid	Electrical Frequency Hz	Nominal Frequency Hz
✓	HV	Chinnaputhur ss	50.	50.
✓	Gen	Chinnaputhur ss	49.75264	50.
✓	Rec Gen	Chinnaputhur ss	49.7523	50.
✓	LV	Chinnaputhur ss	50.	50.
✓	MV	Chinnaputhur ss	49.75264	50.
✓	DC Bus	Chinnaputhur ss	0.	0.
✓	LV(1)	Chinnaputhur ss	50.	50.
✓	MV(1)	Chinnaputhur ss	50.	50.
✓	Gen(1)	Chinnaputhur ss	49.75264	50.
✓	DC Bus(1)	Chinnaputhur ss	0.	0.
✓	Rec Gen(1)	Chinnaputhur ss	49.75264	50.
▶	Terminal	Chinnaputhur ss	49.75264	50.
✓	LV(2)	Chinnaputhur ss	50.	50.
✓	MV(2)	Chinnaputhur ss	50.	50.
✓	Gen(2)	Chinnaputhur ss	49.75264	50.
✓	DC Bus(2)	Chinnaputhur ss	0.	0.
✓	Rec Gen(2)	Chinnaputhur ss	49.75264	50.

**Figure 7.5: Variation in generator and grid busbar frequency**

### 7.3.3 Simulation of E2 feeder system for various wind speeds

The Tables 7.8 shows the performance of G1 in the E2 feeder for the wind speed of 19m/sec. Above the rated wind speed condition, the pitch control mechanism reduce the power extraction from the wind and maintains the constant power generation. It is observed that the generator side converter controls maintains the stator voltage of the generator and the capacitor DC voltage at the fixed reference value. The performance of the generators G1 and G11 in the E2 feeder are the same.

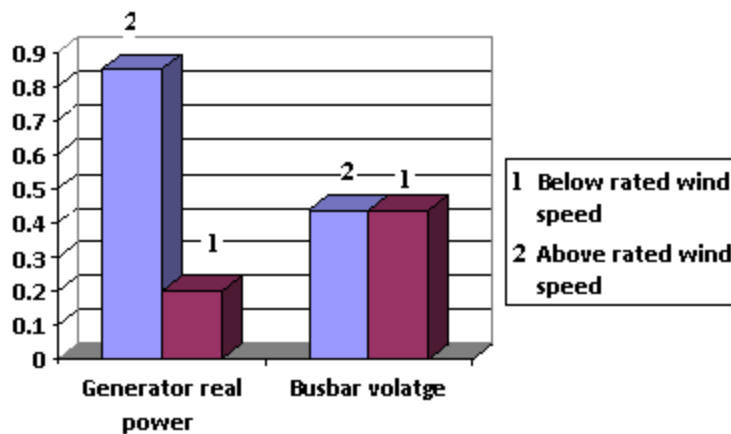
**Table 7.8: Performance for wind velocity,  $v=19$  m/s**

Si. No	Power system component	Real power flow MW		Reactive power flow Mvar		Voltage kV		Current kA	
		G1	G11	G1	G11	G1	G11	G1	G11
1.	Generator	0.85	0.85	0.088	0.086	0.44	0.44	1.122	1.12
2.	Generator side converter	0.85	0.85	0.0	0.0	0.44	0.44	1.122	1.12
3.	Grid side converter	0.85	0.85	0.12	0.12	0.44	0.44	1.122	1.13
4.	Generator bus bar					0.44	0.44		
5.	DC bus bar					0.702	0.702		
6.	LV bus bar					0.44	0.44		
7.	MV bus bar 22					22	22		
8.	HV bus bar 110kV					110	110		

The Table 7.9 shows the value of G1 in the E2 feeder for the wind speed of 8m/s. The generator real power gradually decreases with respect to change in the wind speed but the generator stator voltage remains constant. The Figure 7.6 shows the bar chart of generator real power and bus bar voltage for wind speed below and rated speed.

**Table 7.9: Performance of G1 for wind velocity,  $v=8$  m/s**

Si. No	Power system component	Real power flow		Reactive power flow		Voltage kV		Current kA	
		MW	MW	Mvar	Mvar				
1.	Generator G1&G11	0.20	0.20	0.47	0.47	0.44	0.44	0.66	0.66
2.	PWM Generator side	0.20	0.20	0.0	0.0	0.44	0.44	0.66	0.66
3.	PWM Grid side	0.20	0.20	0.56	0.56	0.44	0.44	0.6	0.6
4.	Generator bus bar					0.44			
5.	DC bus bar					1			
6.	LV bus bar					0.44			
7.	MV bus bar 22					22			
8.	HV bus bar 110kV					110			
9.	Grid power	0.20		0.02				0.6	

**Figure 7.6: Variation in Generator real power and bus voltage for wind speeds below and above the rated speed**

## 7.4 Dynamic simulation of the grid connected wind electric system

Sudden large disturbances in the power system such as change in wind speed, symmetrical fault are considered for the dynamic simulation studies.

As the wind speed is above its rated value,  $v_w = 12\text{m/s}$ , the pitch mechanism is active and limits the power and the speed to their rated values. For lower wind speeds below 12 m/s the pitch mechanism is passive and the pitch angle is kept to its optimal value of zero. Under the variable speed operation, the MPP -tracking assures optimal energy capture.

### 7.4.1 System performance under deterministic wind speeds

The typical variable of the turbine system such as pitch angle, generator speed and active power are considered for the simulation period for varying wind speed. Under this condition, the response of two generators, G11 (8.29KM to the Grid) and G1 (12.35KM to the grid) are considered. The Figure 6.7 shows the wind speed variation, beta, speed of the generators and powers. The green line represents the performance variations of G11 generator and the red line to that of G1 generator. It is seen clearly that when the wind speed decreases below the rated wind speed 12m/s, the pitch angle mechanism becomes inactive and the beta value is maintained zero. The speed and the power of the generator oscillate at every step change in wind speed due to the system damping. The Figure 7.7 shows clearly that the performance of both the generators which are near and far away from the grid are the same as the red line of G1 overlaps the green line of G11 generator.

The Figure 7.8 shows that the DC link voltage and the stator voltage are maintained constant at the reference value with the help of generator side converter control. The damping of the system causes oscillations in the DC-link voltage around its reference value of 0.705kV. The stator voltage is controlled at its rated value.

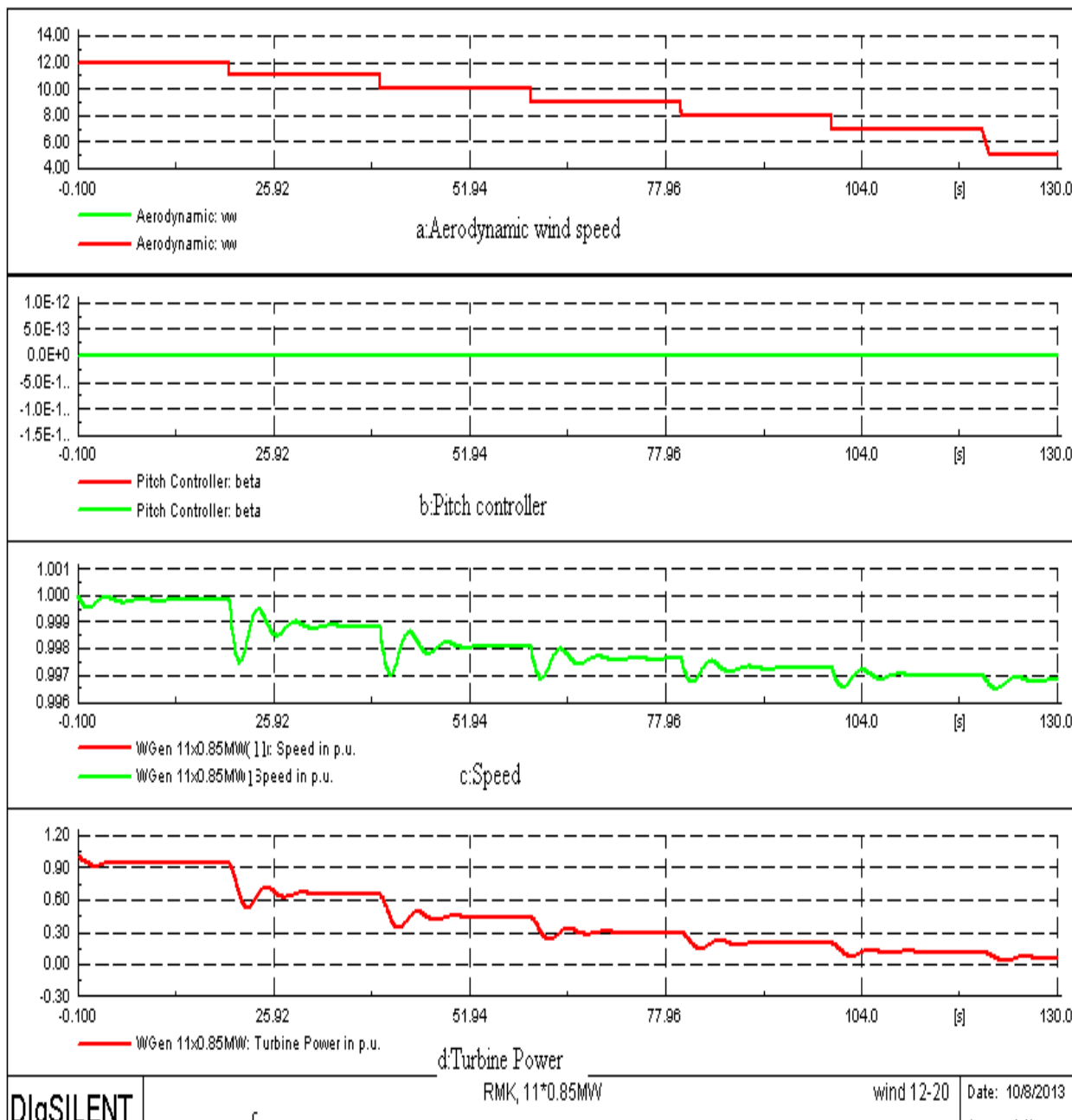


**Figure 7.7: Variation of Pitch angle, Generator speed and Active power of the G1 and G11 for wind speed varying from 12 m/s down to 5 m/s**

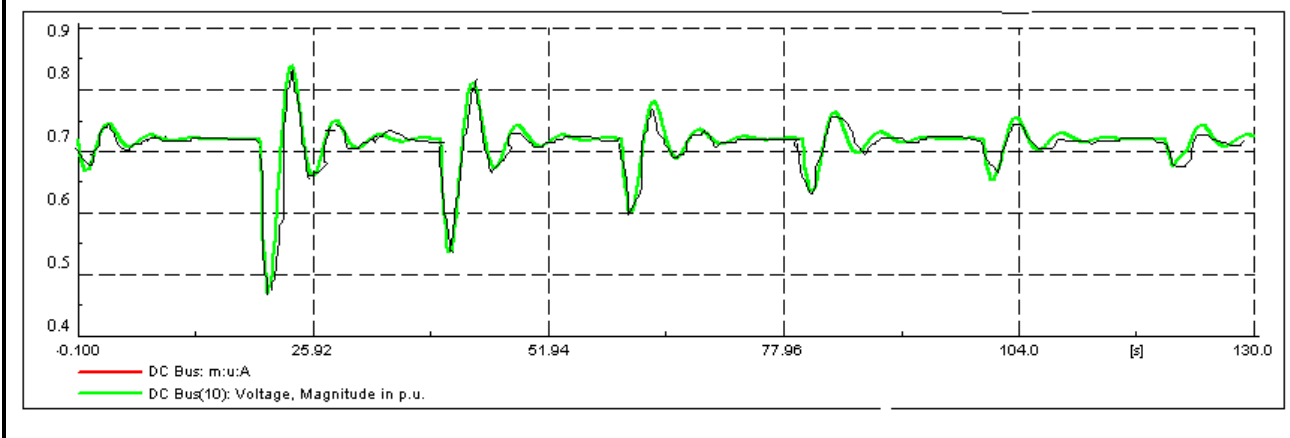


**Figure 7.8: DC-link voltage and stator voltage for the variation of wind speed from 12 m/s down to 5 m/s**

Another case study has been carried out in which the wind speed is increased in steps from 12 m/s to 20 m/s. The response of pitch angle, speed and power is depicted in Figure 6.9. The step variation in the wind speed changes both the pitch angle and the generator speed. The pitch mechanism reacts slowly compared to the power controller. It is noticed that the variations in the generator speed occur at each step change in the wind speed. The response of the pitch angle and the generator speed has oscillations and the generator power is kept at its rated value of 0.85 MW. The speed responses of generator 1 (green line) and generator 11 (red line) are similar with a small deviation of 0.01 p.u. as shown Figure 7.9.

The Figure 7.10 shows the response of DC bus voltage with respect to simulation time. The DC-link voltage is maintained constant at the set value with the help of generator side controller.

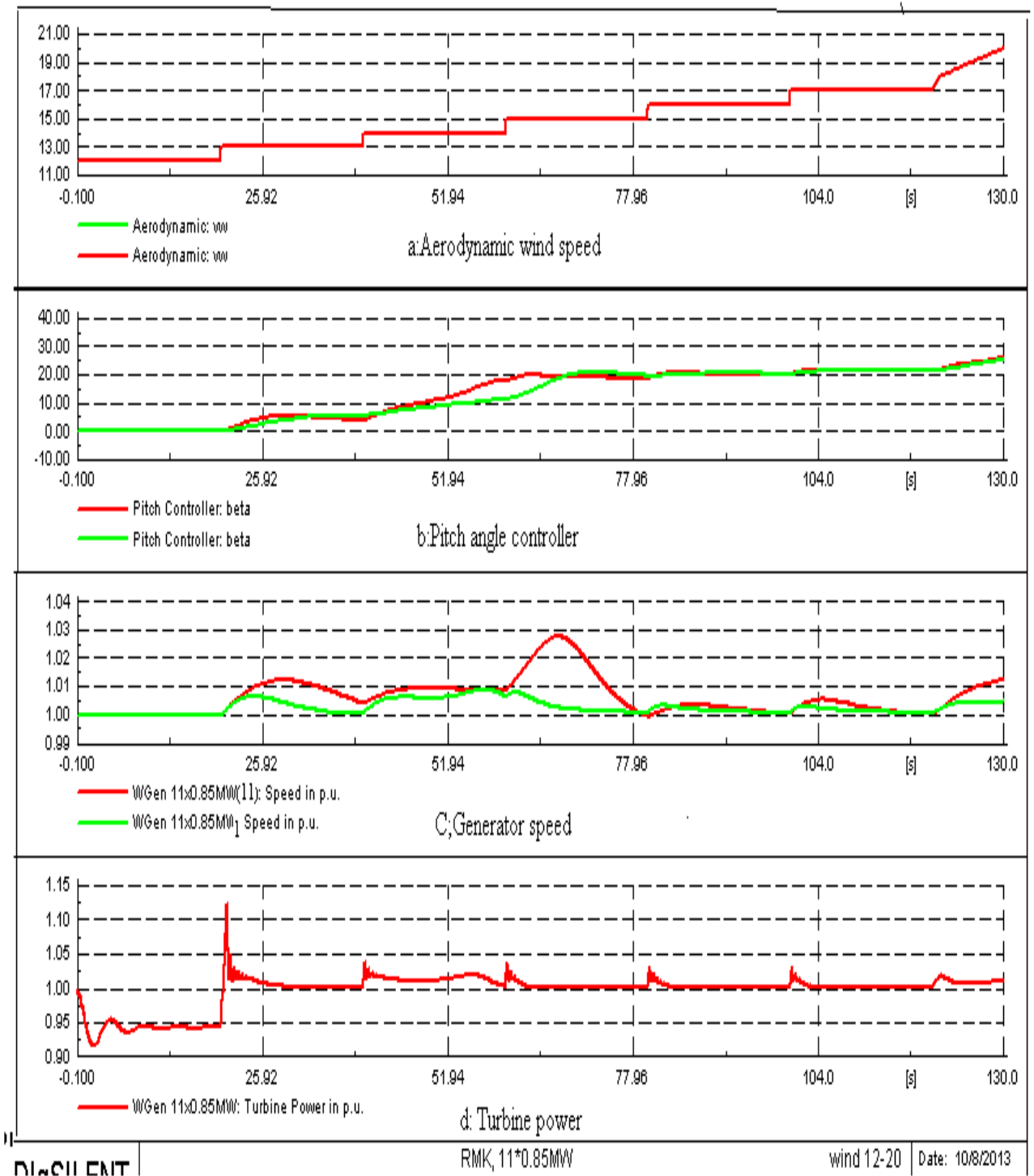


**Figure 7.9: Variation in Pitch angle, Generator speed and Active power for change in wind speed**

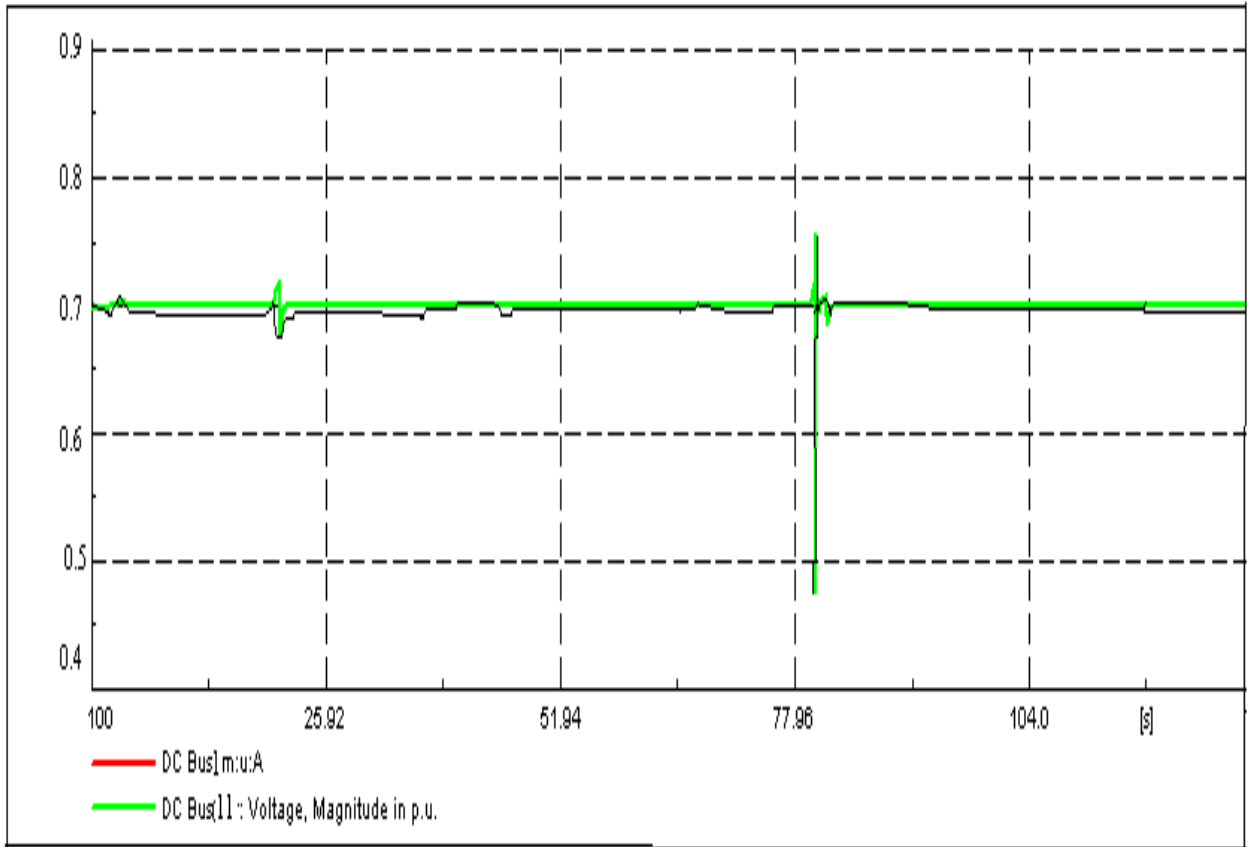


**Figure 7.10: Variation of DC-link voltage for wind speed from 12 m/s to 20 m/s**

#### 7.4.2 Dynamic behavior of the wind turbine driven PMSG under grid faults

In order to evaluate the dynamic behavior of the wind turbines driven PMSG under grid faults, a three-phase grid fault is created at the high voltage grid terminal. The turbine system and its grid connection are illustrated in Figure 7.11.

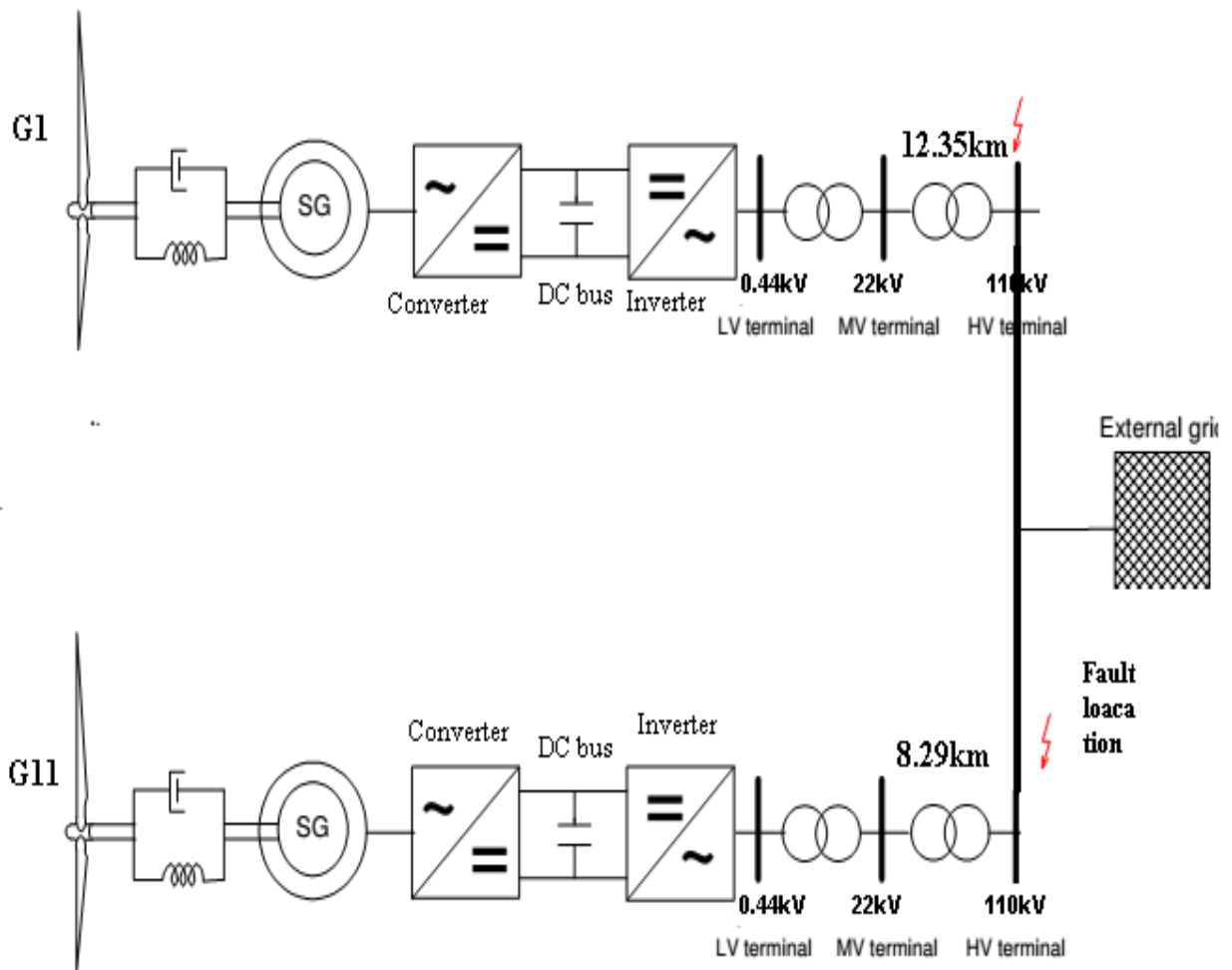


**Figure 7.11: Schematic diagram G1 and G11 of E2 feeder**

A symmetrical three-phase fault is applied at the high voltage terminal at time 10.00 and it lasts for 10 milliseconds. The Figure 7.12 shows the variation in voltage, real power and reactive power. It is inferred that the simulated fault causes 30 % voltage drop of the rated voltage at the MV bus bar of G1 and G11 with 0.01 p.u deviation. The grid side converter continues to restore the reactive power to its reference value and the active power drops.

The Figure 7.13 shows the Constant DC bus bar voltage of G1 and G11. During the fault, the generator side converter control keeps the DC-link voltage constant. This causes a decrease in the absolute value of the actual d-component of the converter current as illustrated. Although the DC voltage is controlled to a constant reference value, a switching transient of the DC-link voltage is observed at the fault incident. It is also noticed that the inner control loop response is fast to

settles down the DC voltage to its reference value with in 4 milliseconds during the fault period. After clearing the fault, the DC-link voltage was found to be oscillating and settles down to the reference value with in millisecond.

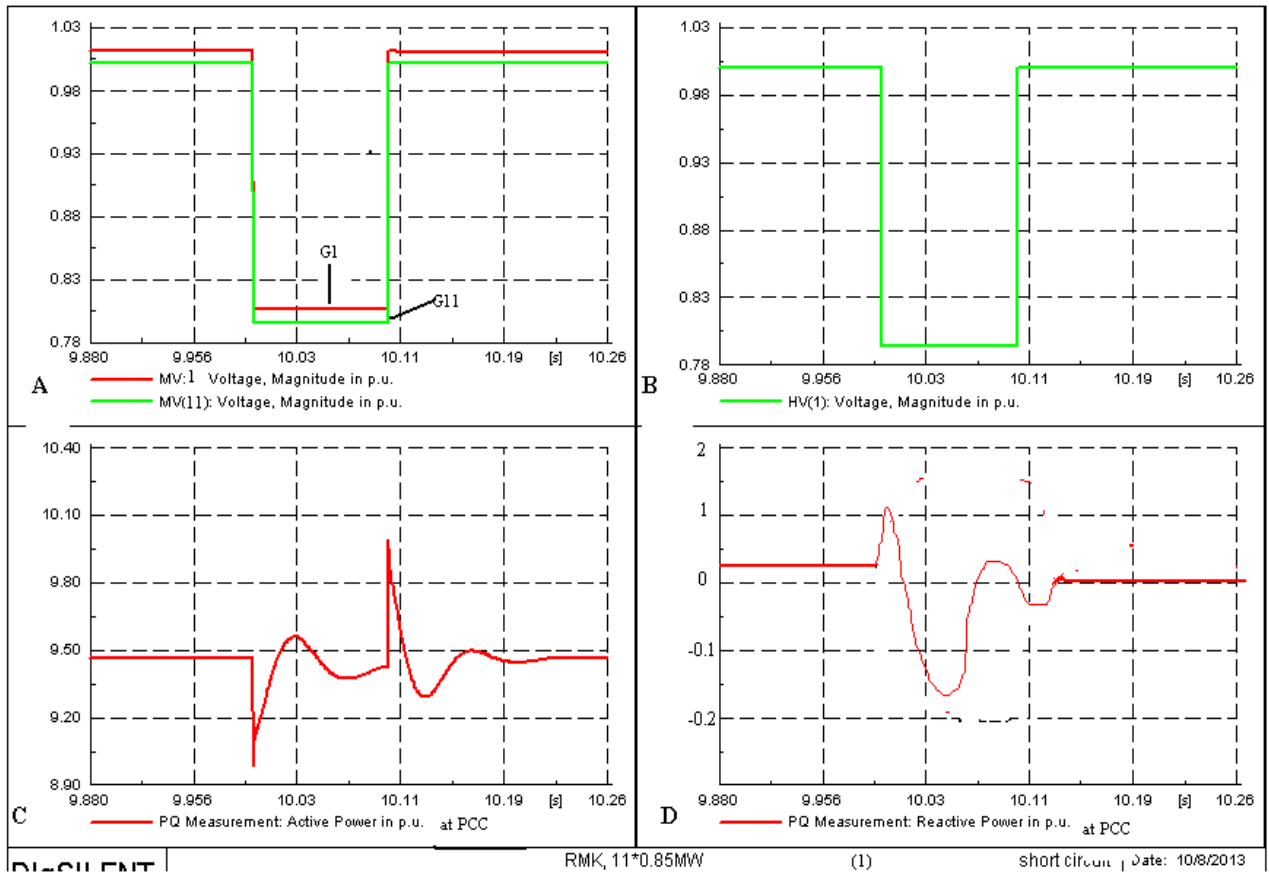


**Figure 7.12 Variation in voltage, Active Power and Reactive power of G1 and G11 generators**

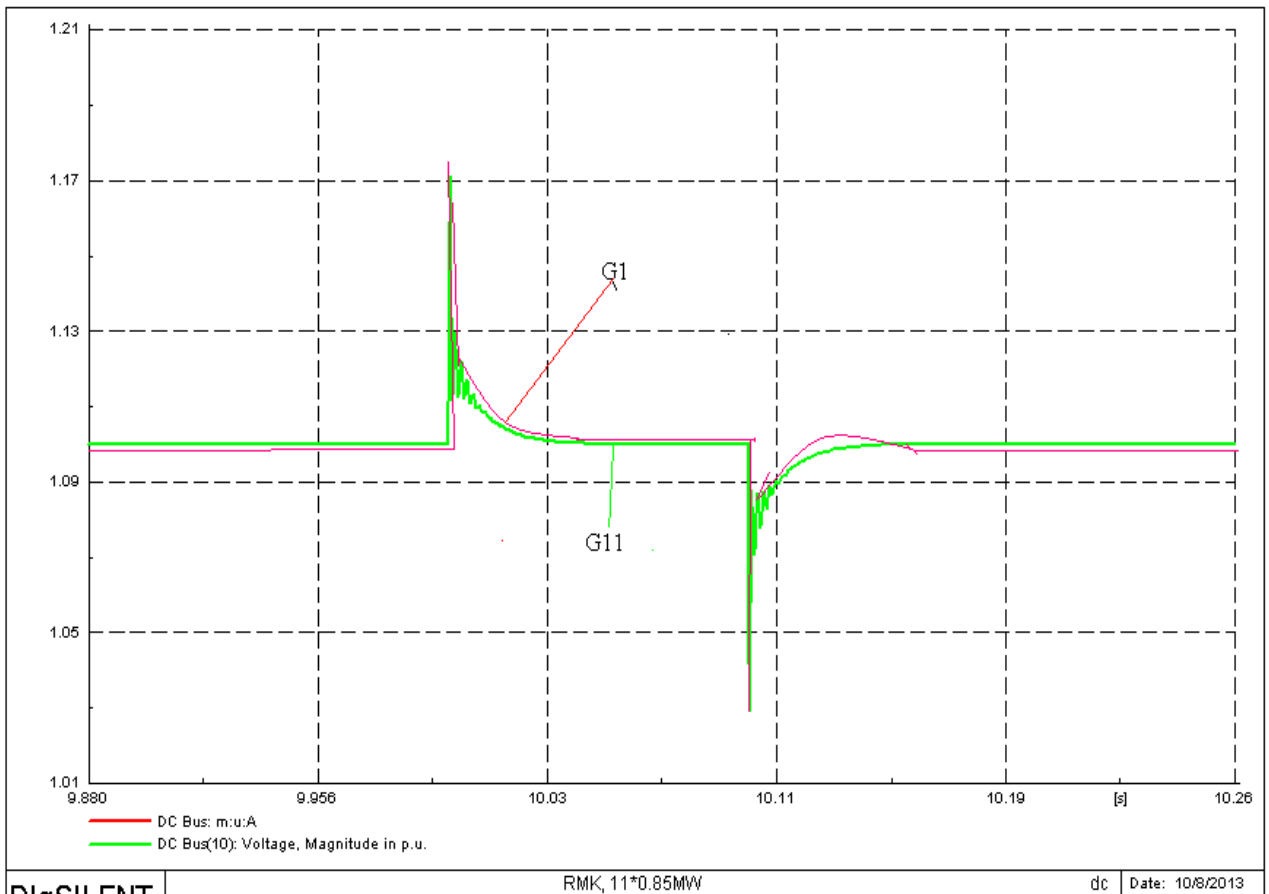


**Figure 7.13: Variation in DC bus bar voltage of G1 and G11**

### 7.4.3 Flickering

With the help of harmonic load flow in the DIgSILENT software the long term and the short term flickering due to continuous and switching operations can be calculated for the constant wind speed and for the various grid impedance angles. The Table 7.10 shows the flicker value appearing at various bus bars for  $50^\circ$  impedance angle.

**Table 7.10: Flickering value at the bus bars for 50° impedance angle**

Si. no	Element	P <sub>st</sub> Continuous Operation	P <sub>lt</sub> Continuous Operation	P <sub>st</sub> Switching Operation	P <sub>lt</sub> Switching Operation
1.	LV bus bar	0.005683	0.006567	0.005126	0.02364
2.	MV bus bar	0.005687	0.002565	0.004532	0.04538
3.	HV bus bar	0.004754	0.006984	0.002526	0.01235

The simulated flicker values for  $P_{st}$  and  $P_{lt}$  are very less when compared to the threshold value of unity. The RMS simulation is executed for minimum of 600sec and the values of  $P_{st} = 0.004563$  and  $P_{lt} = 0.025468$  are measured with the help of flicker meter.

## 7.5 Comparison of simulation result with measurement

### 7.5.1 Introduction

The comparison between the results of the simulations and measurements was performed to validate the model used. The power quality instrument manufactured by Dranetz was connected at the common breaker of the wind farm. During this study, power quality issues such as voltage sag, Interruption, swell and oscillatory transient were recorded.

### 7.5.2 Simulation of voltage sag

Voltage sag is defined as the decrease (between 10% and 90%) in RMS voltage at the power frequency for the duration of 0.5 cycles to 1 minute. In the network design considered, the three phase fault is simulated at 110kV bus bar for 10 ms duration. The sags are momentary in nature as shown in the Figure 7.14. The voltage sag measured at the wind feeder is depicted in Figure 7.15. The dip in the

voltage has occurred due to the fault alone at the grid bus bar but the generator bus bar voltage and DC bus bar voltage are not affected because of the DC link.

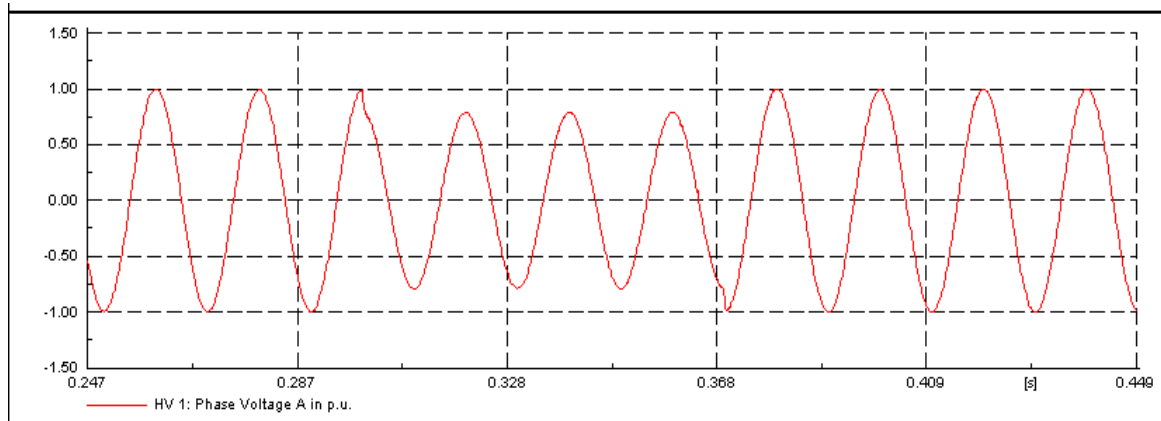


**Figure 7.14: Simulated Voltage Sag at 110kV bus bar at Chinnaputhur Substation**

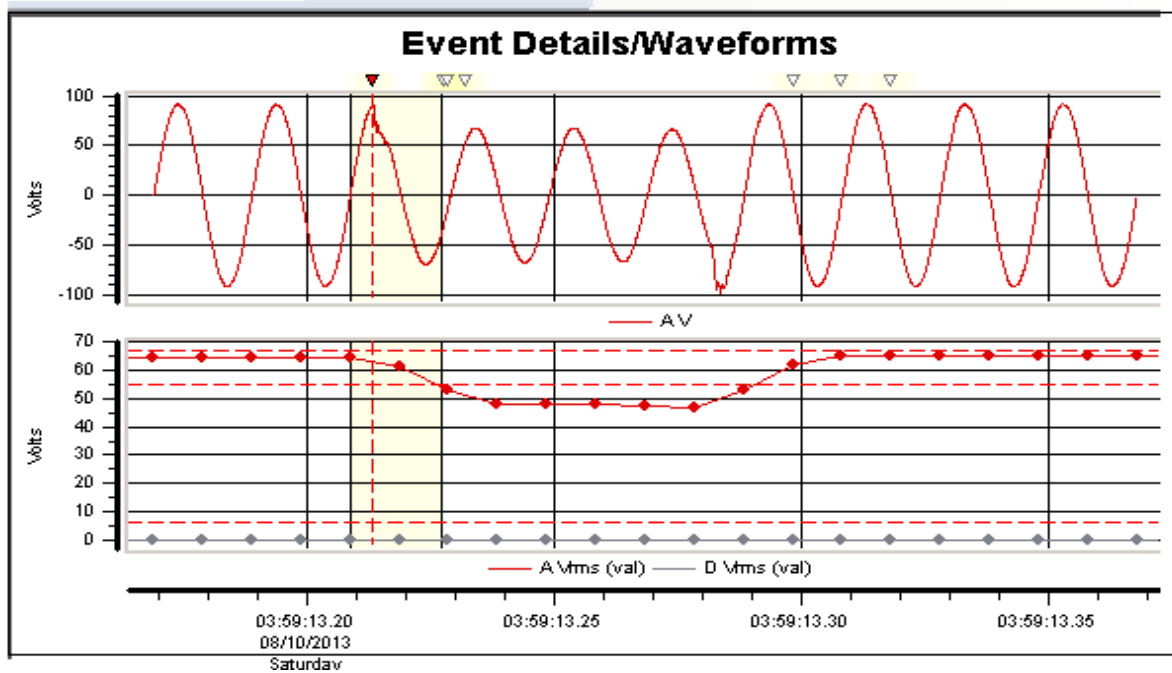


**Figure 7.15: Measured voltage sag at chinnaputhur substation**

### 7.5.3 Tripping of the wind generator

The simulation assumes that the generator 11 is switched out from the network during the concerned interval. The scenario is to switch off the feeder and

then restoring it back. The simulation results of such a scenario show that there is a variation in phase voltage as given Figures 7.16.

The noteworthy observations are: The line-to-line voltage of generator 11 suddenly starts decaying and becomes zero at some point in time. It is restored back to the normal operation after the clearance of fault. The Figure 7.17 shows that the measured voltage interruption wave is very similar to the simulated waveform in the DIgSILENT.

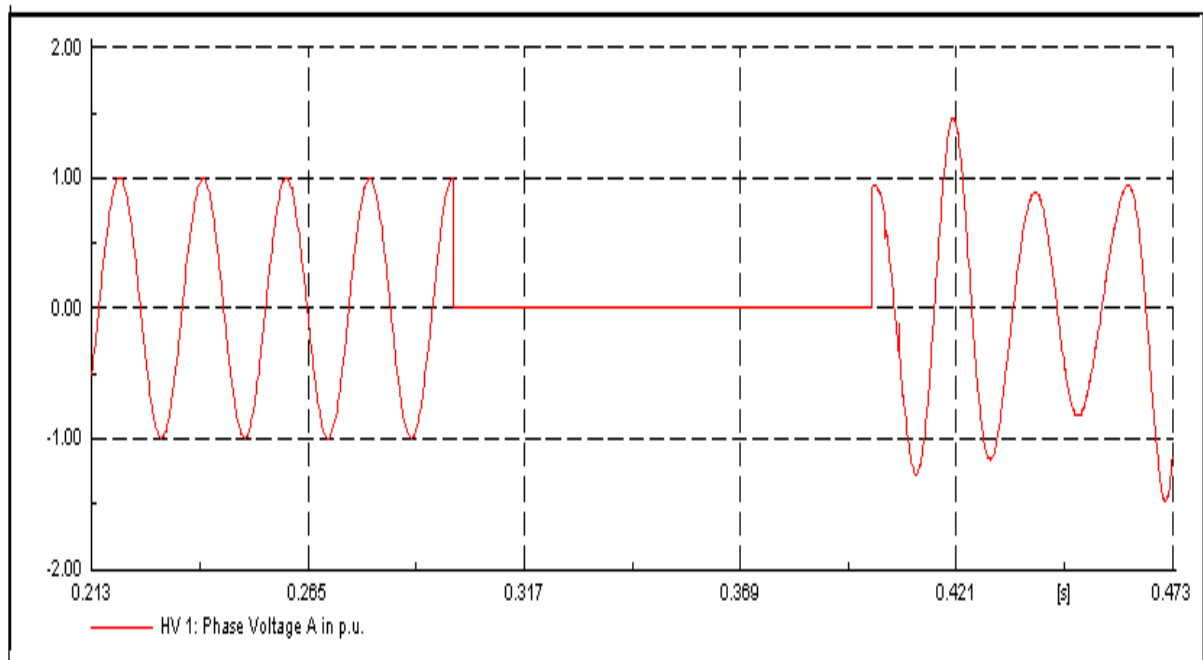


**Figure 7.16: Simulated voltage waveform of generators during tripping**

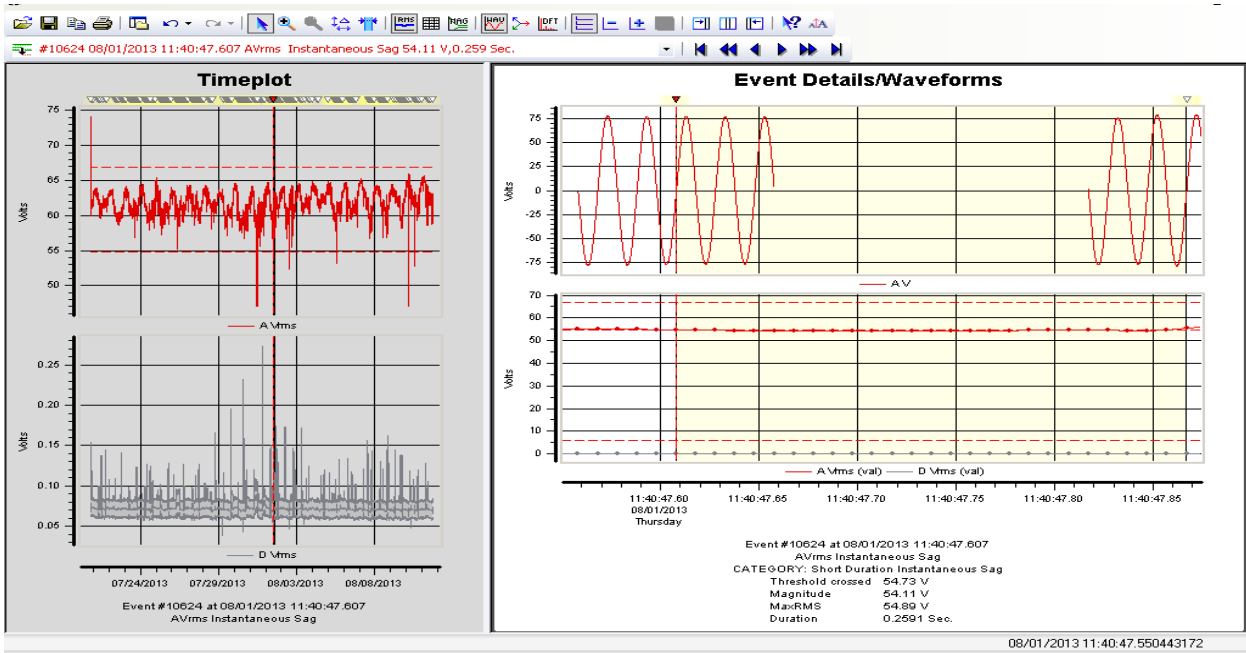


**Figure 7.17: Measured Voltage waveform during tripping**

**7.5.4 Swell**

Voltage swell is an increase (between 10% and 90%) in RMS voltage at a power frequency for duration from 0.5 cycles to 1 min. In the designed network, the load connected to HV bus bar is disconnected. The voltage thus rises from its nominal value of 1 p.u to 1.01 p.u shown in Figure 7.18. The Figure 7.19 shows the measured waveform which is similar to the simulated one.

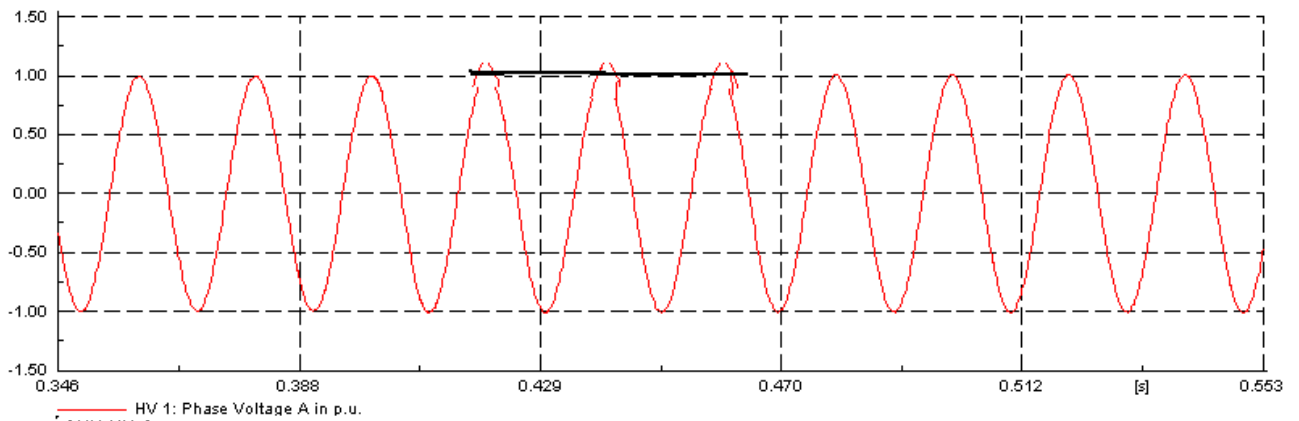


**Figure 7.18: Waveform of simulated Voltage swells at generator bus bar**

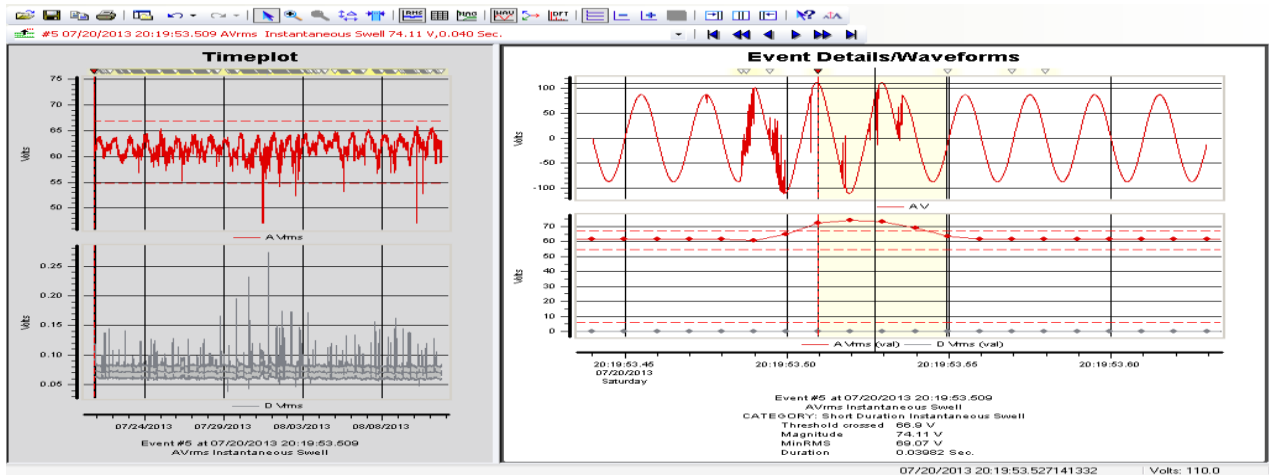


**Figure 7.19: Waveform of measured Voltage swells at 110kV**

## 7.6 Conclusion

The E2 wind feeder of Chinnaputhur substation is modelled as per the layout. It consists of eleven wind turbine of same rating 0.85MW, 0.44kV and total capacity is 9.35MW. As the grid busbar voltage is increased 10%, current flow is decreased and grid reactive power controlled to its reference value. The grid frequency is maintained at 50Hz by the grid side converter control. But the generator frequency varies to change in the wind speed below its rated speed 12m/s. The pitch mechanism is active above the rated wind speed and the generator power of G1 and G11 under consideration is kept at its rated value of 0.85 MW. The speed responses of both generators are similar except a small deviation of 0.01p.u. This deviation is due to the servo mechanism slow response in the pitch control block. The DC-link voltages of G1 and G11 are maintained constant at the set value with help of generator side controller. The symmetrical three-phase fault is applied at the high voltage terminal at the time 10.00s and it lasts for 10 milliseconds. The fault causes a voltage drop of 30 % of the rated voltage at the MV bus bars of G1 and G11. The fault causes drop in the active power.

The wind farm performance and their contribution to the voltage control is assessed and evaluated by means of simulations with the use of a generic and realistic power system model of Chinnaputhur substation at Dharapuram District. The simulation results of PMSG wind farm equipped with voltage control

can participate to re-establish the voltage properly during and after grid fault. The conclusion is that a variable speed wind generator equipped with converter control can help the grid to maintain the voltage stability. It also provides a good dynamic performance for change in wind speed and grid voltage.

## **CHAPTER 8**

### **REMEDIAL MEASURES AND SUGGESTIONS FOR IMPROVING POWER QUALITY**

#### **8.1 Improvement techniques**

Many techniques can be utilized for eliminating voltage drop in electric power system. Few of them are:

1. Capacitor application
2. Re-Conductoring
3. Bifurcation
4. Load balancing
5. Reconfiguration
6. Fact devices

#### **8.2 Capacitor application**

In ac supply, if the load is of purely resistive nature then the apparent power will be equal to the active power. But in case of inductive loads, the active power is less than apparent power. It means that inductive load draws two types of power. One is called active power and other is reactive power. If reactive power is eliminated, then apparent power becomes equal to active power. The total elimination of reactive power from the system is difficult; rather it can be compensated partially by the application of capacitor. Lagging current usually causes greater voltage drop. This is primarily due to the fact that the reactance of the line is generally greater than resistance. Shunt capacitors are utilized to counteract this voltage drop by producing a “voltage rise” across the line. The installation of capacitor also improves the power factor which in turn reduces the line losses. The application of capacitor in the distribution system provides many benefits. The Reduction in voltage drop, enhancement of overall system voltage, improvement in system voltage regulation, release of system capacity, reduction in

the distribution system overloading, increase in system efficiency, reduction in line current, and power factor improvement are the most distinguishable advantages of capacitor utilization in the distribution system.

The other benefits of capacitor application include reduction of power loss in the distribution system, elimination of capital expenditure involved in system rehabilitation and reactive power compensation.

### **8.3 Re-Conductoring**

Re-Conductoring of distribution feeder is another effective method of voltage improvement and voltage drop reduction. However, this method is costly as it involves the replacement of high impedance small capacity conductor by low impedance high capacity conductor. This technique is recommended only when the benefit cost ratio of re-conductoring is equal or greater than unity. Cost is reduced on the installation of new and dismantling of existing conductor. The benefits include reduction of voltage drop and saving in energy losses for a period of about five years and return value of the dismantled conductor.

### **8.4 Bifurcation**

Bifurcation is applied to distribution feeder when it is highly overloaded and simple capacitor application and other techniques do not provide the desired results. The existing feeder is replaced by two or more feeders as per requirement of the locality to supply a portion of the existing area. In this method the re-allocation of loads is carried out. Additional feeder(s) are constructed either from the same grid or from another nearby grid station depending on the economic justification and achievement of maximum benefits. This method is costly as it involves the construction of new feeder(s).

## **8.5 Load balancing**

This technique is economically feasible and can be accomplished quickly. Unbalance of load on the distribution feeder occurs when single phase loads and single phase transformers are not effectively divided among the three phases. If these loads are symmetrically distributed among the three phases of the system, considerable reduction in voltage drop can be achieved. For optimal operation of the distribution feeder, load on transformers should be distributed equally on the basis of their rated power.

## **8.6 Feeder reconfiguration**

Network or feeder reconfiguration is the process of altering the topological structure of distribution feeders by changing the open/close status of sectionalizing and tie switches. Reconfiguration of distribution feeder can be used as a planning as well as time control tool. Modifying the radials of distribution feeder from time to time, by changing the open/closed status of these switches can improve the path of power flow. Transfer of load from heavily loaded feeder to lightly loaded feeder improves the operating condition of overall distribution feeder. Feeder reconfiguration allows the transfer of load from heavily loaded feeder to relatively lightly loaded feeder. Such transfers are effective not only in altering the level of loads on the feeders being switched but also in improving the voltage profile along the feeders.

## **8.7 Fact devices**

A shunt and series device can be connected at the suitable location in the wind farm to improve the power quality issue. The statcom is the shunt device which can inject or absorbs the reactive power from the system to maintain the system voltage at the reference value. The statcom is suitable fact device to reduce the voltage sag under the load variation and fault. The DVR is the series voltage device in the line to control the voltage to the reference value. Transient due to

switching of isolator and capacitance switching are controlled by the dynamic voltage reactor. The UPFC is the combination of shunt and series device. The power flow at the power system is controlled either series or shunt injection or both.

### **8.8 Implication of poor power quality**

Poor power quality in electric power distribution system has many implications. It increases in the line and equipment current leading to additional ohmic losses. The excess line and equipment currents enhance the capital investment. In most of the cases, this increase of current also brings significant changes in the operating temperature of distribution network and electric appliances which not only reduce the life of the equipments but also deteriorate the power quality of the system. The losses in the system increases which in turn minimizes the efficiency of the distribution system. The numbers of outages in the system increases and severely deteriorates the quality of production in the industry. The frequent malfunction of the equipments may also reduce the production completely. The distribution engineers try utmost to eliminate the implications of the poor power quality by implementing the proper and effective system designs.

### **8.9 Custom power solutions**

In the deregulated environment, the manufacturers are less willing to put up with products loss and defects caused by power supply problems. Small outages play significant role among the utilities and customers. Under such circumstances the utilities are bound to mitigate the new and sterner concept of power quality. Custom power solution is implemented on the utility side of the meter and integrates the measures on the customer's side as well. The Majority of the power conditioning devices is custom built to meet certain customer technical performance requirement and target cost. The technical performance is driven by statutory and regulatory requirements, compliance to standard etc. In many cases,

the major driver is the financial incentive arising out of the power conditioning. To ensure the optimality of the solution, it is essential to capture all the performance requirements, cost and benefit elements and arrive at an optimal solution.

### **8.10 Advantages of power conditioning**

The advantages of the power conditioning can be classified into technical and nontechnical types. Technical merits are those that accrue due to improvements in operating efficiency and are directly related to basic laws of physics and are invariant with policies and guidelines to greater extent. The reduction of current in line and equipment minimizes the ohmic losses due to reactive power compensation and harmonic filtering is one example out of many. Non technical benefits are those which can be obtained because of fiscal income due to regulatory norms and compliance and are largely dependent upon the existing policies and norms. Although some of the non technical advantages have their roots in technical aspects of power conditioning, largely depend upon utility policies.

The general merits of power quality improvement include;

1. Minimization of line and equipment currents, losses and thus lowered energy bill.
2. Release of blocked capacity and consequent avoided cost of capital investment.
3. Power factor improvement and avoided penalty for low power factor.
4. Reduction in maximum demand and reduction in demand charges.
5. Benefits in taxes such as accelerated depreciation benefits for installation of power conditioning or energy saving devices.
6. Voltage profile improvement and consequent effective operation of electrical devices.
7. Elimination of harmonic distortion and consequent reduction in copper loss, core loss and stray loss.

8. Prevention of malfunction of equipment and avoided loss of production.
9. Elimination of unplanned outages and reduction in loss of production and revenue.
- 10.Reduction in failure of equipment due to reduced electrical and thermal stresses.
- 11.Increased life and reliability of electrical devices due to lower operating temperatures and lower losses.

### **8.11 Fault ride through**

As a result of the increased wind power development, focus has come to the influence of wind power on the security of the system. An important security issue is the ability of wind turbines to stay connected, or “ride through” when the voltage dips due to a fault in the system. The main fault-ride-through concern is on the possible effect that a fault in the transmission system will have, because such a fault will influence the voltage significantly in a large area. Thus, if many wind turbines are subject to a voltage dip caused by a transmission system fault, it is important that these wind turbines are able to stay connected. Otherwise, significant generation capacity can be lost, causing power and frequency control problems in the system after the fault.

The fault-ride-through demand is also a challenge to the voltage recovery after a grid fault. Before fault-ride-through requirements became relevant to avoid loss of significant generation, the wind turbines had to disconnect to avoid large inrush currents when the voltage recovers, in order to avoid that the inrush current trips a system protection relay. Thus, the fault-ride-through requirements also raise challenges on how to recover the voltage after a dip, especially for wind turbines directly connected to the induction generators.

## 8.12 Suggestions

1. All new wind generation plants must meet WECC LVRT requirements.
2. All new wind plants should be Type 3 or Type 4 generators that are capable of providing dynamic reactive support to help the transmission grid to meet applicable WECC transient stability performance standards and to prevent the potential tripping due to low voltages.
3. In the event that some of the new wind plants are of Type 1 or 2 with no dynamic reactive capability, the generator owner must provide sufficient reactive resources to meet the Low Voltage Ride Through standards and voltage control standard. Additional studies may be required to verify that the generator has been provided appropriate additional external dynamic reactive support to meet the interconnection standards.
4. Re-evaluate the optimal location and size of the dynamic reactive support.
5. Analyze the best solution for improving the nose point of the Q-V analysis for critical 250 kV buses under critical contingency conditions. Potential solutions include the use of series compensation and reduction of proposed shunt compensation.

Type 1 – conventional induction generator

Type 2 – wound rotor induction generator with variable rotor resistance

Type 3 – doubly-fed induction generator

Type 4 – full converter interface

Type 1 machines operate in a very narrow speed range, and always consume reactive power during operation. The reactive power consumption is a function of active power production and grid conditions, and it cannot be controlled. Consequently, both the reactive power consumption of the generator and the

reactive power requirements of the grid must be supplied by additional equipment — usually switched shunt capacitors.

Type 2 machines have wider speed variation and tend to exhibit slower active power fluctuations than Type 1 machines, but have similar reactive power characteristics. Under load, the machines consume reactive power equal to approximately half of the MW output.

Type 3 and Type 4 machines use substantial power electronics to provide wider speed range and fine control of active power production. The power electronics also inherently provide the ability to produce or consume reactive power. It is largely controllable and independent of the active power production. In this regard, these machines resemble conventional synchronous generators with excitation systems and automatic voltage regulators (AVR). The details of performance are different between manufacturers. Generally, wind plants with

Type 3 or Type 4 generators have the ability to provide relatively fast voltage or power factor control. The ways in which each manufacturer controls and coordinates the reactive power production and balance differs

## **Summary**

Electric power quality is an electric power problem manifested in voltage, current or the frequency deviations and results in failure of load side electric equipments. From electric utility point of view, the power quality is the supply of electrical power as per specified standards, whereas from the end user sight, it is the smooth functioning of electrical equipments without any disruption. In the deregulated and competitive environment, both the electric utilities as well as the customers are becoming increasingly concerned about the quality of electric power. The major reason for increased concerns is the availability of sophisticated technology that has developed extremely sensitive electrical/electronic equipment. Any sort of variation in electrical parameters greatly changes the characteristics of such delicate equipments. Widespread use of electronics in the system from home

electronics to the control of massive and costly industrial processes has increased the awareness of power quality. The study of power quality and way to control it is a concern for electric utilities and electricity consumers. Equipments have become more sensitive to even minute changes in the power supply. Different indices are used by distribution engineers for the quantification of electric power quality. These indices have general properties that they are relatively easy to calculate and are calculated using standardized procedures. Majority of these indices are interpreted and applied by distribution engineers. The proliferation of micro-electronic processors in a wide range of equipment, from domestic appliances to automated industrial and hospital diagnostic systems, has increased the vulnerability of such equipment to power quality problems. These problems include a variety of electrical disturbances, which may originate in several ways and have very different effects on various kinds of sensitive loads.

Distributed Generation (DG) is said to be power generation paradigm of the new era because of its ability to resolve many customer problems, especially from power quality point of view. DG is used to provide electricity service at a high level of reliability and power quality than conventional grid power system. DG is capable of protecting sensitive loads from momentary voltage variations. It can provide uninterruptible power supply to ride through any sort of outage until primary or secondary power is restored. It is environmental friendly, promotes renewable energy resources, improves system power factor, and power quality in terms of node voltage drop and power loss reduction. A DG system provides protection from long term outages. Power quality system needs to include important design criteria that relates to system hardening. It is necessary to understand the business mission and the tolerance for outage. To eliminate the power quality and reliability disruptions, a facility may seek to minimize its energy prices by introducing DG.

## REFERENCES

1. Akhmatov V., Knudsen H., Nielsen A.H., Pedersen J.K. and Poulsen N.K., 'Modelling and Transient Stability of Large Wind Farms', *Electric Power and Energy Systems*, Vol. 25, 2003, pp. 123-144.
2. Ana I. Estanqueiro 'A Dynamic Wind Generation Model for Power Systems Studies', *IEEE Transactions on Power Systems*, Vol. 22, No. 3, August 2007, pp. 920-928.
3. Boulaxis N.G., Papathanassiou S.A. and Papadopoulos M.P., 'Wind Turbine Effect on the Voltage Profile of Distribution Networks', *Renewable Energy*, Vol. 25, 2002, pp. 401-415.
4. Chan T.F. and Lai L.L., 'An Axial-Flux Permanent-Magnet Synchronous Generator for a Direct-Coupled Wind-Turbine System', *IEEE Transactions on Energy Conversion*, Vol. 22, No. 1, March 2007, pp. 86-94.
5. Chompoo-inwai C., Wei-Jen Lee, Pradit Fuangfoo, Mitch Williams and James R. Liao, 'System Impact Study for the Interconnection of Wind Generation and Utility System', *IEEE Trans. on Industry Applications*, Vol. 41, No. 1, Jan./Feb 2005, pp. 163-168.
6. Chompoo-inwai C., Yingvivanapong C., Methaprayoon K. and Wei-Jen Lee, 'Reactive Compensation Techniques to Improve the Ride-Through of Induction Generators during Disturbance', *IEEE Trans. on Industry Applications*, Vol. 41, No. 3, May-June 2005, pp. 666-672.
7. Divya K.C. and Nagendra Rao P.S., 'Models for Wind Turbine Generating Systems and their Application in Load Flow Studies', *Electric Power Systems Research*, Vol. 76, 2005, pp. 844-856.
8. Eisenhut C., Krug F., Schram C. and Klockl B., 'Wind-Turbine Model for System Simulations Near Cut-In Wind Speed', *IEEE Transactions on Energy Conversion*, Vol. 22, No. 2, June 2007, pp. 414-420.
9. Julio Usaola, Pablo Ledesma, Juan M. Rodriguez, Jose L. Fernandez, Domingo Beato, Ramon Iturbe and Jose R. Wilhelmi, 'Transient Stability

Studies in Grids with Great Wind Power Penetration - Modelling Issues and Operation Requirements', IEEE Power Engineering Society General Meeting, Vol. 3, 2003, pp. 1534-1541.

10. Muljadi E., Wan Y., Butterfield C.P. and Parsons B., 'Study of a Wind Farm Power System', NREL Report, 2002.
11. Oscar Alexis M.A., 'Issues Regarding the Integration of Induction Wind Turbines in Weak Electrical Networks', Nordic Wind Power Conference, Chalmers University of Technology, March 2004, .-23.